AN ABSTRACT OF THE THESIS OF

Troy A. Hayes for the degree of Master of Science in Materials Science presented on June 14th 1996. Title: Thermal Stability of Surface Treated Zirconium.

Abstract approved:

Redacted for Privacy

Michael E. Kassner

Zirconium press plates have been developed for the production of melamine coated particle board, using shot-peening to achieve the desired plate (and therefore coated particle board) surface texture. Service temperatures of the press plates approach 200°C. This study examined the microstructural effects of extended exposure of shot-peened zirconium to temperatures of 200°C and 300°C. Softening of the surface may reduce wear resistance and possibly the surface morphology of the plate, affecting the usability of the plates. It was discovered that the shot-peened surface of the plates experienced a loss in hardness from approximately 230 VHN (DPH) to about 220 VHN after 560 hrs at 200°C. The same drop in hardness was experienced after only 5.5 hrs at 300°C. This decrease in hardness was determined from hardness profiles before and after heat treating the zirconium to various times from 0.5 hours to 4458 hrs and 2790 hrs at 200°C and 300°C respectively. The decrease in hardness is believed to be a result of static recovery, the annihilation of point and/or line defects and/or alignment of dislocations into relatively low misorientation

substantially relatively close to the shot-peened surface (about 35 μm), and decreased more modestly over the next 100 μm until virtually no drop was experienced further than approximately 150 μm from the surface. The shot peening hardens the surface region which extends about 150 μm from the surface. Thus, the level of recovery appears to depend on the stored energy associated with cold work, or ambient temperature deformation. This increases from about 2-3% cold work (equivalent percent cold reduction from rolling) in the bulk of the specimens to near 99% at the surface resulting from shot peening. The dislocation structure of the shot peened zirconium was examined in the as-peened as well as the annealed conditions using transmission electron microscopy.

Thermal Stability of Surface Treated Zirconium

by

Troy A. Hayes

A THESIS

submitted to

Oregon State University

in partial fulfillment of
the requirements for the
degree of

Master of Science

Presented June 14th, 1996
Commencement June 1997

Master of Science thesis of Troy A. Hayes presented on June 14th, 1996

APPROVED:

Redacted for Privacy

Major Professor, representing Materials Science

Redacted for Privacy

Head of Materials Science Program

Redacted for Privacy

Dean of Graduate School

I understand that my theses will become part of the permanent collection of Oregon State University libraries. My signature below authorizes release of my thesis to any reader upon request.

Redacted for Privacy

Redacted for Privacy

Troy A. Hayes, Author

ACKNOWLEDGMENT

I would like to thank M. Wall for assistance with the TEM study, the Center for Electron Microscopy at Lawrence Berkeley National Laboratory for the use of necessary TEM equipment, P. Danielson of Teledyne Wah Chang for his insight on proper polishing techniques of zirconium, D. Amick of Teledyne Wah Chang for his help with direction of research and his knowledge of zirconium, and X. Li and R. Faber for performing tensile tests. I also wish to express my deepest thanks to Professor M.E. Kassner for making this all possible by recruiting me when I was not really sure which direction I wanted to go. Finally, I would like to thank my wife Natasha, daughter Talisa, and son Shoghi for their enduring support over the duration of this project. It was invaluable to have someone to talk to about the ups and downs of my research work, even if they had no idea what I was talking about. Thank you all.

TABLE OF CONTENTS

Page

TABLE OF CONTENTS (CONTINUED)

TABLE OF CONTENTS (CONTINUED)

LIST OF FIGURES

LIST OF FIGURES (CONTINUED)

LIST OF FIGURES (CONTINUED)

LIST OF TABLES

LIST OF APPENDIX FIGURES

LIST OF APPENDIX FIGURES (CONTINUED)

LIST OF APPENDIX FIGURES (CONTINUED)

Figure Page

DEDICATION

I dedicate this to my beloved wife and children. Thanks.

Thermal Stability of Surface Treated Zirconium

Introduction

Teledyne Wah Chang (Albany, Oregon) is attempting to fabricate zirconium press plates for the production of melamine coated particle board. The surface texture desired for the melamine coated boards will be produced by shot-peening the zirconium plates (impinging the surfaces with cast iron particles) under various intensities and coverage specifications. Intensity is based on the arc height (height of midpoint of bowed strip) that a test strip experiences after being shot peened on one side under the same conditions [1]. Coverage is defined by the percent of the surface that has been dimpled or obliterated when observed under 10X magnification [1]. A coverage of 200% is defined as twice the application time it takes for initial complete coverage (98%). The zirconium press plates would experience thermal cycling (repeated cycling from one temperature to another) to a maximum of 190°C during the manufacturing process for the melamine coated particle board. There is concern that recovery may occur at the deformed, shot peened, surface with prolonged exposure to 190°C. It has been shown by McGeary and Lustman [2] that heavily cold worked zirconium (97% reduced bar) undergoes significant recovery after just 10 minutes at 300°C [2]. Several other authors [3-6] have also observed significant recovery in cold worked zirconium at temperatures around 400°C, however, none have observed a significant amount of recovery at temperatures under 300°C. No long term (>200 hours) softening studies appear to have been performed at temperatures as low as 190°C for cold worked zirconium. The

reduction in hardness results reported by McGeary and Lustman are illustrated in Figure 1 below.

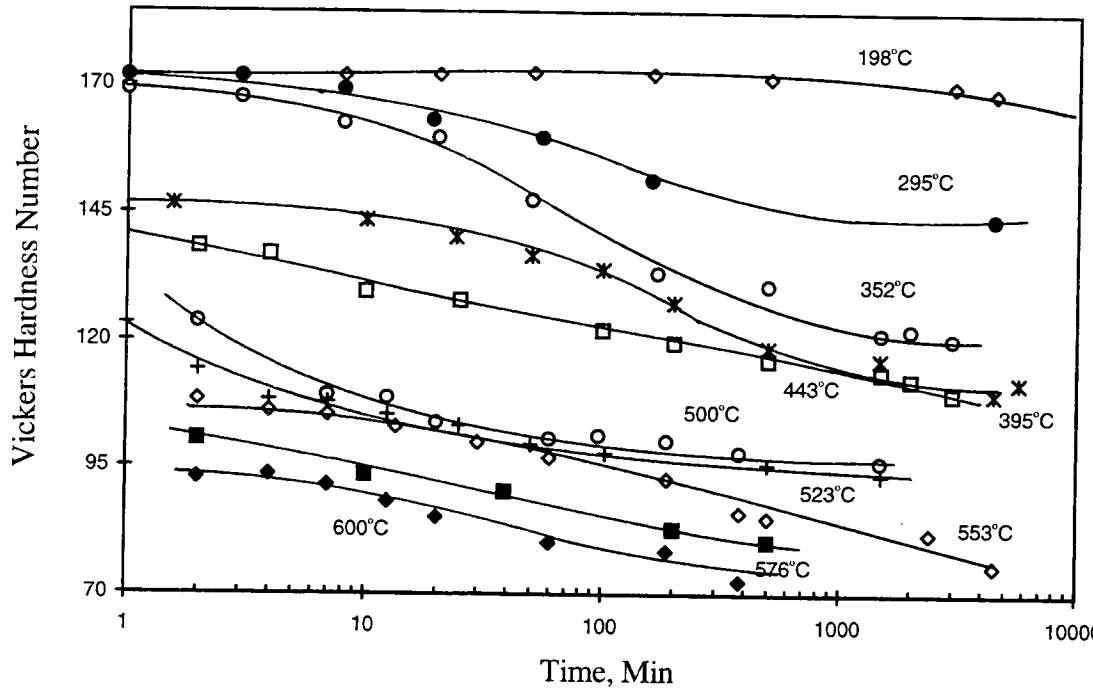

Figure 1 Hardness-decrease for isothermal annealing of 97% cold rolled zirconium at various temperatures [2]

Desalvo et al. [4] has observed a so-called "stage I" of recovery over the temperature range of ambient temperature up to about 315°C in 80% cold worked reactor grade (99.5% Zr) plate. This "stage I" recovery was also reported at 30 to 35°K by Swanson et al. [7] for a study of 99.9% zirconium cold worked in tension at 4°K (liquid helium) and by Merle et al. [8] in a study of 82% cold-rolled Zircaloy-4 sheets at temperatures up to 100°C. The authors proposed that "stage I" recovery was due to interstitial migration [7] or short distance dislocation rearrangement which is too small to be observed under the electron microscope at that time [4]. Bostrom et al. [9] also observed restoration

of resistivity at low temperatures. "Stage I" recovery has been observed by electrical resistivity studies and has not been associated with a reduction in hardness (no hardness data were reported). Further, it is not clear what mechanism of recovery was associated with "stage I" and the so called "stage I" is very sensitive to the purity of the zirconium as impurities may pin dislocations [4]. In the present study, recovery is considered to be a change in hardness associated with a change in point (vacancy) concentration or line (dislocation) density and/or arrangement as will be discussed later. This study will determine if softening of variably cold worked (shot peened) zirconium occurs after extended exposure to temperatures of 200°C and 300°C and possibly determine the softening mechanism.

Teledyne Wah Chang is advertising superior features of the zirconium plates when compared to the currently available, very hard, chromium plated stainless steel (SS) plates manufactured in Germany (300 series austenitic SS with about 18% Cr, 8% Ni). These properties include the resistance to incidental damage during the manufacturing of the melamine boards. This advantage is realized because zirconium has a yield strength similar to that of SS (300 MPa for zirconium compared to about 240 MPa for SS) and an elastic modulus about half that of SS (99.4 GPa for zirconium compared to about 200 GPa for SS). This results in approximately doubling the energy that the zirconium plates can absorb before experiencing permanent plastic deformation. The chromium layer does not effectively improve the damage resistance of the stainless steel plates. The yield strength at the surface of the shot peened zirconium is actually higher than the above measured bulk yield strength since the surface has been shot peened or heavily cold worked (the surface yield stress is approximated at 420 MPa, as will be shown later). Teledyne also claims to be able to repair a small area in the plate if it does become damaged which is impossible with electroplated SS. The SS plates cannot be practically re-electroplated to obtain the original texture. Repairing the zirconium plate entails removing, by cutting, the damaged section, followed by replacement

using Tungsten Inert Gas (TIG) welding, grinding the repair area and finally shot-peening the surface to achieve the original texture.

If recovery (decrease in dislocation density or point vacancy concentration) or recrystallization (nucleation of new, relatively dislocation-free grains) occurs, these advantageous characteristics could be dramatically affected. For instance, recovery and recrystallization are associated with a reduction in surface hardness or yield strength, which would allow the plate to become damaged more easily. Also, if recovery or recrystallization occurred, the surface morphology could change due to plasticity associated with residual stress relaxation. These effects would also complicate repair since the recovery must be reproduced in the repair area for homogeneity of the surface.

The goal of this project is to determine if there is any softening in the shot-peened zirconium surface in the vicinity of the service temperature. Recovery and/or recrystallization of the shot-peened surface layer would be manifested by structural change, perhaps detectable by changes in the micro-hardness and by optical and transmission electron microscopy (TEM). Although hardness testing has previously been regarded as a poor measure of recovery [10,11], it has been utilized in this study due to the variable amount of cold work with depth associated with shot peening. The variable cold work with depth complicates the use of electrical resistivity measurements. Hardness testing was also chosen because the commercial community is interested in the change in hardness of the surface of the shot peened plates independent of resistivity or microstructural changes.

Experimental Procedure

One means by which softening or "restoration" of the shot peened zirconium was assessed was by determining initial hardness profiles from the shot-peened surface to the interior of the metal. The zirconium was subsequently heat treated at 200°C and 300°C for various times, increasing (in each instance by a factor of ten or so) from an initial 0.5 hour heat treatment. New hardness profiles were determined from the identical specimens after heat treatment and compared to the initial profiles. If a loss in hardness occurred, the grain and dislocation microstructure would be examined using optical microscopy and TEM both before and after heat treatment to determine the possible source of the loss of strength (hardness) of the zirconium.

Plate Fabrication [12]

The plate was fabricated from a triple arc-melded ingot (melted three times in a consumable electrode vacuum arc furnace), 68.6 cm in diameter and 2.74 m in length. The ingot was commercially pure zirconium 702 with the nominal composition listed in Table 1.

Element compositions in Table 1 were determined using inert gas fusion (H, O, N), inert gas fusion with non-dispersive infrared detector (C), flame photometry (P), and ICP emission spectroscopy (Si and all metallic elements).

Zr - 99.17%	Al - 120 ppm	Nb - 50 ppm	Sn - 1800 ppm
C - 142 ppm	H - 30 ppm	Ni - 98 ppm	Ta - <100 ppm
Cr - 1022 ppm	Hf - .276%	O - 1320 ppm	Ti - 84 ppm
Cu - 25 ppm	Mo - <10 ppm	P - 10 ppm	V - <25 ppm
Fe - 1547 ppm	N - 55 ppm	Si - 58 ppm	W - <25 ppm

Table 1 Nominal composition of zirconium 702 [13]

The ingot was homogenized at 1040°C for 8 hrs and slow cooled to ambient temperature. The ingot was open die hot forged (heated zirconium ingot pressed between cold flat plates) to 10-13 cm thickness, 76 cm width and 3 m length, with intermittent re-heats to 1040°C when the ingot temperature dropped below 650°C. The minimum temperature of 650°C was necessary avoid cracking. A phase transformation ($\beta \rightarrow \alpha$ transition at 862 ± 5 °C [14]) occurs during forging over the above temperature range (this transformation was allowed because the next step includes β phase recrystallization). After the final reduction, the plate was heated to 1040°C to allow β phase recrystallization and water quenched from the high-temperature β body centered cubic (bcc) region, resulting in a "metastable" β phase texture with an α hexagonal closed packed (hcp) crystal structure via a martensitic transformation (the β texture is not eliminated until subsequent cold working and recrystallization, as noted later). The pressed plate was then blasted with 30-60 grit (see Table 2 for grit/size conversion) silicon carbide to remove the oxide scale that developed during hot working. Next, about 0.07 cm were removed from both plate surfaces using 8-10 grit aluminum oxide or silicon carbide on drums to remove any remaining surface oxides and ensure a level surface. Up to 0.26 mm of metal (as much as needed

to remove "smeared" material from silicon carbide grinding) was then chemically removed using an etching solution of 5% HF, 25% HNO_3, 70% H_2O at 38 °C. "Smearing" is the plastic flow of the surface of the zirconium that may cover surface defects such as cracks. The chemical etching process (pickling) exposes the surface crack defects. The plate surfaces were spot ground to remove defects. The plate was then subjected to ultrasonic tests to detect macroscopic defects (cracks, voids, low density inclusions, etc.) within the plate interior. A small hole was drilled in the plate to mark or eliminate any exposed defect. Any defects were avoided when the plate was sectioned for specific applications. The plate was hot rolled in a reversing hot roller from about 10 cm to 0.95 cm after pre-heating to 780 +/- 14°C for 80 to 100 minutes. The plate was rolled in increments of approximately 25% reduction in thickness per pass (8-10 total passes) which were interrupted by re-heating to 780°C if the temperature dropped below 540°C (to maintain dynamic α phase recrystallization). This step eliminates all residual β texture that resulted from water quenching the β zirconium and yields a uniform grain α phase. The plate was then annealed at 790°C for 30-60 minutes to ensure stress-relief and full recrystallization of the plate (the final passes of the hot rolling may have been at a temperature too low for complete dynamic recrystallization, thus resulting in a certain amount of residual work in the plate). If warpage occurred during annealing, the plate was roller leveled at 650°C leaving 2-3% residual plastic deformation (2-3% is allowed by Teledyne Wah Chang, since this level is not believed to have any significant effects on the material properties). The plate was shot blasted (similar to shot-peening, but utilizes a more variable shot size and is applied without intensity and coverage specifications) with 330 to 550 (0.84 to 2.0 mm diameter) size 1 wt % carbon cast iron shot to remove all surface oxides that developed upon annealing. The plate was again pickled to remove the cold worked layer resulting from the shot blasting, and to highlight any remaining surface oxides remaining from the blasting. These could be

individually removed by spot grinding. The pickling also ensured a smooth surface for a favorable appearance. Finally, the edges of the plate were trimmed according to the dimensions required for the specific application.

Grit No.	8	10	30	50	60	80	120	150	180	220	240	280	320	400	600
Avg. particle size (μm)	2400	2000	590	350	270	190	115	80	70	62	54	35	29	23	17

Table 2 Silicon carbide grit/ particle size correlation [15, 16].

Press Plate Surface Treatment

Surfaces of a 15.0 cm by 21.6 cm plate were wet ground from 0.86 cm thickness to 0.65 cm (0.11 cm from each side) with a 220 grit silicon carbide belt yielding a 20 microinch rms (root mean square as described in [17]) finish. The plate was then shot-peened with cast iron S-550 shot (1.19 to 2.00 mm diameter particles) at 16A Almen intensity (described subsequently) [18] with 100% coverage, or saturation of the surface [1]. A small amount of bending was observed after peening one side (15.0 cm by 21.6 cm sample plate experienced a maximum arc height of 0.457 mm) resulting in a bending stress of about 30 MPa (see Appendix D), however this bending was elastic (yield stress of zirconium is 300 MPa) and the plate was flat after both sides were peened. The tolerance for the S-550 shot size is based on screening of the shot through a sieve with 1.19 mm openings followed by a sieve with 2.00 mm openings with a maximum of 2% of the particles passing and being retained by the sieves, respectively [19]. The Almen intensity is specified using a shot-peening test strip that is shot-peened on one side while bolted to a rigid surface. The intensity number (16) corresponds to the arc height that the 76.2 mm long by 23.8 mm wide strip experiences as a result of the peening and the letter (A)

specifies the thickness of the test strip (1.29 ± 0.02 mm in this case) [18]. Coverage is determined by visual inspection under a ten power magnifying glass. Peening to the point where the dimples do not quite overlap is considered 98% coverage (100% coverage is a factor of 1.02 larger than the time required for 98% coverage) [1].

Sample Preparation

Seven samples were removed from various localities (see Figure 2) from a 15.0 cm by 21.6 cm by 0.65 cm thickness test plate using a water cooled silicon carbide abrasive cutoff saw. Approximate dimensions of each sample were 1.6 cm by 0.65 cm by 0.65 cm with the long dimension parallel to the rolling direction of the plate. Corners of the samples were ground smooth with wet 240 grit silicon carbide paper prior to cold mounting in Buehler epoxy resin (5-6 hour cure). A side transverse to shot-peened surface was subsequently polished. The backsides of the samples extended beyond the epoxy mount so that the pressure on the sample could more easily be controlled during polishing. This step was critical, because if the backsides of the samples were level with or covered by the mounting material, the pressure applied to the sample could not easily be controlled and high quality polishing was not possible (free of large scratches, not over-etched, etc., as will be described subsequently). The samples were polished according to the following procedure.

Sample Polishing

Polishing proceeded in three steps; grinding, rough polishing, and final polishing as will be described in detail subsequently.

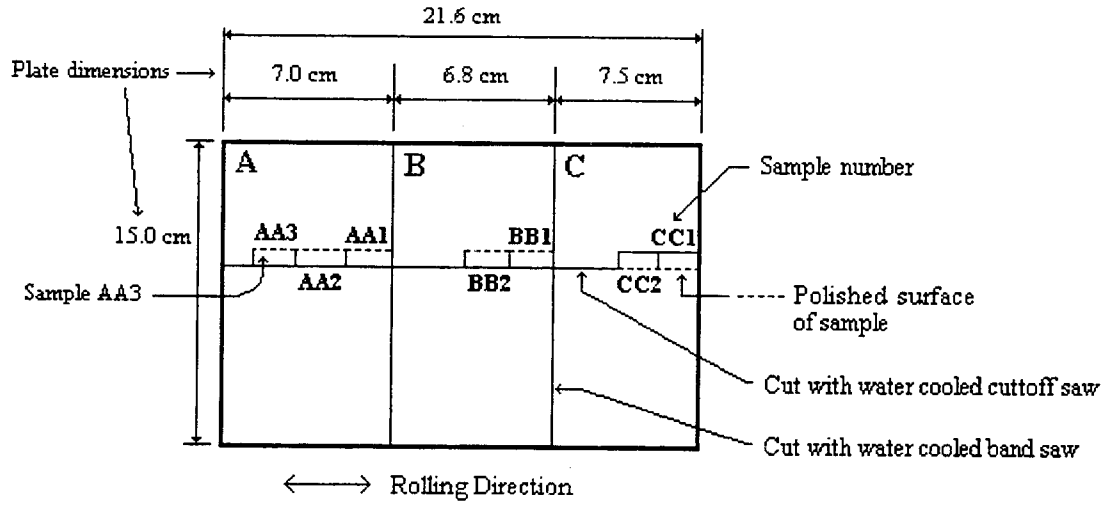

Figure 2 Sample orientation

Grinding

The samples were ground on H_2O lubricated 240 grit silicon carbide paper in order to attain a flat surface and remove any mechanical damage resulting from the abrasive cutoff wheel. The thickness of the sample were then recorded to allow a determination of the material removed from each grinding/polishing step. The samples were ground according to Table 3. The surface of the samples appeared to have uniform scratches accompanied by small pits when observed under 100X magnification and bright field illumination after each grinding increment. The specimens were ground until all scratches from the previous grinding step were removed. The pits or chips had a diameter of roughly three scratch widths (pit size scaled with finer grinding steps). The cause of the pitting was unclear.

Description	Material Removed (μm)
320 grit H_2O lubricated silicon carbide	10 - 20
400 grit H_2O lubricated silicon carbide	5 - 15
600 grit H_2O lubricated silicon carbide	5 - 10

Table 3 Rough grinding procedure

Samples were turned 90° after each wet grinding stage so as to ensure that the surface remained flat. Turning the sample also allowed visual inspection of the surface uniformity. A grinding step was complete after doubling the time necessary to remove "transverse" scratches resulting in new uniform scratches over the entire surface. After the 600 grit wet grinding step, the sample was rinsed thoroughly with fresh water and cleaned in a vibrator for approximately one minute followed by an alcohol rinse.

Rough Polishing

The next step (rough polishing) was completed using a Buehler Chemomet I final polishing cloth (so called "rough polishing" cloths were too coarse as will be discussed later) on a 20.3 cm diameter anodized aluminum polishing wheel. An acid and alumina slurry (polishing solutions defined in Table 4 below) was chosen over various mechanical polishing methods because it yielded a better surface finish using less time. Some other polishing techniques that proved unsuccessful will be detailed in a following section.

A small flow of fresh tap water was supplied to the perimeter (outermost 2 cm) of the wheel during the rough polishing stage. This water ensured that the wheel maintained a sufficient lubricating fluid base throughout the polishing so

that friction between the wheel and the sample remained low. The friction greatly increased if the wheel was dry, causing "smearing" or plastic flow at the surface of the zirconium samples.

The polishing wheel was coated with 1 μm alumina slurry (refer to Table 4 for all polishing compounds) and a 1-2 ml application of rough polishing acid (Table 4) at a speed of about 550 rpm. The sample was then polished by moving the sample in small circles from the inner portion of the wheel to the wetted perimeter region while applying a moderate force (3-5 pounds) to the back of the sample that protruded from the mounting material. The sample was oriented with the long dimension tangential to the wheel so that the entire sample was at virtually the same radial distance from the center of the wheel and was polished consistently. The goal of this polishing technique is to remove the material by the acid and the alumina slurry at approximately equal rates. Smearing occurred if removal was dominated by the slurry, and the surface would brown and become porous if removal was dominated by the acid. Polishing in small circles was continued for about 45 seconds and the sample was then immediately rinsed with fresh water. The polishing wheel was rinsed and the process was repeated with new applications of acid and slurry for a total time of about 3 minutes (3-4 repetitions). The surface of the material appeared shiny and free of scratches without magnification. Samples often required longer times for polishing to the same surface finish because of the pressure sensitivity which was affected by the sample mounting material (the quantity of mounting material holding each sample varied some). The samples could not be polished without the mounting material (where application pressure could be more easily controlled) because the shot peened surfaces of the sample would become rounded and be attacked by the etchant precluding effective imaging and hardness testing. It is very important during the rough polishing stage not to excessively polish the sample. With increased polishing time, the sample surface becomes recessed from the mounting material. This occurs because the acid does not attack the mounting epoxy. Further polishing does not yield the

desired surface finish because, even with the application of higher pressures to the back of the sample, the slurry on the polishing wheel can not reach the sample and the critical shot peened edges of the surface turn brown and porous from acid etching. This typically occurs after about 4 minutes, and varies with the pressure applied to the sample and the amount of acid and slurry used. Following the last repetition of the rough polishing step, the samples were again rinsed thoroughly with fresh water and cleaned in a vibrator while immersed in tap water for about one minute followed by an alcohol rinse.

Step	Description	Duration	Composition
Rough Polishing	Acid	3-4 min	250 ml H_20, 22 ml HNO_3(70%), 3 ml HF(48%)
	Slurry		300 ml H_20, 20gm of 1 μm alumina powder
Final Polishing	Acid	4 min	200 ml H_2O, 30ml HNO_3, 20 ml H_2O_2 (70%), 8-10 drops HF
	Slurry		200 ml H_2O, 3gm of 0.05 μm alumina powder
Etching	Acid Etchant	6-8 sec	18 ml H_2O, 18 ml HNO_3, 4 ml HF

Table 4 Polishing Solution Compositions

Final Polishing

Another polishing wheel (same configuration as used for rough polishing stage) was coated with a 0.05 μm slurry of alumina and a 3-5 ml application of the "final" polishing acid (Table 4) for final polishing. The wheel operated at a speed of about 550 rpm. The sample was oriented with the long dimension of

the sample pointing radially toward the center of the wheel. This orientation was adopted so that if any deep scratches occur during final polishing, they were easily avoidable when hardness testing (scratches occurring in the long direction could extend across the entire sample in the critical region near the shot-peened surfaces). The sample was then polished at half the radial distance from the center of the polishing wheel (applying about 1 to 2 pounds of force) for 45-60 seconds. The wheel was rinsed and the process was repeated with new applications of acid and slurry for a total time of about 4 minutes (4-5 repetitions) or until no scratches were visible under 550X magnification. Repetitions were necessary because the lubrication on the wheel from the acid and slurry was diminished (polishing without sufficient lubrication caused smearing) if polishing proceeded longer than about 1 minute. Another 45 second final polish was necessary if the sample was examined using a microscope before etching (samples were only observed under a microscope periodically before etching to ensure that the final polishing was yielding a desirable surface finish). This is because the sample requires etching immediately following final polishing so as to minimize surface oxidation.

The rough and final polishing cloths were changed after polishing about 15-20 specimens. Deep scratches would often result on the surface if the rough polishing cloth was not changed with this frequency. The final polishing procedure did not experience the same diminished polished surface quality if the final polishing cloth was not changed, however, the rubber base of the cloth would begin to deteriorate. It was then extremely difficult to remove the cloth from the polishing wheel. Reference [20] has a general summary of a similar rough and final polishing technique for zirconium.

The sample was rinsed briefly immediately following final polishing and etched in a solution of 45 ml H_2O, 45 ml HNO_3 (70%), and 10 ml HF (48%) (as recommended by Leco [15]). This etchant was lightly swabbed on the sample surface using a cotton tipped applicator for about 6-8 seconds and immediately rinsed with cold water followed by an alcohol rinse. A total of 1 to 2 μm were

removed during etching (determined with an optical microscope). The cotton tipped applicator was first rinsed thoroughly with alcohol and dried with hot forced air before swabbing. If the swab was applied with "excessive" force, the surface quality was diminished due to the associated differential acid removal rate at the tip of the swab. The etching was occasionally repeated following the cold water rinse if the surface did not appear uniform, but the total etching time did not exceed 10 seconds. Etching longer than ten seconds caused too much distortion (undulation) of the surface because of the increased removal rate in the highly cold worked grains near the shot-peened surface compared to the removal rate in the bulk interior grains. It was also observed that the sample would rapidly increase in temperature and boil the etchant, emitting brown nitrogen dioxide gas if the sample was etched continuously for more than about 12 seconds. This will be discussed in greater detail later.

The sample appeared shiny and uniform across the surface after proper etching. The grains in the interior region of the sample appeared uniformly polished and etched when observed under polarized light at 100X magnification, while the shot-peened region was slightly recessed due to the differential rate of etching of cold worked and non-cold worked metal. The epoxy mount was removed from the sample for hardness testing.

The above polishing technique is superior to, exclusively, mechanical polishing because as the zirconium was removed from the surface by the alumina slurry, it was dissolved and/or washed away by the acid. This precluded the mechanically removed material from scratching the surface.

The adopted polishing procedure also led to a higher surface quality than the other techniques because it reduced the etching time required after final polishing. The etching time was reduced because there were only very small uniform (0.05 μm) scratches to remove. Other techniques resulted in an "orange peel" surface and/ or had additional larger scratches for unclear reasons.

In order to ensure that the above polishing technique did not leave any mechanical damage (e.g. increased dislocation density or microtwins) from the

abrasive polishing, a "true" unpolished (undeformed), or baseline hardness was determined. This hardness was then compared to the hardness measured after polishing a sample using the above polishing procedure. This allowed a determination if any mechanical damage was caused to the sample surface region resulting from polishing.

Over 1.5 mm of material were removed from 5 shot peened specimens taken from another shot-peened test plate of the same nominal composition using only an acid etchant (specimens used in the heat treatment study were not yet fabricated). A solution of 45% H_20, 45% HNO_3, and 10% HF was used as it rapidly and evenly reacts with zirconium across the grains [15]. This left a surface with no residual surface deformation due to sample preparation. An average hardness value of about 160-165 Vickers Hardness (VHN) was obtained by averaging 40 to 50 hardness tests in the interior (over 3 mm away from the shot-peened surfaces) of each of the 5 samples. A hardness profile (procedure detailed in a subsequent section) was then developed from a shot-peened sample that had been polished using the above acid/ slurry polishing technique. The interior region of the hardness profile reached a similar hardness of about 160-165 VHN, confirming that the acid/ slurry polishing technique did not produce measurable surface damage. A 100 gram force (gf) was used for the initial hardness tests but a 300 gf indenter was later used for greater accuracy, as will be discussed subsequently.

Unsuccessful Polishing Techniques

The first attempted polishing technique utilized wet grinding using 240 to 600 grit silicon carbide paper. This was followed by polishing with 5 μm, 1 μm, and 0.05 μm water based alumina powder on a polishing wheel at low and high speeds (~500 and ~1000 rpm). The pressure applied to the sample, the water to alumina ratio and length of time on the polishing wheels were varied at each of the wheel speeds. The surface immediately pitted or smeared giving an "orange

peel" appearance regardless of any changes in the variables. The reason this occurred is unclear.

Another process tested used dry alumina coated lapping paper on flat glass plate for the final polishing stages rather than wet polishing wheels. This seemed to leave a good polish (no "orange peel") without "smearing", but visible scratches on the surface of the metal were evident for unclear reasons. These scratches could be removed using a longer acid etching time, but this led to an uneven surface because the acid attacked the shot-peened region much more rapidly than the undeformed regions.

A similar method utilized alumina lapping paper under a flow of water to wash away any possible small fragments from the surface. This method was ineffective and scratches were still produced. The zirconium was next polished while the alumina lapping paper was submerged in the etching solution. This seemed to work initially, but the excessive time required to attain the desired surface quality resulted in a greatly distorted (undulations that precluded effective imaging and hardness testing) shot-peened region due to acid erosion. It was also very cumbersome to secure the lapping paper while submerged in the acid.

Once choosing the procedure utilizing acid/ alumina slurry, detailed in the previous section, minor variations were attempted in an effort to decrease polishing time. The acid/ alumina slurry technique was performed with Buehler Texmet 1000, Texmet 2000, and Metcloth covered with nylon, but all of these cloths produced inferior results to those that resulted from using the Chemomet I final polishing cloth. These cloths removed material faster than the Chemomet I polishing cloth, but the scratches left from rough polishing took much longer to remove during final polishing, resulting in a longer polishing process with a less desirable surface finish.

It was found that all of the techniques could lead to a surface without a damage layer simply by increasing cumulative etching time after the polishing was complete. The problem is that the longer the material was etched, the

greater was the localized attack of the deformed material near the shot-peened surface, as was discussed previously. As the region near the surface is obviously the most critical, any more than slight undulation near the surface renders the hardness tests inaccurate. Therefore, the etching time must be minimized by achieving a good surface quality from polishing.

Etching Techniques

Etching techniques were evaluated with respect to surface quality (pitting of the surface and/ or undulation from localized attack), and sample temperature resulting from etching. A thermocouple was attached to one sample and the temperature was recorded as the material was removed during the acid etching. It was found that rapid heating occurred if the sample was allowed to remain immersed in the etchant for more than about 12 seconds. The sample initially increased slowly (about 12 seconds) from ambient temperature to about 40 to 50 °C followed by a very rapid (about 1 second) increase to about 100°C. It was important to minimize specimen heating from this etching as this study consisted of controlled experiments on thermal stability of shot-peened zirconium at low temperatures. The maximum etching time was reduced to 12 seconds to preclude heating during etching. When determining the baseline hardness discussed above, however, extensive etching was required to remove 1.5 mm of material. Here, the samples were intermittently cooled by rinsing with cold water after a maximum etching time of 12 seconds. Intermittent cooling was chosen over pouring etchant across the sample surface, which would have been a continuous process using fresh, cool etchant to simultaneously cool the sample. This is because small pitting of the surface resulted for unclear reasons. The same swabbing technique was used as it left a flat, uniform finish for the short etching times (6-8 seconds) required after the polishing of the samples for hardness profiling,. The above etching technique was developed to yield a good

surface finish for imaging and hardness testing as well as maintaining low temperatures during etching.

Safety Precautions

When working with zirconium, several precautions are needed. Welding glasses must worn while cutting zirconium on the abrasive cutoff saw. It is also important to make sure that small shavings or dust from the specimens are not allowed to accumulate, as they can spontaneously combust or explode, even while submersed in water.

All polishing using etch attack polishing (combination of acid and alumina with water) must be completed in a well ventilated area. Two layers of latex rubber gloves were worn while polishing, with a full length lab coat, plastic apron, and a full face shield. Thicker neoprene gloves are too bulky to allow for control of the sample during polishing. Because all polishing involved the use of hydrofluoric acid, any spillage or splashing on the clothing requires thorough flushing with fresh water. Etching was always performed under a fume hood.

Hardness Testing

A Leco M400A microhardness testing machine was utilized for all hardness determinations. A Vickers Hardness (VHN) diamond tipped indenter was chosen because of availability. Using a Vickers Hardness indenter also resulted in more consistent hardness measurements (less scatter) than a Knoop indenter. The M400A had a load range from 1 gram force (gf) up to 1000 gf using free weight loading. All hardness testing performed for this study utilized a 300 gf load. The loading cycle was arbitrarily set to 15 seconds from the time of first contact with the sample until the time when the tip cleared the surface during retraction. This timing was used consistently throughout the study. The

diamond pyramid indenter was oriented so that the diagonals formed a cross parallel and perpendicular to the shot-peened surface. The indenter was manufactured by Leco Corporation. The diamond tip was cleaned after every 20-30 hardness tests with a dry lens wipe to ensure that the tip was free of oil or any small dust particles. The instrument was regularly checked for calibration on a Leco testing block. Hardness values ranged from about 2.5% under to 1.5% over the known hardness value of the test block of about 712 VHN (DPH). The samples were rinsed with alcohol and dried with hot forced air before being secured in a self leveling stage for indentation as shown in Figure 3. The self leveling stage ensured that the top surface of the sample was perpendicular to the hardness indentation loading direction. This was accomplished by leveling the sample in accordance with the top surface with the "adjustable clamps" (see Figure 3) while the "self leveling stage" moved freely on a ball and socket joint to accommodate the bottom surface (which may not quite be parallel to the top surface). The secured sample was observed through a 55X magnifying lens and a 10X magnifying eyepiece under bright field illumination for a total magnification of 550X.

A 300 gf load was used to develop a hardness profile for about 800 μm nearest the shot-peened surface. The indentations were "staggered" as illustrated in Figure 4, leaving at least 5 indentation widths between each indentation to avoid erroneous measurements due to the effects of the previous indentation. The first hardness measurement was taken about 35 to 50 μm from the shot-peened surface. Any measurements closer than about 35 μm gave superficially low results because the free surface results in diminished resistance to the plastic flow of material. Hardness measurements were determined in depth increments of 10 to 20 μm for the nearest 100 μm to the shot-peened surface. The spacing was then increased to about 20 to 40 μm for completion of the profile. This "graduation" was used so that more data could be obtained in the most critical region near the surface while still fully extending

through the depth of the shot-peened "damage layer". This "graduation" is also illustrated in Figure 4.

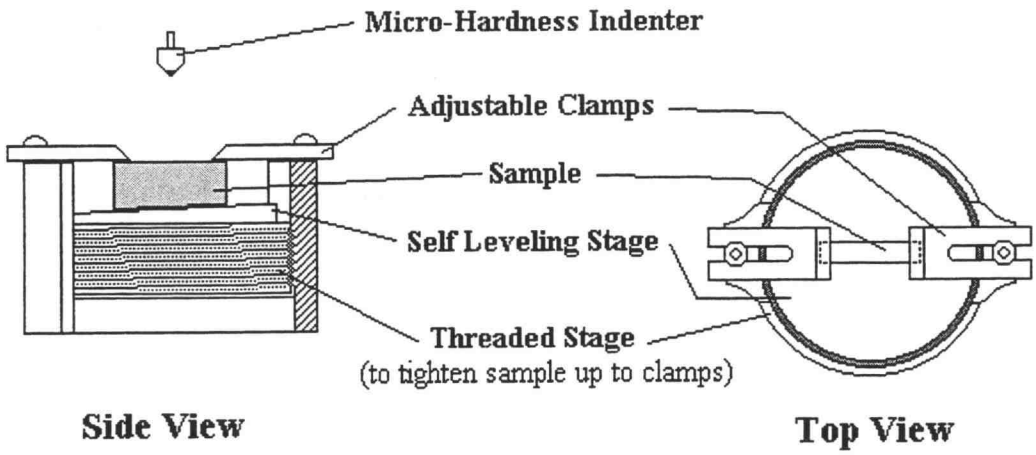

Figure 3 Sample and mounting stage configuration for hardness testing

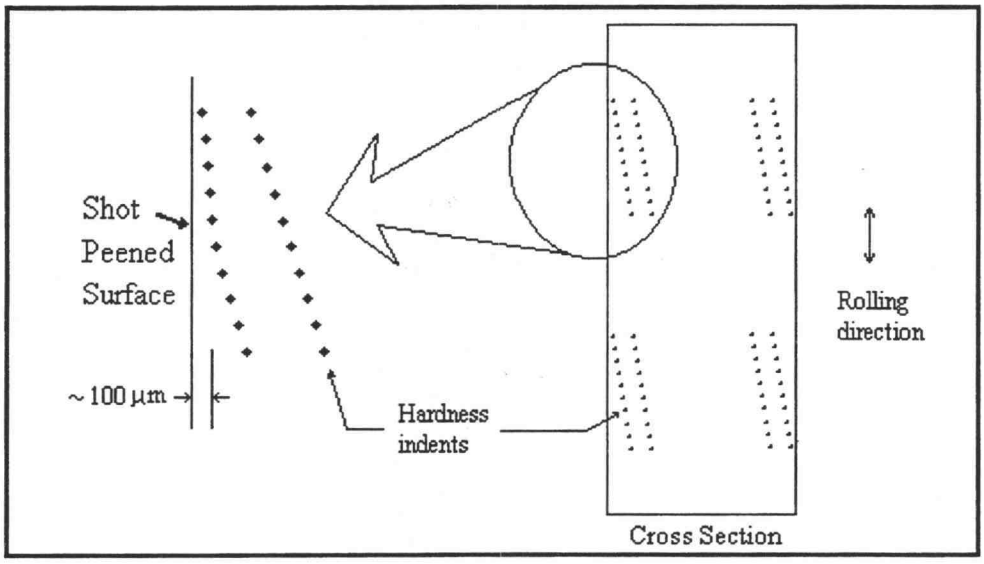

Figure 4 Hardness indentation orientation

Following hardness measurements for the initial hardness profiles, the samples were photographed under polarized light using color Polaroid film at 51.3X and 100X magnifications. The higher magnification was used to determine the depth of the mechanically twinned (known damage) layer with respect to the hardness indentations to ensure that the profile extended beyond the twinned region. The higher magnification was also used to determine if any new grain nucleation occurred after heat treatments. After the initial hardness profiles were completed, all photo-micrographs of subsequent hardness profiles used bright field and 51.3X magnification because it was not practical (the time of exposure was excessively long under the dim polarized light) to take a large number of photographs using polarized light. Distances from the edge were measured to the center of each hardness indentation and a plot was developed of the Vickers hardness values versus the distance from the shot-peened surface.

Three steps were taken to eliminate variations of the hardness measurements due to inhomogeneity within the sample or variations in the sample preparation and/or hardness testing equipment. First, as can be noted in Figure 4, a total of four hardness profiles were developed on each sample. These profiles were combined to form a single profile in order to eliminate possible scatter due to variations with the location within the sample. Since profiles were combined from both sides of the sample, the possibility of incidental scatter (due to changes in shot peening conditions rather than actual changes in hardness due to heat treatment) was further reduced as both sides of the plate were shot-peened independently. Second, three samples, extracted from different sections of the test plate (see Figure 2), were profiled as outlined above and the resulting profiles were combined for a single complete hardness profile. This yielded a final combined hardness profile consisting of twelve profiles for a given heat treatment temperature and time. A best fit curve (3rd order polynomial) was formulated for the initial, or non-heat treated zirconium. This was compared to data measured after 200 and 300°C thermal treatments

for various times. As a third precaution, a control sample (un-heat treated) was polished and profiled along with each set of heat treated samples and this sample was compared to the initial pre-heat treatment profiles. This step was necessary to ensure that some variation did not occur in the polishing procedure or hardness testing apparatus between profile sets.

A set of hardness profiles was developed, as outlined above, for six samples in the initial, or pre-heat treated, condition. Three of these samples (AA1, BB1, CC1) were then used for 200°C testing and three (AA2, BB2, CC2) for 300°C testing. Hardness profiles were developed again after each specified heat treatment time and temperature and these were compared to the initial profiles to determine if any changes (e.g. decrease) in hardness occurred.

The baseline hardness of zirconium varies substantially with composition changes. This was illustrated by Bailey [21] who measured the effect of oxygen and nitrogen on the hardness of commercial grade and zirconium crystals. Bailey found that the hardness for commercial grade zirconium with about 0.1 wt % of oxygen and nitrogen had a hardness of 185 ± 5 VHN while higher purity (~0.03 wt % oxygen and nitrogen) had a much lower hardness of 100 ± 3 VHN. This would indicate that direct comparison between experiments [e.g. by different investigators where small changes in composition (often not reported) can exist] may be less useful than relative changes in hardness within an experiment with zirconium from a given production heat (fixed composition).

Analyses of Hardness Data

A third order polynomial curve fit was performed on each hardness profile. Third order was chosen for the consistency of shape that resulted, which could not be obtained using higher order polynomials, over the shot peened damage depth. The bulk portion (beyond the shot peened damage) was fit with a straight line not obtainable from the polynomial fit. One might argue that the polynomial may not accurately characterize the hardness trend in the region nearest the

shot peened surface (≤ ~30 μm) as there were no hardness measurements inside this region, however this extrapolation allowed a reasonable measurement of the changes in hardness at the surface. Also, the absolute hardness at the surface of the sample is not as important as relative changes in the hardness at the surface because, as mentioned above, the hardness of zirconium can vary a great deal from one investigation to another. The consistency using a polynomial description was superior to "hand fitting".

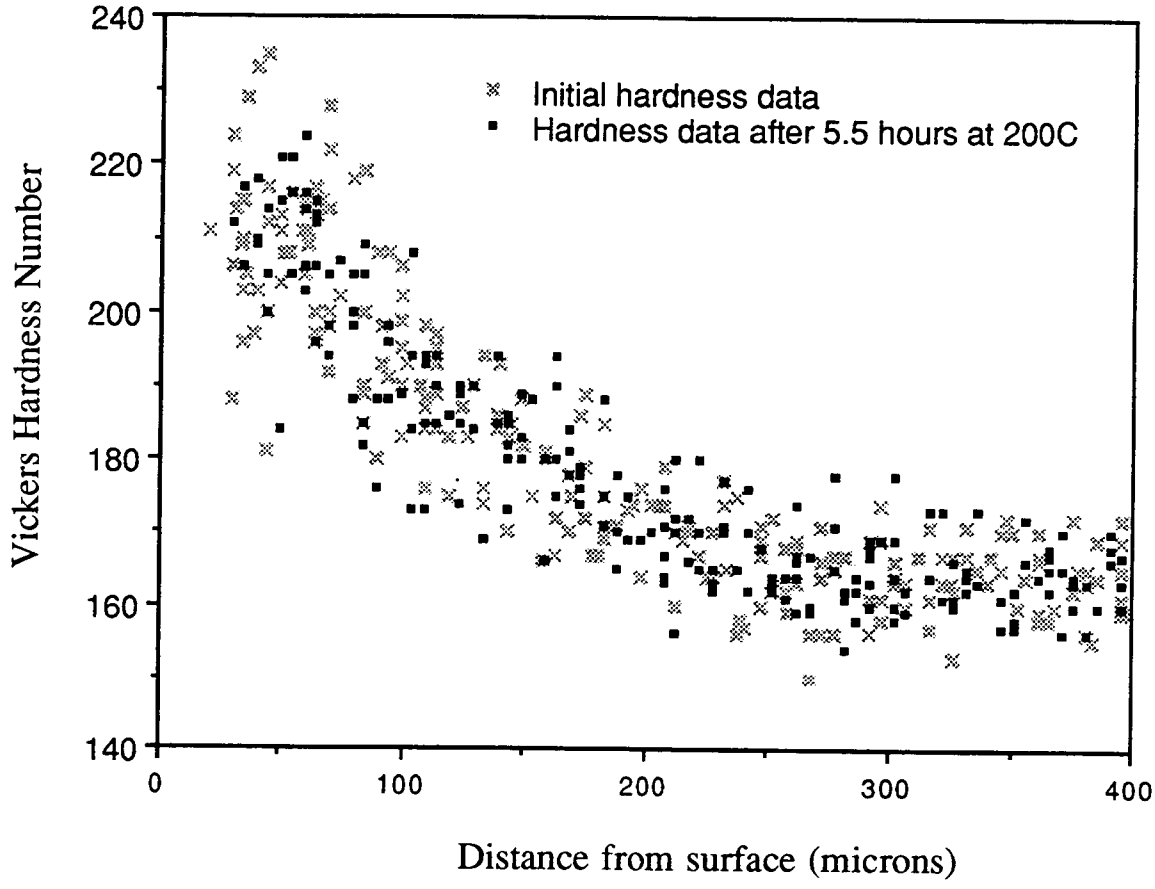

Figure 5 Comparison of hardness measurements for the initial shot peened condition and after 5.5 hours at 200°C

Each (combined) hardness profile formed a fairly distinct trend but also a scatter band. Subtle changes in the hardness profiles were sometimes difficult

to detect due to this scatter. It was noted, by comparing hardness profiles visually, that, although the curve fit after the first few 200°C heat treatments (0.5, 5, 50 hrs) appeared to coincide with the initial profiles, a few of the maximum hardness values appearing for the non-heat treated specimens near the surface were absent in the annealed zirconium (see Figure 5 above). This indicated that the hardness near the surface had possibly decreased slightly. This change was not illustrated by the polynomial curves because the majority of the data were coincident, so the small number of "absent" high hardness points near the surface had little effect on the curves. To evaluate this possible decrease, the number of points above certain hardness values (200, 210, and 220 VHN) was recorded for each profile for all data less than 150 μm from the surface. The hardness values of 200, 210, and 220 VHN were chosen because they appeared to span the general range of hardness for the nearest 150 μm of the surface in the initial hardness profile. Because the number of data points within 150 μm varied between samples (ranging from 80 to 110 points), the absolute number of points above a given value was converted to a percentage of the total number of data points within 150 μm. The initial hardness profiles developed from samples AA1, BB1, CC1, AA2, BB2, and CC2 were combined with all control sample AA3 profiles (purpose of AA3 is explained in next section) to make a single initial profile for this analysis. If the hardness profile for a set of samples was re-measured for verification of results (after the first major changes in a hardness profile were noted for a given temperature), only the first profile developed was used in the analysis of the hardness distribution within 150 μm of the surface. The re-profiles were not used because they had a higher distribution of points very close to the shot-peened surface (nearest 75 μm) to verify that this region had actually experienced a decrease in hardness. Because of this skewed distribution near the surface, the analysis of the percentage of hardness measurements above a given value within 150 μm of the surface would also be skewed toward higher numbers, and give results that were not consistent with

other specimens of the analysis. The results of this analysis are plotted in Figure 16 in the results section.

Developing a Profiling Technique

In determining a hardness, the most repeatable obtainable hardness value uses the highest possible force on the hardness indenter [22], because it averages the hardness over a larger area and a greater number of grains (zirconium is very plastically anisotropic, so hardness can vary a great deal with grain orientation because slip occurs primarily along the prism planes). It has been shown that the DPH (VHN) hardness decreases with increasing load [23]. The scatter associated with multiple hardness tests also decreases with increasing loads indicated the largest possible load should be used. However, the larger indentations created from larger loads must be positioned further from the shot-peened edge to avoid surface effects as described above.

The first attempt at developing a hardness profile used a 100 gf load, but significant scatter (see Appendix B) in the data led to the application of a larger load. A large variation could be detrimental to the outcome of the experiment since small changes in the average hardness could be obscured. Profiles were also developed using 300 and 500 gf loads, and the data are shown in Appendix B. As the load force was increased, the scatter tended to decrease, but the distance between the shot-peened surface and the first VHN indentation increased. This minimum distance was determined by the point where the hardness dropped to an excessively low hardness (outside of the normal scatter apparent in the remainder of the hardness profile) as a result of surface effects (discussed previously). As a compromise, one profile used a 100 gf load for the first 40 μm from the surface, a 300 gf between 40 and 110 μm, a 500 gf load between 110 and 400 μm, and a 1000 gf load beyond 400 μm of the surface. Although using a "graduated" profiling technique seemed to alleviate some of the problems of scattered hardness values for interior regions, significant scatter

near the surface persisted, although measurements relatively close (25 μm) to the shot-peened surface were possible. A concern also arose whether the different loads would give different hardness values in the same region as was suggested by Chubb et al. [23]. To verify (for the current experimental conditions) the results reported by Chubb et al., the variation of hardness with loading force was tested in the interior region of a sample by averaging a large number of tests at various loads. It was found that as the load increased, the observed hardness value decreased (from 175 with a 100 gf load to 162 with a 1000 gf load). This is consistent with the results presented by Chubb et al. [23]. The reason for the reduction in apparent hardness with larger loads is unclear.

It was noted that using a 300 gf load allowed profiling almost as close to the surface as the 100 gf load and yielded much more consistent results. Extensive tests were performed using a 300 gf load and the hardness profiles developed appeared to have modest scatter. These profiles were also relatively reproducible between samples and locations within a sample. As a result, the final hardness profiling procedure in this study utilized a 300 gf load.

Heat Treatment

A cylinder furnace was-fabricated by Zircar Corporation specifically for 200 - 300°C heat treatments. The furnace used zirconia insulation with a Sigma MDC4E temperature controller and was capable of maintaining a temperature variation of less than 1°C at either 200 or 300°C (over 500 hours at 200°C, one point was recorded at 199°C while recording data every 5 minutes with a Fluke Data Acquisition unit with 1°C resolution).

A thermocouple was spot welded to a sample of zirconium of similar size to the actual samples being studied in order that an accurate record of the temperature could be obtained. The samples to be heat treated were then tied on to this sample using chromel wire. The thermocouple could not be wired

directly to the actual specimens because of the temperatures associated with spot welding as well as the damage associated with welding. Soldering the wire to the samples was not an option because, even if low temperatures were maintained, the solder would not adhere to the zirconium surface.

The first heat treatment cycle for samples AA1, BB1, and CC1 was 0.5 hours at 200°C. This and subsequent time-temperature (TT) curves are illustrated in Appendix A. The temperature was measured using a Fluke Data Acquisition System and recorded on a computer using LabView at one minute intervals throughout the heat treatment. The samples were air cooled on a porous ceramic brick after heat treatment. All samples were re-polished and new hardness profiles were developed. The same samples were then treated at 200°C for 5 hrs, 50 hrs, 504 hrs, 1684 hrs, and 2214 hrs (cumulative time of 4458 hours), hardness profiling after each heat treatment. Again, the temperatures were recorded by a computer throughout the heat treatments (with larger time increments between recorded points for longer heat treatments to simplify data processing). Samples AA2, BB2, and CC2 were similarly treated at 300°C for 0.5 hrs, 5 hrs, 50 hrs, 502 hrs, and 2233 hrs (cumulative time of 2790 hours), re-polishing and determining hardness profiles after each heat treatment. The TT profiles for each heat treatment are in Appendix A.

Upon determination of the first distinct change in the hardness profiles of a set of samples at a given temperature and time, the samples were re-polished and re-profiled together with a control sample AA3 (remaining in initial pre-heat treated condition). The un-heat treated control sample AA3 with an established hardness profile was polished with the heat treated samples to ensure that the observed changes in hardness in the heat treated specimens were not just due to variation in the sample preparation procedure. The profile obtained from sample AA3 was compared to the initial profiles to ensure consistency in procedure. The non-heat treated control sample AA3 was polished after each subsequent heat treatment of the samples AA1, BB1, CC1, AA2, BB2, and CC2. Control specimen AA3 hardness profiling was performed only in those cases

where heat treatments appeared to result in hardness decreases from the initial pre-annealed hardness profile.

Oxygen Effects

As mentioned previously, the effects of oxygen on the hardness of zirconium were studied by Bailey [21]. Bailey observed that commercial grade zirconium with about 0.1 wt % of oxygen and nitrogen had a hardness of 185 ± 5 VHN while higher purity (~0.03 wt % oxygen and nitrogen) had a much lower hardness of 100 ± 3 VHN. This raised some concern with longer air annealing because the solubility of oxygen in zirconium is about 30 at. percent at the temperatures used in this study. If a significant amount of oxygen diffused into the samples, the softening due to recovery could be countered by an increase in hardness due to the absorbed oxygen. Although the effects of oxygen could have been minimized by vacuum annealing, annealing in ambient air was still performed since this is the service condition that the shot peened plates would actually experience. The difference in hardness as a function of oxygen content was also investigated by Sauby et al. [24] for Zircaloy-2. The diffusion rate of oxygen in annealed, polycrystalline bulk zirconium is about 3.22×10^{-21} and 2.58×10^{-19} m^2sec^{-1} at 200°C and 300°C respectively (interpolated from reference 25) and is enhanced due to cold work in the present study as will be discussed subsequently.

Oxidation Mechanism

It has been shown in previous work [26,27] that oxidation of zirconium proceeds in three stages at temperatures between ambient temperature and 327°C. The first involves absorption of oxygen up to the maximum solubility limit of about 30 atomic (at) % (α-Zr(O) formation). The second stage is the

precipitation and development of ZrO_2 at the surface of the zirconium. The final stage is the growth of the oxide layer. It has been shown [27] that the growth of ZrO_2 occurs away from the surface as a result of oxygen diffusion, rather than diffusion of Zr to the surface. An oxidation growth model at temperatures below about 330°C is not clear. The oxide growth rate has been modeled to fit experimental data at low temperatures (up to about 400°C) as a cubic rate law [28,29], a parabolic rate law [30], and a logarithmic rate law [31]. These observations of apparently different oxide growth models may be the result of experimental conditions such as sample preparation, sample purity, and variations of temperature during oxidation [32]. A parabolic model was adopted here because our concern was only to calculate an approximate oxide thickness and significant oxygen penetration depths, and the above variations in oxide growth rate appeared to be within one order of magnitude [33]. A more accurate model was not necessary for the current study because the purpose of these calculations was to determine if oxygen diffusion depths were on the order of the distances from the surface at which hardness measurements were performed.

Estimate of Diffusion Coefficients

The diffusion coefficients for oxygen in ZrO_2 and Zr(O) were determined and are shown in Table 5 below for previous work [26]. The parentheses in Zr(O) shown in the table are simply a convention used in the literature to indicate the region in the zirconium where oxygen is completely soluble and has not yet formed ZrO_2.

Temperature (K)	D in α-Zr(O) (m^2/s)	D in ZrO_2 (m^2/s)
320	2×10^{-23}	3×10^{-24}
420	3×10^{-22}	3×10^{-23}
530	4×10^{-21}	5×10^{-22}

Table 5 Oxygen diffusion coefficient in α-Zr(O) and ZrO_2 [26]

An approximate value for diffusion in ZrO_2 at 200°C and 300°C (current experimental conditions) was calculated with a diffusion equation derived using previous experimental data as follows. First,

$$\ln D = \ln D_o - Q_d/R\ (1/T) \qquad \textbf{(1)}$$

where $\mathbf{D_o}$ is a temperature independent constant, $\mathbf{Q_d}$ is activation energy for diffusion, **R** is the ideal gas constant and **T** is the absolute temperature. Using the data in Table 5 above, average $\mathbf{D_o}$ and $\mathbf{Q_d}$ values of 1.55×10^{-18} m^2/sec and 35.8 kJ/mol, respectively, were calculated. The resulting diffusion coefficient equation for diffusion of oxygen in ZrO_2 is

$$D_{ZrO_2} = 1.55 \times 10^{-18} \exp [(-35.8\ kJ/mol) / RT]\ m^2/sec \qquad \textbf{(2)}$$

over the temperature range used in this experiment (200 to 300°C). Using the same method and the data in Table 5, the equation 3 was determined for the diffusion of oxygen in Zr(O).

$$D_{Zr(O)} = 1.47 \times 10^{-17} \exp [(-36.5\ kJ/mol) / RT]\ m^2/sec \qquad \textbf{(3)}$$

The same analysis was applied to oxygen diffusion in bulk zirconium to determine equation 4 using data from reference 25.

$$D_{Zr} = 2.61 \times 10^{-10} \exp [(-98.8 \text{ kJ/mol}) / RT] \text{ m}^2/\text{sec} \qquad \textbf{(4)}$$

Solving equation 2 gives a value for $D_{200°C}$ in ZrO_2 of 1.72×10^{-22} m^2/s. Similarly, $D_{300°C}$ is found to be 8.44×10^{-22} m^2/s for oxygen in ZrO_2. The values of $D_{200°C}$ and $D_{300°C}$ in Zr(O) calculated from equation 3 are 1.38×10^{-21} and 6.96×10^{-21} respectively. Diffusion coefficients for oxygen in bulk zirconium calculated from equation 4 are 3.22×10^{-21} and 2.58×10^{-19} for 200°C and 300°C, respectively. Diffusion in zirconium is, obviously, somewhat faster for lower concentrations than diffusion through the nearly 30 at. % oxygen present in Zr(O) regions because more interstitial diffusion sites are occupied. This has been simplified assuming a constant diffusion coefficient through Zr(O) and a higher (constant) diffusion coefficient through zirconium of a lower oxygen concentration. There is, however, another factor that must be considered when analyzing diffusion through the Zr(O) and Zr regions and this is discussed subsequently.

Deformation Effects

As was discussed previously, the surface of the zirconium was shot peened, resulting in a severely plastically deformed surface region. The dislocation density increases significantly as a result of this deformation at ambient temperature, or cold work. Having a high dislocation density can lead to "short circuit" diffusion, which yields a higher diffusion coefficient than would be expected in bulk, annealed material. In this case "short circuit" diffusion involves diffusion along dislocation lines where the lattice is distorted perhaps

creating more "room" for diffusing atoms. Dislocation pipe diffusion effect can dominate at lower temperatures.

"Short circuit" diffusion would effect the diffusion coefficient in the Zr(O) and Zr regions. The dislocation density in ZrO_2 is presumed to be low and short circuit diffusion is not expected to occur in this region.

The magnitude of increase in the diffusion coefficient via dislocation pipes can be calculated following the analysis presented in reference 34, where the following equation for the apparent diffusion coefficient is given:

$$D = D_p g + D_L(1-g) \qquad (5)$$

where **D** is the apparent diffusion coefficient, $\mathbf{D_p}$ is the pipe diffusion coefficient, $\mathbf{D_L}$ is the lattice diffusion coefficient and **g** is ratio of time spent on the high diffusivity zone around the dislocation core to time spent in the bulk lattice. The equation for **g** can be described by:

$$g = C\rho \qquad (6)$$

where **C** is a constant and ρ is the dislocation density. The ratio of $\mathbf{D_p g}$ to $\mathbf{D_L}$ was calculated [34] for silver and appears in Table 6 for a dislocation density of $10^8/cm^2$.

$\mathbf{D_p g / D_L}$	**Temperature (°C)**	$\mathbf{T / T_m}$
0.08	590	0.7
0.90	465	0.6
27	345	0.5
4500	220	0.4

Table 6 Values of at various temperatures for Ag [34]

Assuming that zirconium diffusivity trends are similar to silver, at the temperatures of concern (T/T_m = 0.26 and 0.31 for 200°C and 300°C respectively), the ratio of $\mathbf{D_p g}$ to $\mathbf{D_L}$ should be very large. The term $\mathbf{D_L(1-g)}$ can then be neglected and the result is

$$D \approx D_p g \qquad (7)$$

Because **g** is proportional to ρ, the dislocation density, the following proportionality can be written.

$$D \propto \rho \qquad (8)$$

Typical increases in the dislocation density with severe cold working can be four orders of magnitude (from 10^8 /cm^2 to 10^{12} /cm^2). This is not an unreasonable increase in dislocation density as a result of shot peening where the engineering percentage cold work at the surface was about 99% (determined experimentally by a cold rolling/ hardness experiment which will be described later). Because the amount of cold work decreases dramatically with distance from the surface, it would be useful to consider an average dislocation density. If an average dislocation density of 10^{10} /cm^2 is used, then the short circuit diffusion analysis will yield a first order approximation of diffusion through the damaged surface region. Applying the above analysis with a change in dislocation density of two orders of magnitude due to dislocation short circuit diffusion, the diffusion coefficients of oxygen in Zr(O) (30 at. % O) increase from 1.38×10^{-21} and 6.96×10^{-21} to 1.38×10^{-19} and 6.96×10^{-19} m^2/s at 200 and 300°C respectively. Similarly, the diffusion coefficients in bulk (low oxygen concentration) zirconium increase from 3.22×10^{-21} and 2.58×10^{-19} to 3.22×10^{-19} and 2.58×10^{-17} for 200°C and 300°C respectively. The above assumptions are conservative and imply that any prediction of low oxygen diffusivity is reliable.

Depth Calculations

Using a parabolic model,

$$d^2 \approx D\,t \qquad (9)$$

where **d** is the diffusion depth, **D** is the diffusion coefficient and **t** is time. Solving for **d** (diffusion depth) using 4458 and 2790 hours for 200°C and 300°C respectively (cumulative heat treatment time) yields the following results.

$$d_{200°C\text{-}ZrO2} = [(1.72 \times 10^{-22}\ m^2/s)(16.03 \times 10^6\ s)]^{1/2} = 5.3 \times 10^{-8} = 0.05\ \mu m$$

$$d_{300°C\text{-}ZrO2} = [(8.44 \times 10^{-22}\ m^2/s)(10.04 \times 10^6\ s)]^{1/2} = 9.2 \times 10^{-8} = 0.09\ \mu m$$

This estimate may be slightly low based on the color of the zirconium samples after long term annealing. Both sets of samples (200 and 300°C annealing) were dark blue or gray-purple in appearance, roughly corresponding to at least a 4000 Å thickness [32] or 0.4 μm. This depth is still much smaller than the depths which are of concern in this study.

The same technique can be applied to determine the depth of the Zr(O) region using the "short circuit" diffusion coefficients. The results are as follows.

$$d_{200°C\text{-}Zr(O)} = [(1.38 \times 10^{-19}\ m^2/s)(16.03 \times 10^6\ s)]^{1/2} = 1.5 \times 10^{-6} = 1.5\ \mu m$$

$$d_{300°C\text{-}Zr(O)} = [(6.96 \times 10^{-19}\ m^2/s)(10.04 \times 10^6\ s)]^{1/2} = 2.6 \times 10^{-6} = 2.6\ \mu m$$

Because very small changes in the oxygen concentration may affect the hardness, a slightly different analysis was used that accounted for the small

concentration change. The concentration/diffusion coefficient relationship is given by

$$\frac{C_d - C_0}{C_s - C_0} = 1 - \mathrm{erf}\left(\frac{d}{2\sqrt{Dt}}\right) \qquad \textbf{(10)}$$

where $\mathbf{C_d}$ is the concentration at the depth **d**, $\mathbf{C_0}$ is the initial concentration and $\mathbf{C_s}$ is the surface concentration. For this analysis, the change in concentration of concern (concentration that may cause some appreciable change in hardness) was assumed to be 100 ppm (0.01 at.%). The initial concentration as given by Table 7 below (in a subsequent section) is 1350 ppm and the surface concentration was taken as 30 at. % O (approximately the maximum solubility limit of oxygen in zirconium). Equation 11 predicts

$$d \approx 5.2\,(D\,t)^{1/2} \qquad \textbf{(11)}$$

The following depths to which a change in oxygen concentration of 100 ppm occurred as a result of diffusion were calculated as:

$$d_{200^\circ C} = 5.2\,[(3.22 \times 10^{-19}\ m^2/s)(16.03 \times 10^6\ s)]^{1/2} = 12\ \mu m$$

$$d_{300^\circ C} = 5.2\,[(2.58 \times 10^{-17}\ m^2/s)(10.04 \times 10^6\ s)]^{1/2} = 84\ \mu m$$

Because these depths are on the order of the depths at which hardness testing is initially performed, and the analysis used some very crude assumptions, experimental confirmation of oxygen within the shot peened surface is appropriate.

Vacuum Annealing

A zirconium sample was removed from the same shot peened test plate and annealed in a vacuum furnace in order to determine if the softening effects that were realized upon annealing in air were affected by the absorption of oxygen (that would tend to independently increase the hardness). Annealing was performed in a Mellen three zone alumina insulated tube furnace evacuated by a Varian mechanical vane pump. Honeywell controllers maintained the 300°C temperature within ± 1°C. Pressure was monitored using a Hastings thermocouple vacuum gauge. Samples were wrapped in about 15 layers of zirconium foil to act as a "getter" for residual oxygen. The wrapped zirconium sample was then inserted into a stainless steel envelope with three welded sides to further protect the sample from any residual oxygen. The bag was hand pressed around the sample to eliminate the majority of air and then creased on the fourth side to seal the bag. Initially, the furnace was evacuated to 25 mTorr at ambient temperature. This vacuum was maintained for about 12 hours to allow for outgassing of absorbed water vapor and other gasses from the sample or furnace walls before the furnace was brought to the desired annealing temperature. The sample was then annealed at 300°C for 1.5 hours. An annealing time of 1.5 hours was chosen because the exact heat up time for the sample is not known (see below). The sample was allowed to anneal longer to be sure that it spent at least 0.5 hours at 300°C. This time and temperature were chosen because a significant drop in hardness was observed after 0.5 hours at 300°C in air.

In order to determine the heat up time, a dummy zirconium sample was inserted into the furnace with a thermocouple attached to it. The thermocouple wire was fed through a rubber cork which was then used to plug a bleed through hole in one of the stainless steel end caps to the furnace (plates that sealed the vacuum tube) and sealed with hot glue and high vacuum grease. A vacuum of 57 mTorr was attained and, after outgassing for 2 hours, the furnace was

allowed to heat up and the temperature was recorded using a Fluke linked to LabView on a Macintosh computer. Although the vacuum achieved was not quite as good (normally a solid plate was used for the end cap), this experiment yielded a good estimate of the time necessary to heat the sample to 300°C. Using this method, a heating time of 60 minutes was measured.

Superior vacuum testing may have been achieved by enclosing the samples in evacuated quartz tubes. Unfortunately, the facilities were not readily available at OSU. The samples enclosed by Teledyne specifically for the present study were not useable because a piece of zirconium (sponge) was also enclosed with the sample, separated from the sample by a smaller diameter glass tube. This sponge was intended to effectively absorb oxygen once the quartz tube was sealed. Unfortunately, the zirconium sponge contained a substantial amount of absorbed water vapor and other impurities that were released when heated. The evacuated tubes were thus unusable.

The vacuum annealing performed in the vacuum furnace appeared to effectively minimize oxidation of the surface of the zirconium specimen. The outermost layers of the zirconium foil wrapping appeared to be slightly golden with respect to its natural color, while the innermost layers appeared visually the same as the original foil. This indicates that a slight oxide (much less than in air) was developed. Oxidation of zirconium proceeds through various interference colors, gold being the first or thinnest oxide. The sample surface was also very slightly yellow in appearance when compared to a non-heat treated sample. The thickness of the oxide is not easily determined from the color without an in depth analysis of the refractive index of the material and measuring the phase change occurring in reflections from the surface. Douglass et al. [32], however, attempted to measure a range of oxide thickness' over the interference color regime for oxidation in air at 250 to 450°C. The minimum thickness Douglass et al. estimated (roughly corresponding to the initial gold color) was about 100 Å. The maximum thickness that could be examined (under TEM) by Douglass et al. was estimated to be about 4000 Å and corresponded to a gray purple surface

color. Although this does not give an exact thickness, it indicates that very little oxidation (on the order of 100 Å) occurred in the sample vacuum annealed in this study.

Quantification of Cold Work Induced by Shot Peening

Previous studies on the effect of thermal heat treatment on deformed zirconium was only relevant to uniformly cold worked zirconium. The equivalent amount of cold work associated with shot peening needed to be quantified as a function of depth from the shot-peened surface. This would allow comparisons to be made with other studies to determine if shot peened specimens respond to thermal exposure consistently with similarly deformed zirconium. Characterizing the amount of cold work induced by the shot peening would also allow more usability of the thermal stability results and over a much broader range of cold work than is currently available for low temperatures.

A single level (single set of rollers) cold rolling mill was utilized to cold work a zirconium plate over a range from approximately 3% to 57%. Ideally, the rolling reductions would have continued to higher level of cold work, but the cold rolling mill could not achieve any further reductions (rollers on the mill were in contact with each other prior to the last two rolling passes, but deflected around the sample due to the fact that the rolling mill was not rigid). A new (not surface treated) zirconium 702 plate was used for this purpose. Using a new plate for the study was chosen over the following options. The surface treated samples could have been annealed at 790°C (alpha HCP phase) to restore the dislocation density through recrystallization, but the grain structure may change, possibly changing the cold working response. A second option included annealing at 1000°C (in the BCC β regime) in a vacuum furnace, but this can result in a β texture that cannot be eliminated without significant deformation at intermediate temperatures and dynamic recrystallization or warm working in the

α regime. Warm working would be necessary because without the extra strain energy added by deformation at low or moderate temperatures, recrystallization in the α region, to the extent where the β texture is eliminated, is extremely slow, even at temperatures approaching 862°C (alpha to beta transition at 862°C [14]). A texture similar to that of the original shot peened specimen is desirable for accurate results, as zirconium is very anisotropic and the hardness profiles of a given cold work level or surface treatment may significantly change with texture. Because the above options were not feasible, another zirconium 702 plate fabricated under the same conditions (without any surface treatment) was used. Using a new plate, however, was still not an ideal solution, as the (new) plate used for this part of the study was manufactured at a different time and the plate production procedure could vary somewhat, leading to a slightly different texture. The date of manufacture of the new plate and spectrographic analysis [35] (see Table 7 below) indicated that the plate used for the cold work study was probably manufactured from the same ingot as the plate used for the shot-peening/ heat treatment study. The level of impurities for all of the observed elements from both plates was practically identical except Ti which varied from 62 ppm to 250 ppm between plates and this variation may have been due to compositional variations throughout the ingot. The exact verification of the ingot from which the two plates were produced was not possible due to incomplete records. The texture and hardness of the new plate were also compared with the bulk region of the shot peened specimens to ensure that the material was relatively similar. The specimens were compared under 200X magnification and polarized light for any gross texture differences. Although this technique is marginal, it still allowed some comparison of preferred orientation, as it would appear as a dis-proportional percentage of a particular color grain under polarized light. As shown in Figure 6, the texture appeared to be fairly consistent with respect to grain orientation. Grain sizes of the plate for the cold rolling study and the shot peened plates were not consistent (new plate had a

grain size of about 3-4 times larger than the bulk of the shot peened plate), although the effect of this may be relatively minor and will be discussed below.

Specimens→	Shot Peened	Cold Rolled	Tensile
C	136 (ppm)	98	117
Fe	1110	1150	1150
H	10	5	5
N	56	47	41
NB	70	64	67
O	1370	1370	1350
Ti	62	250	260

Table 7 Compositions of zirconium 702 specimens [35]

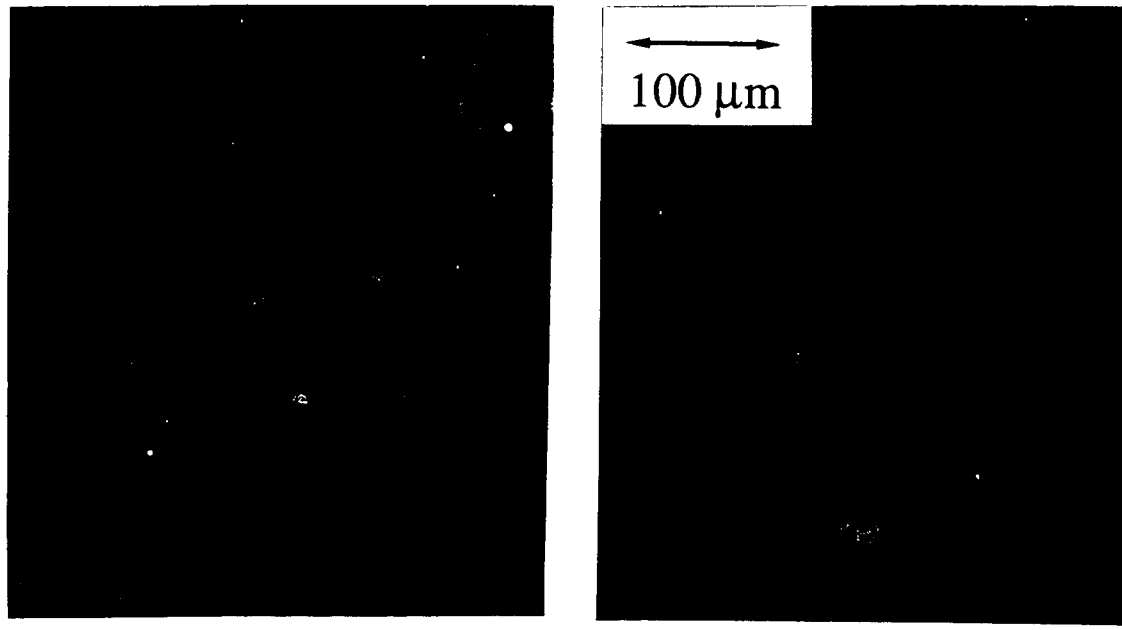

(a) (b)

Figure 6 Comparison of grains for zirconium plates used for a) shot peening/ thermal heat treatment study and b) cold work study

Cold rolling procedure

The un-peened plate (DD) used in this cold work study was approximately 250 mm long (rolling or longitudinal direction) by 180 mm wide and had an original thickness of 4.91 mm. The 4.91 mm thickness was obtained by averaging numerous points across the surface of a 2.5 cm by 18 cm strip that was sheared off with a metal shear press prior to any cold rolling operations. The plate was cold rolled according to Table 8, shearing off a 2.5 cm by 6.5 cm strip with a metal shear after each rolling step.

Thickness (mm)	4.91	4.74	4.54	4.09	3.62	3.18	2.73	2.33	2.13
% Reduction (cw)	0	3.4	7.5	16.7	26.2	35.3	44.3	52.6	56.7

Note: All reduced dimensions in this table are approximate because the surface thickness subsequent to rolling varied across the plate by about ± 0.05 mm.

Table 8 Rolling dimensions after cold reduction of the plate DD used for the cold work study

Determining a baseline hardness value for the cold work study

A baseline hardness of a fully annealed sample from the plate DD was determined before hardness studies were conducted on the cold rolled zirconium plate DD. The small amount of "equivalent residual cold work" resulting from plate production of the as fabricated (pre-cold rolled) plate DD was then approximated by comparing the as-fabricated hardness to the fully annealed hardness. A 2.5 cm by 18 cm strip of plate DD (pre-cold rolled condition) was cut into thirds using a water cooled silicon carbide abrasive cutoff wheel to

determine the baseline hardness. One of the three pieces was set aside in the as-fabricated state. The second of the three pieces was annealed at 790 °C for 1 hour and air cooled. The third of the three samples was annealed at 790 °C for 24 hrs. The two annealed specimens allowed a determination of the unworked hardness of the plate DD while the third specimen was used for an as-fabricated hardness, allowing the approximate determination of the as-fabricated "equivalent" percent cold work. There was no further softening of the zirconium after the 1 hr anneal as will be discussed later.

Three samples were similarly cut out of the shot peened test plate BB (same plate from which specimens were removed for the shot-peened/ thermal stability study) to compare with the plate DD for general texture (grain orientation as observed under polarized light) and hardness consistency for the as-fabricated and fully annealed conditions. One of the three BB samples was set aside to serve as the as-fabricated/ shot-peened, non-annealed condition. As with the DD samples, the second of the three BB samples was annealed for 1 hr at 790 °C and the third for 24 hrs at 790 °C and air cooled. These six samples (one sample from BB plate and one from DD plate in the as-fabricated, 1 hr annealed, and 24 hr annealed condition) were then etched and hardness values were determined as will be discussed subsequently.

Hardness characterization

Two samples (approximately 13 mm by 5 mm by 5 mm) were cut out of each of the as-fabricated, 1 hr annealed and 24 hr annealed plates, BB and DD, discussed previously. One of the samples was removed in the longitudinal orientation and the other in the transverse orientation with respect to the rolling direction during fabrication (see Figure 7a) so that the long dimension of the extracted samples were parallel to these orientations. Two samples were similarly removed from each of the cold rolled strips, with the longitudinal direction being parallel to the cold rolling direction (which was consistent with

the fabrication rolling direction). This resulted in a total of 28 specimens (14 longitudinal, 14 transverse). Each sample thickness was measured and recorded so that the cold work could be calculated. The samples were removed from the middle of the each strip, away from the leading edge (see Figure 7b), as this edge was more deformed due to the nature of the rolling operation (leading edge is sloped from entering the two rollers as the rollers are "pushed apart". The two orientations were used so that the cold work versus hardness plots could be reasonably compared since cold work versus hardness trends may change for transverse and longitudinal directions. In order to characterize a third orientation (plane parallel to rolling planes), the samples were acid etched from the top face to the middle of the sample so that hardness could be tested in a similar region of the rolled zirconium as was tested in the other orientations (see Figure 7c). It was important to perform hardness tests in a similar region of each sample because the amount of cold work may be different near the outer surface of the plate than in the interior. In order to reach the middle of the sample in this third orientation, nearly half of the thickness of the sample would have to be removed to reach a common region of the sample examined in the other orientations. This took an excessive amount of time, therefore, the orientation parallel to the rolling plane was not examined.

After the samples were removed, the desired cross sectional surface was etched in a 45 ml H_20, 45 ml HNO_3, and 10 ml HF solution until approximately 0.5 to 1.0 mm of material was removed from the surface. Removing such a large amount of material ensured that no surface damage from cutting was left on the material and the surface was smooth and uniform for hardness testing. The etchant was applied continuously using a cotton tipped applicator under a fume hood. As outlined previously, after about 15 seconds, the sample heated up to about 100°C and a violent reaction ensued. This reaction was necessary to remove large amounts of material in a relatively short amount of time (~5 minutes). Although the samples were allowed to heat to 100°C, the short time that the samples were exposed to this temperature (approximately 5 minutes)

had a negligible effect on the hardness (no noticeable decrease in hardness was experienced after 0.5 hours at 200°C in the current study). The samples were rinsed thoroughly with water, rinsed again with methanol alcohol and dried with forced heated air following etching. Each sample was then mounted in the Vickers hardness machine.

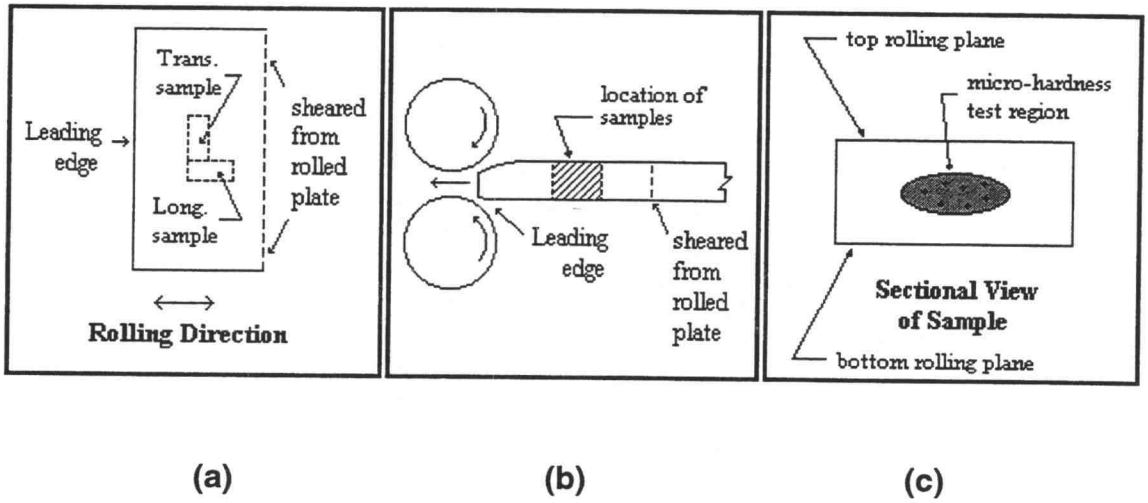

Figure 7 Sample configuration for cold rolling analysis; (a) transverse and longitudinal orientation; (b) sample location with respect to leading edge; (c) placement of hardness tests

Hardness tests were conducted at random locations in the interior region of each sample (Figure 7c) from the annealed, as-fabricated and cold rolled conditions, leaving at least 5 indenter widths between each test. These tests were performed using the same apparatus used for the developing hardness profiles of the shot peened specimens.

It was noted that the plate DD had an average grain size of about 3-4 times larger than that of the shot peened plate BB (see Figure 6). This had no apparent effect on the hardness indicating only a mild grain size strengthening effect. This was confirmed by determining a hardness value of about 165 VHN from a third plate with a third grain size between the two grain sizes just

discussed. Although the average hardness was consistent, the scatter was significantly higher from test to test on the larger grain size plate DD (+/- 25 VHN in the DD samples as opposed to +/- 10 VHN in the BB samples). This scatter may result from the fact that the indenter only contacts one or two grains when it strikes the surface of the larger grain size metal rather than possibly three or four with the smaller diameter grain size material. To compensate for this scatter, approximately 20 hardness tests were averaged for the DD specimens while only 10 tests were averaged for the original shot peened BB specimens used in this part of the study.

Plots were developed of hardness versus cold work for each orientation. The change in hardness that occurred as a result of the first two rolling reductions (3.4 and 7.5%) of plate DD was then compared to the difference in hardness between the annealed BB and DD specimens and the as-fabricated BB and DD specimens. Based on these comparisons, the equivalent amount of cold work present in the "as-fabricated" state was estimated. This value (percentage) was then added to the original thickness to determine a "new" (theoretical) original thickness (without the small amount of cold work present in the as-fabricated state). This "new" original thickness was used to calculate the cold work of each specimen after rolling. After new curves were developed (one for each orientation) based on the "new" original thickness, the process was iterated until a consistent curve was established. The results obtained from this hardness study are summarized in Table 9 and are plotted in Figure 19 in the results section. It was found that the data could best be approximated using a parabolic shaped function for each orientation (longitudinal and transverse to the rolling direction).

The longitudinal hardness versus cold work equation was then extrapolated to 99% cold work. The predicted values were compared to the hardness values at the surface of the shot peened specimens as determined from the hardness profiles. The longitudinal orientation was chosen because all of the hardness profiling of the shot peened samples was performed in the

longitudinal direction, or parallel to the plate production rolling direction. A cold work percentage was then assigned to each point along the best fit curve for the initial (pre-heat treatment) hardness profile of the shot peened specimens. From these values, a new curve was developed of cold work versus distance from the shot peened surface (Figure 20 in Results). The hardness values corresponding to a given percentage cold work allowed comparison of the present work, on the softening of shot peened surfaces with annealing, to the previous studies on recovery and recrystallization of zirconium.

Tensile Testing

Tensile tests were performed on three longitudinal and three transverse zirconium 702 flat tensile specimens on an Instron 4505 at OSU. A constant strain rate of 6.67×10^{-4} sec^{-1} was applied to the specimens. The specimens were cut from a 4.8 mm thick zirconium 702 plate according to Figure 8. Machining of samples was performed by Teledyne Wah Chang, Albany, Oregon.

These tensile tests were performed so that the shape of the true stress strain curve in the plastic regime could be compared to the hardness versus cold work curves developed in the cold rolling study. The shape of these curves should be generally consistent. Tensile testing also allowed determination of a yield strength/ hardness relationship. An approximate yield strength at the surface of the shot peened specimens was then determined to compare damage resistance with the currently available stainless steel press plates.

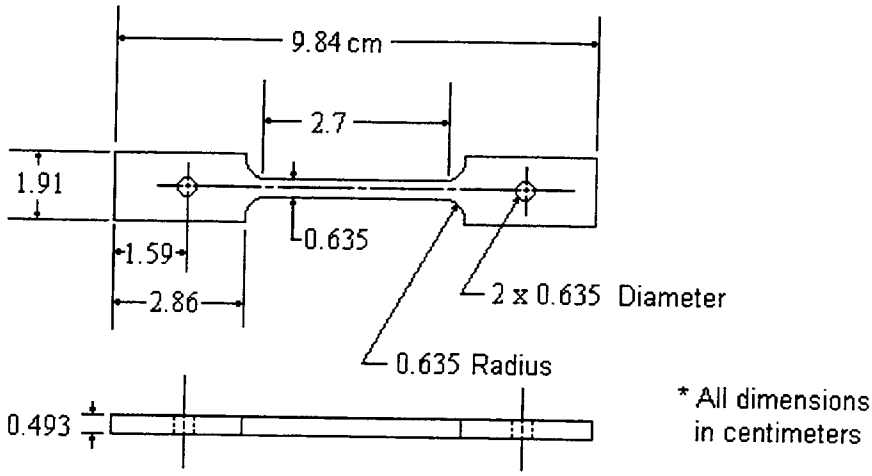

Figure 8 Flat zirconium tensile specimens [36]

Transmission Electron Microscopy

Transmission electron microscopy (TEM) was utilized in order to examine the dislocation microstructure of the heavily deformed surface region of the shot peened zirconium, and to observe changes after annealing. A slice of about 6.5 mm (parallel to the shot peened surface) was removed from each shot peened surface of the specimens using a low speed diamond saw using oil lubrication. Saw speeds from 120 to 280 rpm were maintained. The slice was then lapped down to 300 to 400 μm using wet 600 grit silicon carbide paper. TEM specimens were then removed from the slice using a 3 mm disk punch.

Each disk was electropolished to perforation using Fischione twin jet electropolishing unit with a solution of 5% perchloric acid, 5% methanol and 35% butoxy ethynol (butocelusol), 34 volts, 25 mA and a medium jet speed setting. Two jets of acid were applied to the sample, one on each side.

The diameter of the opening in the sample holder was 2.3 mm. For samples polished with both sides exposed, the area for current flow was 8.3 mm^2. This resulted in a current density of 3.0 mA per mm^2 for a typical current of

25 mA. Samples that were etched from one side only experienced an increase in the current density because the current did not change proportional to the area (area decreased by half while the current only decreased to 18 mA). While being polished on one side, these samples experienced a 4.3 mA per mm^2 current density.

Liquid nitrogen was used to keep the electrolytic polishing solution cool during polishing. The initial polishing temperature was approximately -25°C. This temperature increased to about -20°C over the duration of polishing one sample to perforation (around 3-5 minutes).

The samples were preferentially etched from one side of the specimen in order to examine varying depths from the shot peened surface to about 200 μm from the surface. For specimens close to the surface, the surface oxide on the shot peened surface (exposed surface during heat treatment) did not etch away as quickly as the freshly exposed side. After a period of etching using the oxide as a barrier, the surface oxide was removed by scraping the surface with the tip of the tweezers so that the oxide could be etched away and the desired depth of perforation could be achieved. The scraping of the oxide also allowed uniform perforation which did not occur if the oxide was left intact. In order to examine regions deeper in the sample, the oxide on the shot peened surface was lapped away using 600 grit silicon carbide paper and the opposite side was covered with plastic to protect it from the etchant. The plastic cover was removed after a certain amount of electropolishing so the desired depth of perforation could be achieved.

Most samples electropolished according to the above procedure resulted in a single perforation with enough electron transparent region to allow adequate TEM characterization. Many samples, however, resulted in multiple perforation with small electron transparent regions. For this reason, many samples were utilized so that adequate TEM imaging could be achieved for all of the desired depths.

The depth of the perforation from the shot peened surface was determined using an optical microscope with a micrometer on the vertical stage. The accuracy of this method was estimated to be about $\pm$ 5 μm.

Three foils with depths determined by this method were examined from the initial or pre-heat treated condition. The depths of these foils were 54, 62, and 118 μm. Two additional specimens were examined at approximate depths of 120 and 150 μm below the shot peened surface in the initial condition as well as three specimens at approximate depths of 40, 70, and 90 μm below the shot peened surface from a sample annealed for 0.5 hrs at 300°C. The depths on the last five specimens are only approximate because they were determined based on etching times assuming equal rates of etching from either side of the samples when no etch barrier was used. A more accurate determination using an optical microscope as described above was not possible as the samples were lost (misplaced) after TEM imaging. These foils were examined at 10,000 and 30,000X magnification on a JEOL JEM200CX (200 kV) transmission electron microscope at the National Center for Electron Microscopy at Lawrence Berkeley National Laboratory (LBNL).

Results

Thermal Stability Study

The initial hardness profiles (before annealing) determined for both sets of samples (AA1, BB1, CC1 for 200°C testing and AA2, BB2, CC2 for 300°C testing) dropped from about 230 - 240 VHN at the surface to about 165 VHN in the interior of the metal. The initial profiles developed for the pre-heat treated shot peened zirconium are illustrated in Figures 9 and 10 along with their respective 3rd order polynomial curve fit.

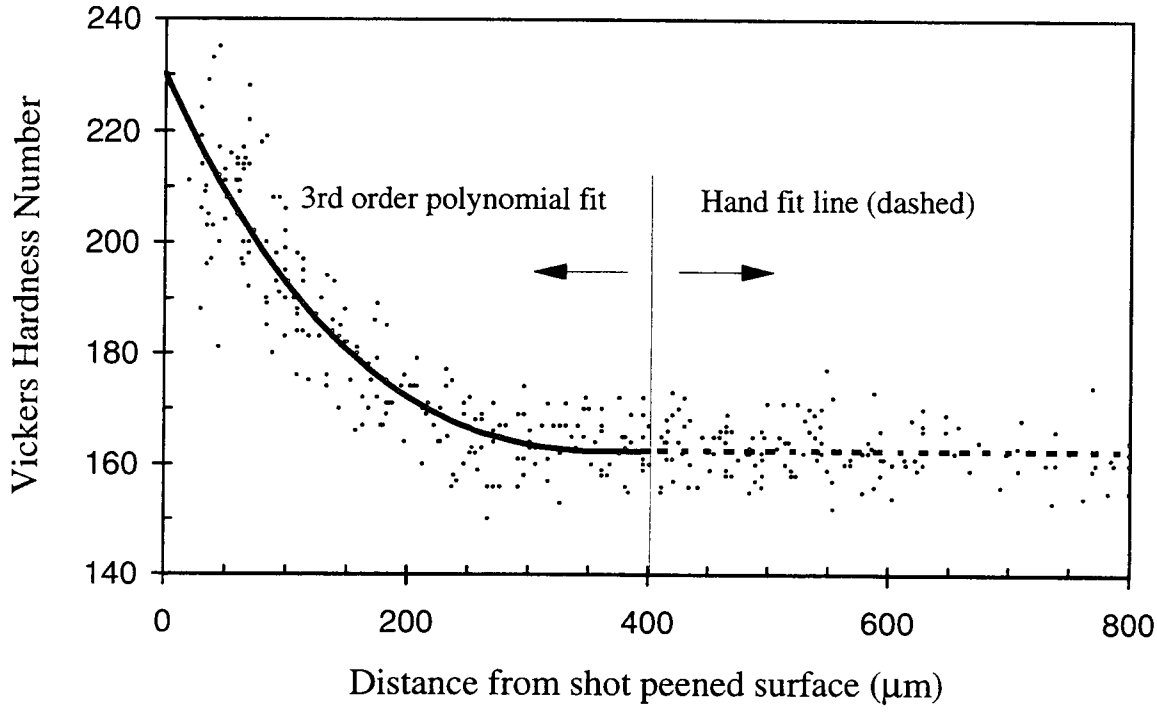

Figure 9 Initial hardness profile from samples AA1, BB1, CC1 later used for 200°C annealing

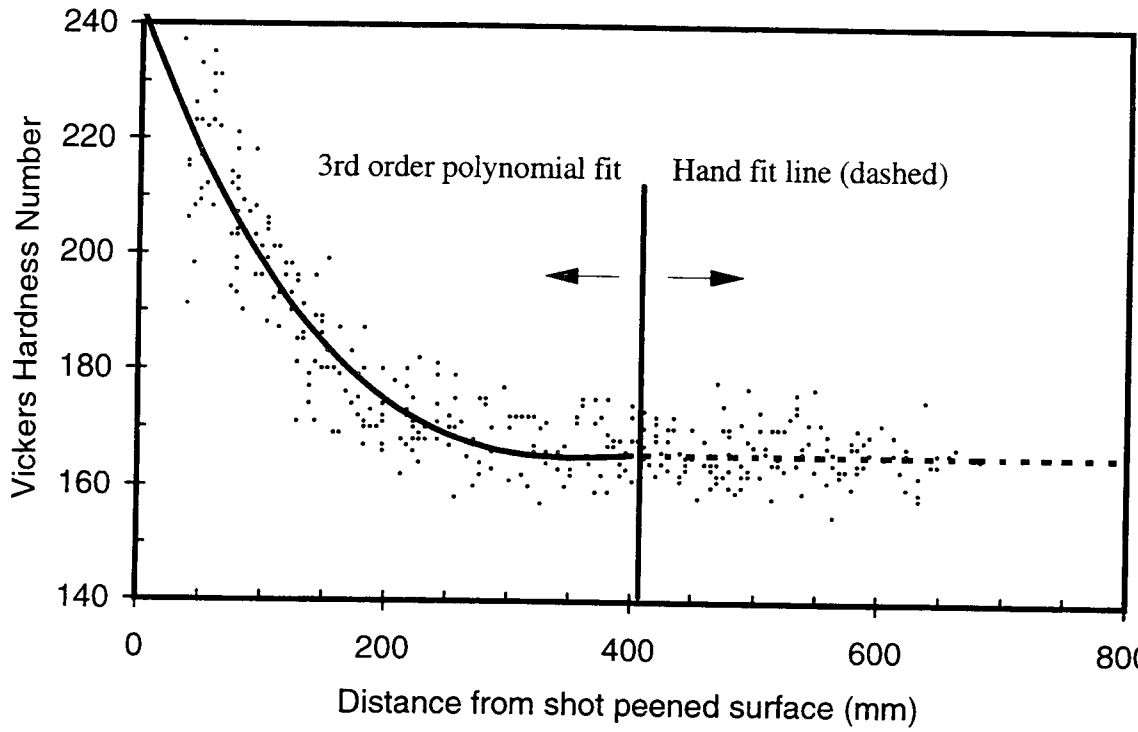

Figure 10 Initial hardness profile from samples AA2, BB2, CC2 later used for 300°C annealing

Each of the third order polynomial curve fits from the hardness profiles developed at 200°C after 0.5 hrs, 5 hrs and 50 hrs did not show a significant decrease in hardness from the initial profile shown above. The plotted data of these profiles appear in Appendix B, while the third order polynomial best fit curves from these plots appear in Figures 14 and 15 below. After 500 hrs, the hardness near the surface dropped noticeably. The "nose" of the curve, corresponding to the nearest 100 μm to the surface, seems to drop while the remainder of the curve remained essentially the same. The surface hardness from the best fit curve dropped from 230 VHN to 220 VHN. Similar results were observed after only 0.5 hrs at 300°C. The surface hardness dropped from 240 VHN to 217 VHN after 0.5 hrs at 300°C. These results, yet larger drops in hardness at the surface after longer annealing times, and the drop in hardness that occurred further away from the surface are plotted in Figures 11-15 below.

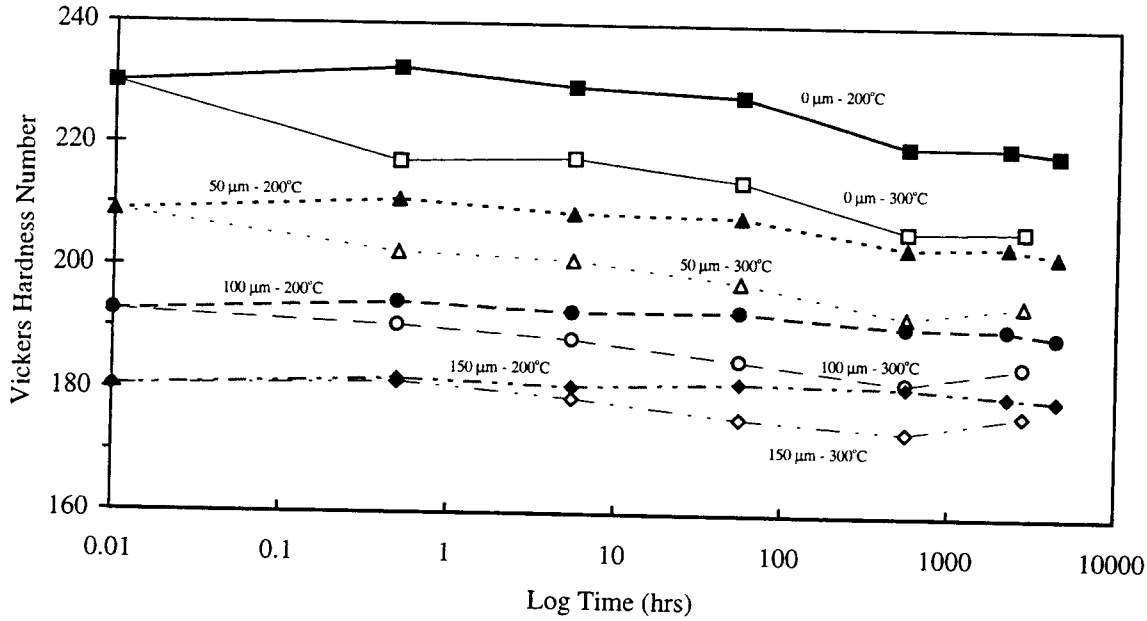

Figure 11 Decrease in hardness as a function of time, temperature and distance from the shot peened surface

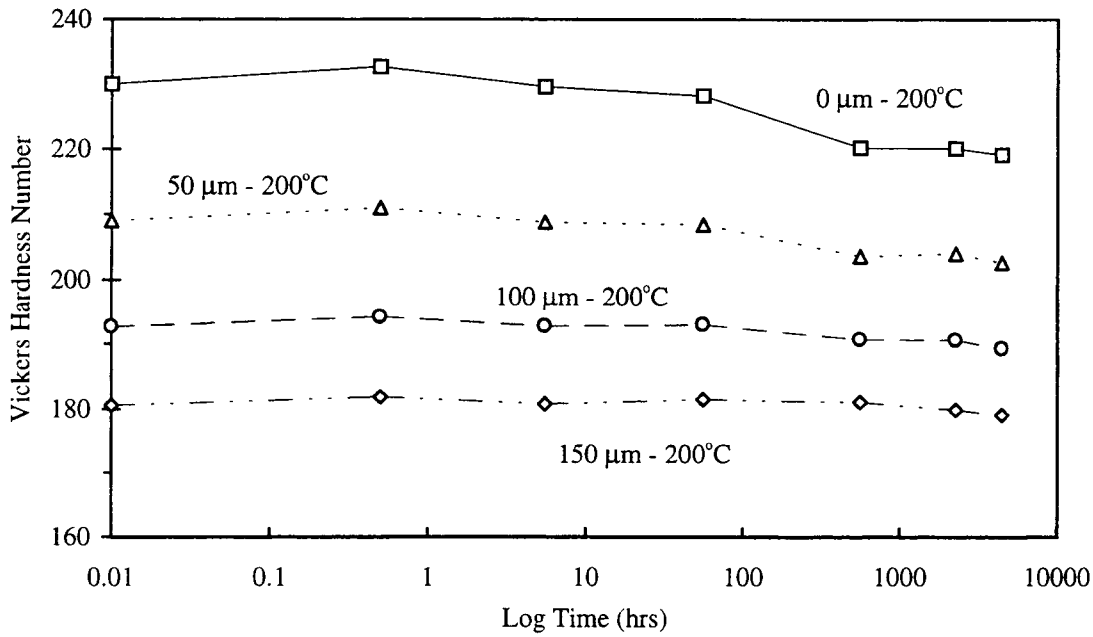

Figure 12 Decrease in hardness as a function of time and distance from the shot peened surface at an annealing temperature of 200°C

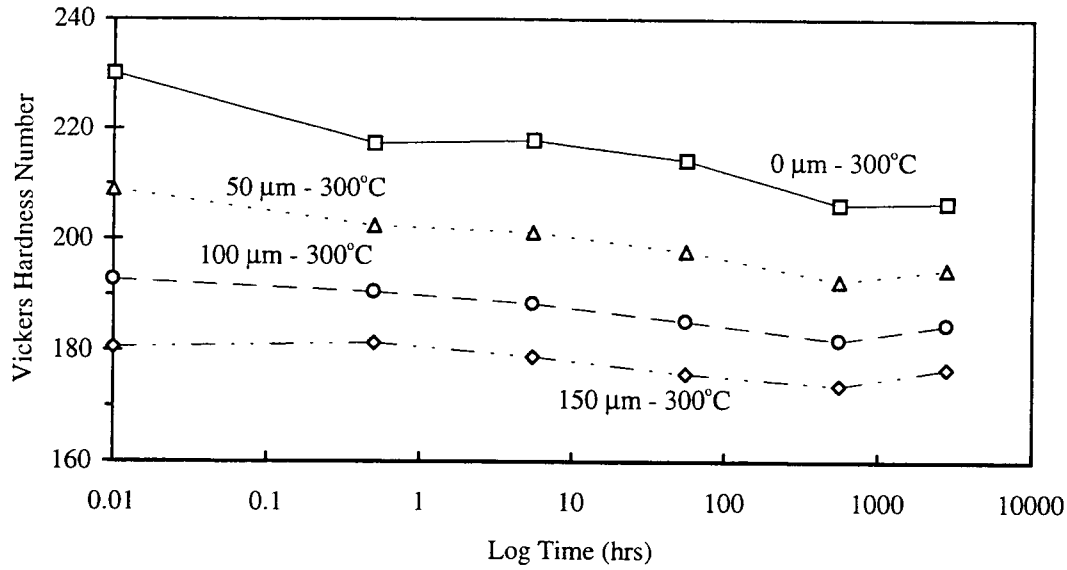

Figure 13 Decrease in hardness as a function of time and distance from the shot peened surface at an annealing temperature of 300°C

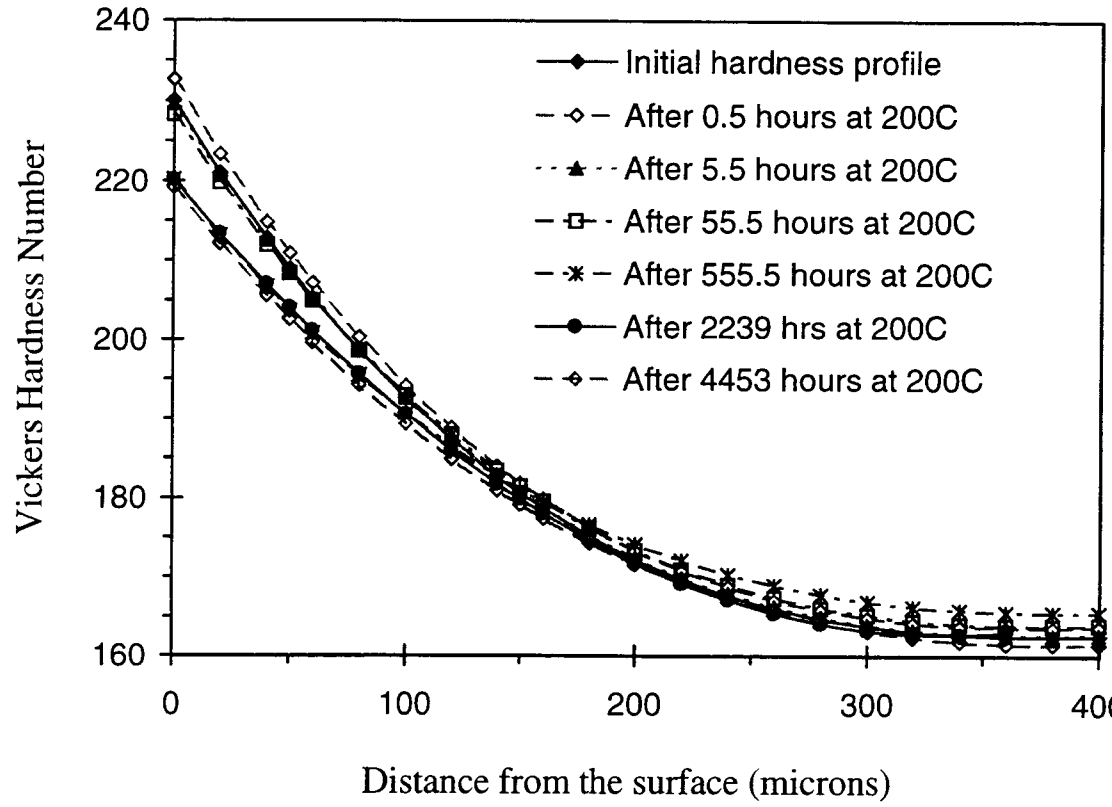

Figure 14 Hardness profiles after 200°C annealing times (see Appendix B for individual hardness profiles)

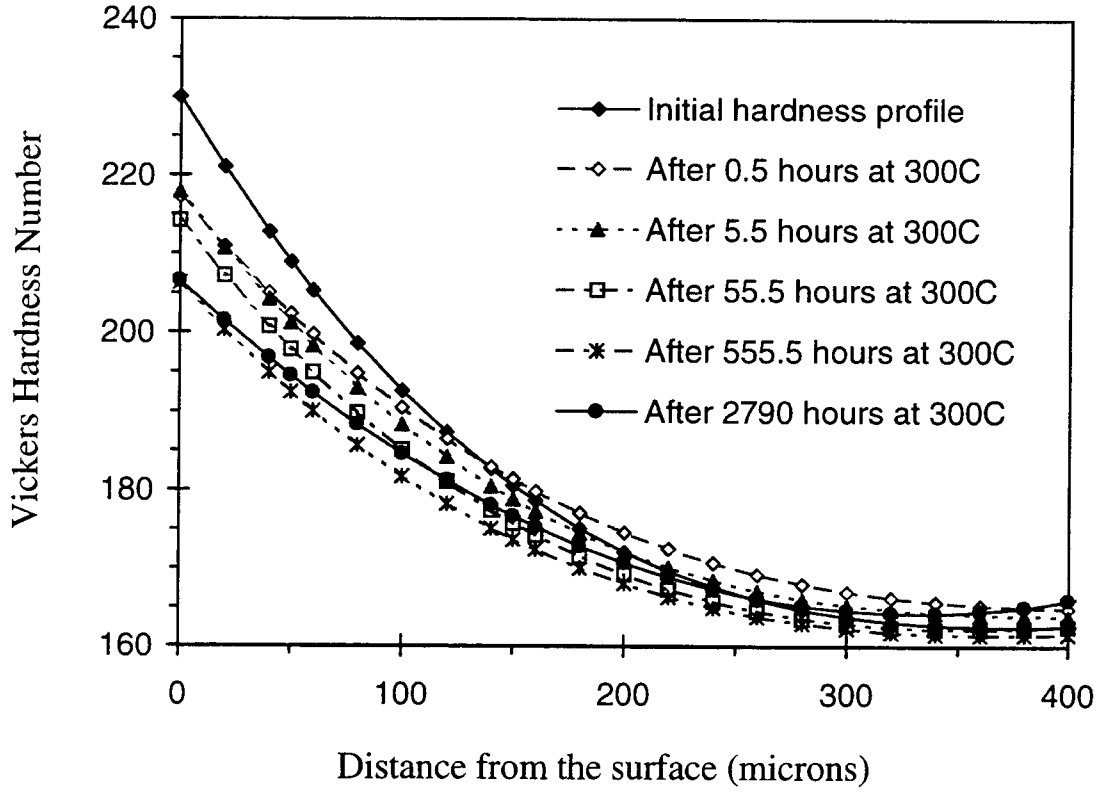

Figure 15 Hardness profiles after 300°C annealing times (see Appendix B for individual hardness profiles)

As was noted previously, the more subtle hardness changes were analyzed by comparing the percentage of data points above a given value for the nearest 150 μm of the surface. These results are plotted below in Figure 16 which illustrate the drop in the percentage of hardness measurements above given values as a function of time for the 200°C, 300°C air and 300°C vacuum annealing experiments.

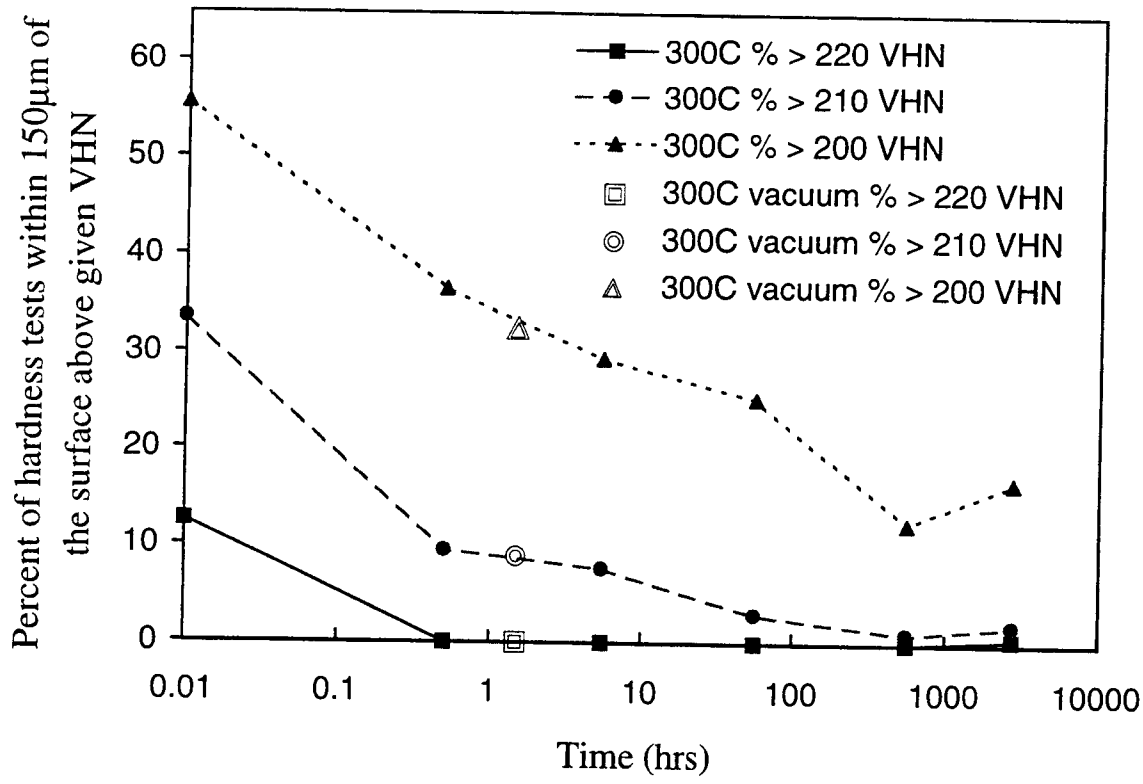

Figure 16 The percentage above given VHN values within 150 µm of the shot peened surface

It is apparent from Figure 16 that there is a consistent trend toward the softening of the material, even after only 5.5 hours at 200°C or 0.5 hours at 300°C. This may indicate that if cold worked zirconium experiences even very short term exposures to low temperatures (200 - 300°C), the material properties such as hardness (yield strength) can be detrimentally effected. There appears to be a more abrupt drop in the hardness between the 0.5 hour anneal and the 5 hour anneal at 200°C, but the reason for this was unclear. Possibly, the variation was only a result of experimental variations such as the variation in spatial distribution of the data points inside 150 µm (some profiles had slightly more points concentrated near the surface). The reason for the increase in the percentage of hardness measurements above 200 VHN that appears in Figure

16 after the final heat treatment for both 200°C and 300°C is not clear. The same trend was not observed for data above 210 VHN or 220 VHN and was not apparent in the 3rd order polynomial curve fits illustrated in Figures 13 and 14.

Vacuum Annealing

No distinct oxide was observed in optical micrographs taken after the above air heat treatments. In another experiment using the same grade of zirconium as used in this study [37], a thick oxide layer was visible under the same observation conditions used in this study (polarized light and approximately 200X magnification), indicating that, in the current experiments, the oxide layer is too small to be visible using optical microscopy.

A hardness profile was developed after 1.5 hours at 300°C under vacuum. The third order polynomial curve from the resulting profile is plotted below in Figure 17 along with the profiles from 0.5 hours and 5 hours at 300°C in air illustrated previously in Figure 15. The actual data plot can be found in Appendix B. Figure 17 illustrates that the softening observed under vacuum appears coincident with the other two curves. Figure 18 plots the data from the vacuum anneal hardness profile with the 300°C air anneal data for hardness as a function of time and distance from the shot peened surface. Figure 16 above also includes data after vacuum annealing. As can be observed in Figures 16 and 18, the vacuum data again coincides fairly well with the 300°C air anneal data. Also, no increases in the surface hardness or change in the hardness profile shape were observed after long term anneals as might be expected if oxygen had diffused to a significant extent (curve shape would change where the effect of oxygen on the hardness becomes apparent). This indicates that oxygen diffusion did not occurred to any significant extent, since it is expected that any small increase in oxygen content has a dramatic effect on hardness [21,24].

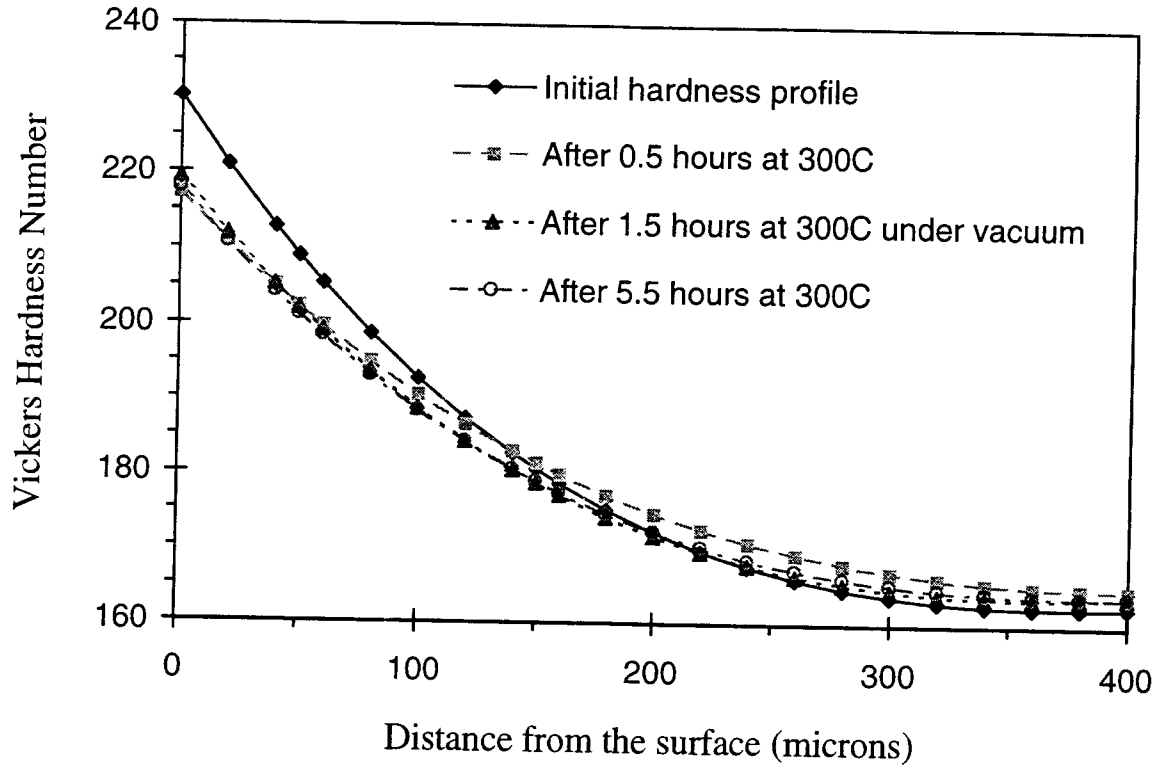

Figure 17 Hardness profiles after 1.5 hours at 300°C under vacuum compared to annealing in air for 0.5 and 5.5 hours at 300°C

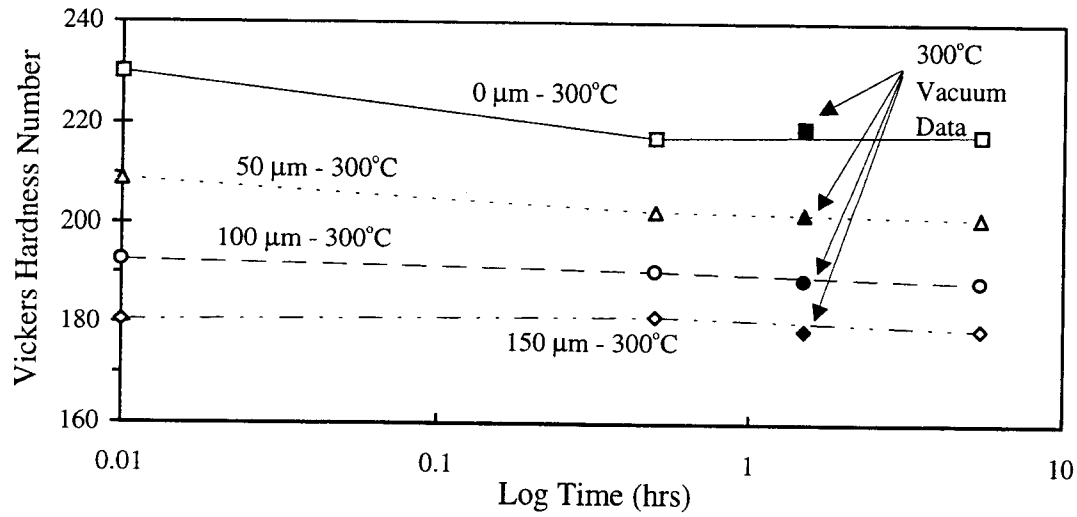

Figure 18 Decrease in hardness as a function of time and distance from the shot peened surface with annealing at 300°C in both air and vacuum

Hardness/ Cold Work Study

The pre-cold rolled longitudinal hardness of the samples used for the cold work study (from non-shot peened plate DD) in the as-fabricated condition was 164 VHN. This compared to a 164 VHN initial average hardness (before annealing) in the interior region of the shot peened specimens used in the thermal stability study. In the transverse orientation, a 148 VHN was observed from the pre-cold rolled DD specimens, while 156 VHN was observed from the interior region of the pre-annealed shot peened specimens. These initial values served as the "as-fabricated" bulk hardness for the plate DD before cold rolling and before any annealing of the shot peened specimens BB. After a 1 hour anneal at 790°C to relieve any possible residual cold work, the hardness of the longitudinal shot peened specimens dropped from 164 VHN to 155 VHN as opposed to the DD specimen that only dropped to from 164 VHN to 161 VHN. The annealing seemed to have less effect on the transverse orientation, where the hardness only decreased from 156 VHN in the as-fabricated shot peened plate to 152 VHN after 1 hour at 790°C. The plate DD had similar results in the transverse orientation where the hardness stayed about the same (148 as-fabricated to 149 after a 1 hour anneal). Further annealing for 24 hours (to be sure that the hardness did not continue to drop after the 1 hour anneal) had little or no effect on either orientation (see Table 9 below). The hardness values that were determined after annealing were compared to the "as-fabricated" hardness values for the pre-annealed shot peened specimens BB and the pre-cold rolled specimens DD. As discussed earlier, this comparison allowed an approximate determination of the "equivalent" cold work present in the "as-fabricated" condition for both plates [pre-annealed shot peened BB and pre-cold rolled (non-shot peened) DD].

The difference between the fully annealed specimens and the as-fabricated DD specimens was about 3 on the Vickers hardness scale. This amounts to an approximately 2% change in hardness. A change in hardness of

3 to 5 on the Vickers scale is observed from the as-fabricated state to the first reduction in thickness (3.0% CW in the longitudinal direction, 3.9% CW in the transverse direction, see Table 9 below). This would tend to indicate that the plate had an "equivalent" cold work in the as-fabricated state of about 2%. The "adjusted original thickness" was 5.01 mm based on an actual original thickness of 4.91 mm (adjusted for the 2% cold work in the as-fabricated state). After re-plotting the hardness versus cold work data based on an "adjusted" as fabricated thickness and iterating the initial cold work estimate to best fit the general trend of the plot, a value of 0.9% cold work was determined corresponding to a 4.95 mm initial thickness. The iteration process, as explained previously, was simply evaluating the change in hardness after the first few rolling reductions using cold work percentages calculated based on the new or "adjusted" original thickness. This change in hardness was compared this to the difference in hardness between the as-fabricated and the annealed states to obtain an "iterated" estimate of the amount of residual cold work present in the as-fabricated state.

The as-fabricated interior (baseline) hardness of the shot peened metal BB was 164 VHN, compared to 155 VHN for the fully annealed plate. Comparing this change to the change in hardness after the initial rolling reductions indicates that the shot peened plate had residual cold work to about 2.4%. This "equivalent" cold work was probably a result of working during the fabrication stage.

Longitudinal Orientation	Vickers Hardness Number		Transverse Orientation	Vickers Hardness Number
BB as-fabricated	164		BB as-fabricated	156
BB after 1hr at 790°C	155		BB after 1hr at 790°C	152
BB after 24hr at 790°C	153		BB after 24hr at 790°C	150
DD as-fabricated	164		DD as-fabricated	148
DD after 1hr at 790°C	161		DD after 1hr at 790°C	149
DD after 24hr at 790°C	161		DD after 24hr at 790°C	151
DD after 3.0% reduction	167		DD after 3.9% reduction	153
" 7.3% "	182		" 7.6% "	168
" 17.0% "	198		" 16.5% "	179
" 26.6% "	193		" 25.9% "	182
" 35.9% "	204		" 34.7% "	194
" 44.5% "	206		" 44.1% "	197
" 52.9% "	212		" 52.2% "	204
" 57.1% "	212		" 56.3% "	211

Table 9 Cold work and hardness values for BB (shot peened) specimens and DD (cold rolled) specimens in transverse and longitudinal orientations

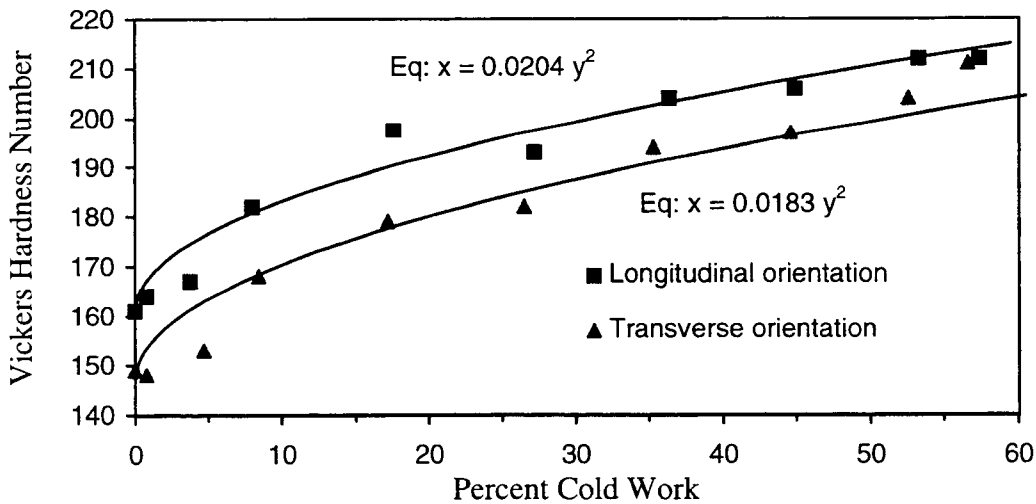

Figure 19 Cold work versus hardness curves for longitudinal and transverse orientations

The shape of the curve is consistent with data reported by Gray [5] for cold rolled zirconium. The relationship between the longitudinal and transverse hardness is fairly consistent with the data presented by Treco [11] for iodide zirconium although the divergence in the hardness curves between the two orientations did not increase with increasing cold work as was observed by Treco. A difference in hardness between the longitudinal and transverse orientations is probably due to texture and the plastically anisotropic nature of zirconium. Zirconium can develop a preferred orientation under deformation and the result is a slightly different hardness with orientation [11,23,38].

The values shown in these curves (Figure 19) have been curve fit using a parabolic function of the form $\mathbf{x = Cy^2}$, where **x** is the percent cold work, **C** is a constant, and **y** is the difference between the baseline hardness (fully annealed), and the hardness at a given percent cold work. The constant C was solved by averaging the C values obtained from the highest seven data points (the first two data points would skew the data since they are so close to the origin). The following equations were determined:

Transverse Orientation	$x = 0.0204\ y^2$	**(12)**
Longitudinal Orientation	$x = 0.0183\ y^2$	**(13)**

A value of about 230 VHN is calculated in the longitudinal orientation and 220 VHN in the transverse orientation when evaluating the equations near 100% cold work. The highest values observed in the shot peened zirconium were about 230 VHN (hardness of shot peened specimens measured in the longitudinal direction) at a distance of 40 μm from the shot peened surface (see Figures 8 and 9). A value of approximately 230 - 240 VHN is predicted (longitudinal orientation) by extrapolating to the surface of the shot peened zirconium using a best fit third order polynomial curve. These values correspond fairly well with value of 230 VHN that would be obtained by evaluating the parabolic equation at a cold work level approaching 100%.

Because the cold work/hardness relationships for the rolled plates were best approximated by parabolic functions, a similar curve was assumed for the shot peened induced cold work. As the maximum initial surface hardness of the shot peened specimens was about 230 VHN and the maximum extrapolated hardness value of the cold rolled plates was about 230 VHN at nearly 100% cold work, it was assumed that the surface of the shot peened specimens was cold worked to nearly 100%. Using 155 VHN as a baseline hardness (fully annealed shot peened specimen) and an average maximum hardness of 230 VHN at the surface of the pre-annealed shot peened specimens, the following parabolic function was derived:

$$\text{Longitudinal Orientation} \quad x = 0.0178\, y^2 \qquad \textbf{(14)}$$

Equation 14 is slightly different than equation 13 so that the hardness value evaluated at a cold work level approaching 100% is exactly 230.

The hardness values from a typical pre-heat treated shot peened specimen were converted to percent cold work using equation 14 and appear in Figure 20 below.

The extrapolated hardness value near the surface of the shot peened specimens was used to compare the results of this investigation to those of the McGeary et al. [2] study on the recovery of 97% cold worked zirconium. As can be observed in Figure 20, the equivalent cold work of the shot peened zirconium reaches 97% within about 5 μm of the surface. After each heat treatment, a hardness value was estimated at this depth using a best fit curve and these hardness values were compared to the changes observed over the 80 hourduration of the McGeary et al. study. An illustration of these comparisons appear in Figure 21, below. Figure 21 is a plot of the relative change in VHN as a percent, versus time. The relative change in VHN was calculated by dividing

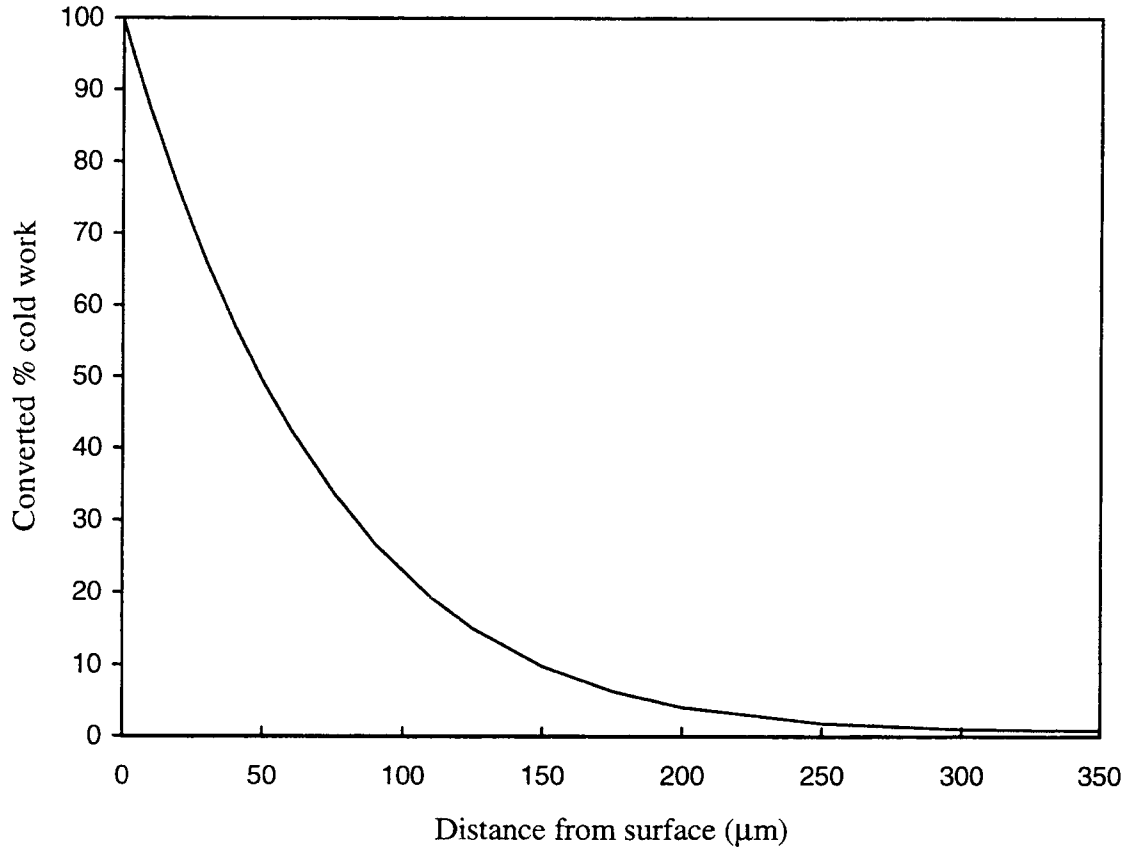

Figure 20 Plot of cold work versus distance from the shot peened surface

any change in hardness experienced after annealing at the given temperatures by the total change in hardness between the cold worked (to 97%) zirconium and the annealed zirconium for the respective studies. Normalizing the data in this fashion allowed comparison of the changes in hardness with the data reported by McGeary et al. by accounting for composition, grain size, texture, etc., which all effect the baseline hardness.

The hardness value that McGeary et al. [2] determined for zirconium with 97% CW is substantially lower than the hardness observed for a similar amount of cold work in the shot peened samples (172 VHN versus 230 VHN). This difference may be due to texture as a result of the reduction method. McGeary

et al. used cold swaging rather than rolling as was used in this study. As well, production and thermo-mechanical processing, the composition [23], or even the load used for hardness testing [23] can effect the measured hardness. It is common to see such variations in the hardness of zirconium [23]. The purpose of this comparison, however, is to compare hardness change trends as a result of annealing. As can be seen in Figure 21, the observed softening in the current study at 200°C and 300°C is fairly consistent with the results obtained by McGeary et al. [2].

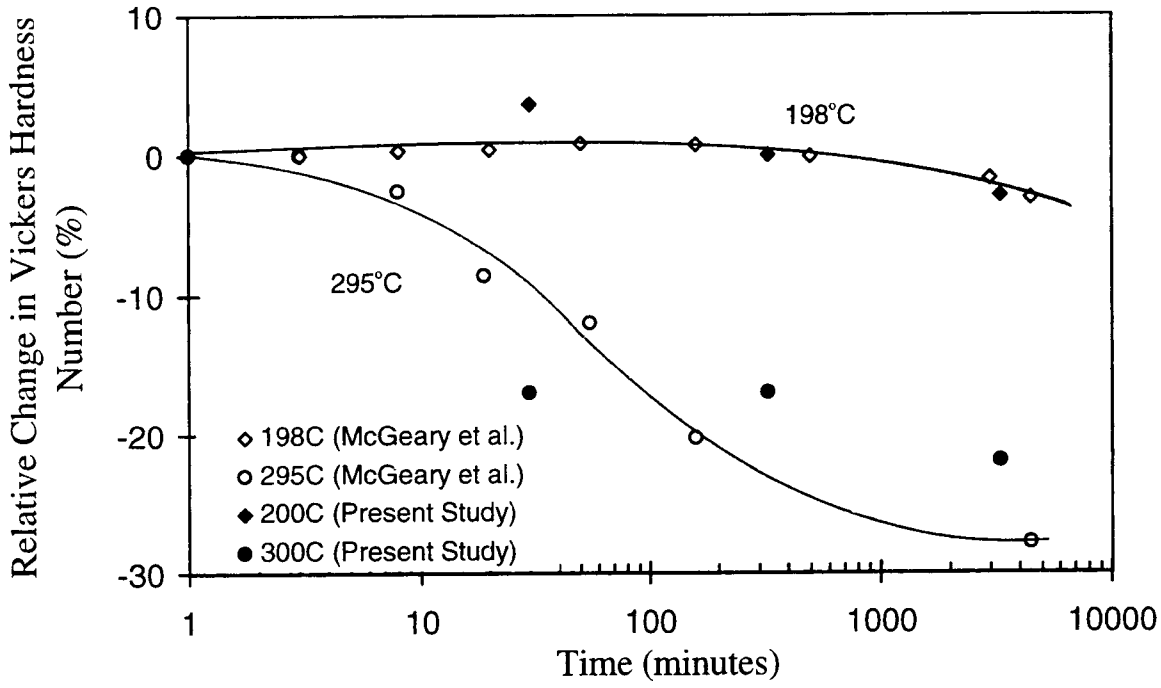

Figure 21 Comparison of current study to 97% cold work (CW) study by McGeary et al. [2]

Tensile Testing

Figure 22 illustrates one tensile test in both longitudinal and transverse orientations. Results from all performed tensile tests can be found in Appendix C "Tensile Tests."

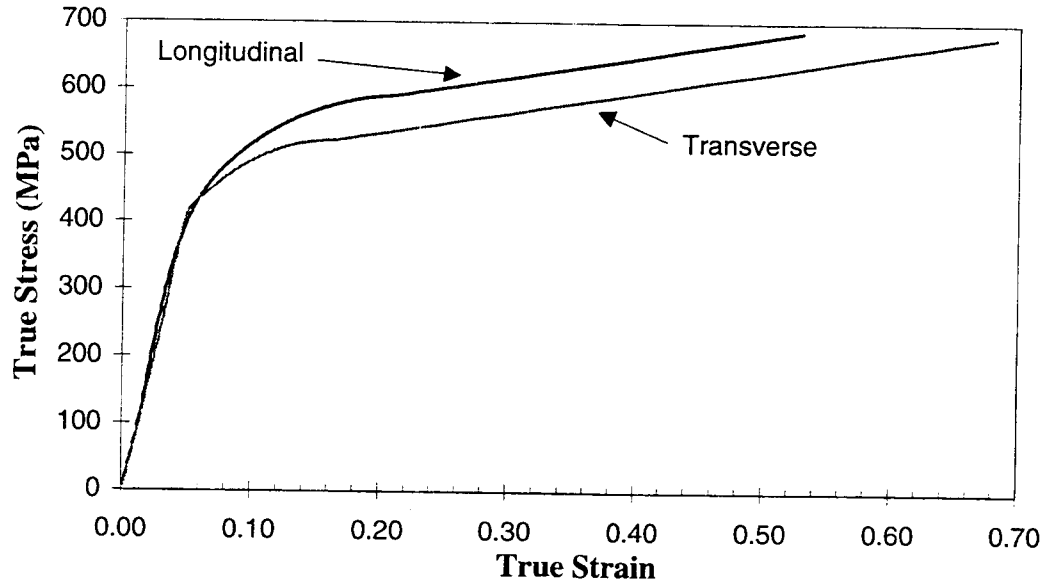

(a)

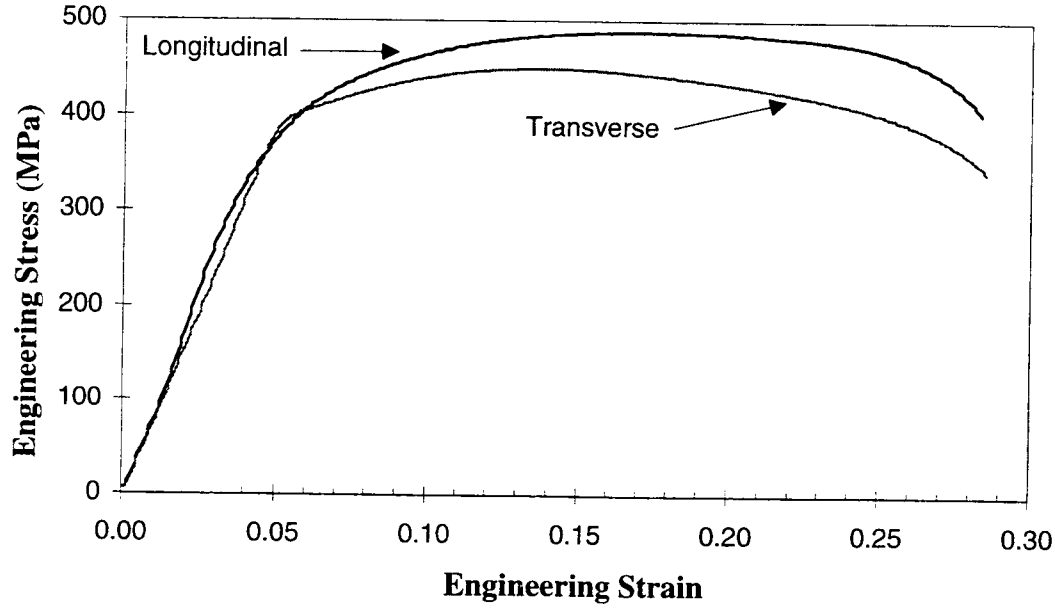

(b)

Figure 22 (a) True stress-strain curves (b) Engineering stress-strain curves. Other stress-strain curves performed in this study are in Appendix C.

Tensile testing was performed on the material to determine the shape of the true stress versus true strain curve as well as determine the yield strength of the zirconium used in this study. The curve shape of the true stress versus true strain in the plastic regime (parabolic) gave an indication of the curve shape that should be expected for the hardness versus percent cold work curves developed during the cold rolling experiments. The curve shapes were, indeed, consistent showing that the data obtained in the hardness/ cold work study were reasonable.

The yield strength was used to develop a hardness versus yield (or flow) strength relationship so that a yield strength could be estimated at the shot peened surface. The yield strength of zirconium is roughly proportional to the hardness [23], or,

$$\sigma_y \approx N\ (VHN) \qquad \textbf{(15)}$$

where σ_y is the yield strength and **N** is a constant.

The constant **N** is calculated to be 1.82 using an approximate yield strength measured in this study of 300 MPa and a corresponding as-fabricated hardness of about 165 VHN. A value for the yield strength at the shot peened surface of the zirconium, corresponding to a 230 VHN, was calculated to be approximately 420 MPa. The ultimate strength of the zirconium was about 480 MPa, so a value of 420 MPa seems reasonable. This surface yield strength was used for comparison with the chromium plated stainless steel plates.

Transmission Electron Microscopy

General microstructure TEM micrographs have been taken at a few depths for the initial condition and after 0.5 hrs at 300°C as mentioned above. At this time no conclusive evidence has been found as to the nature of the

observed softening or recovery. Further TEM analysis (to be performed at a later time) should lead to a more definitive conclusion. Some typical micrographs are shown below in Figures 23 and 24 for the initial condition and after 0.5 hours at 300°C. The TEM micrographs are superimposed on a hardness profile so that the depth of the TEM foil can be correlated to a specific cold work level (hardness value).

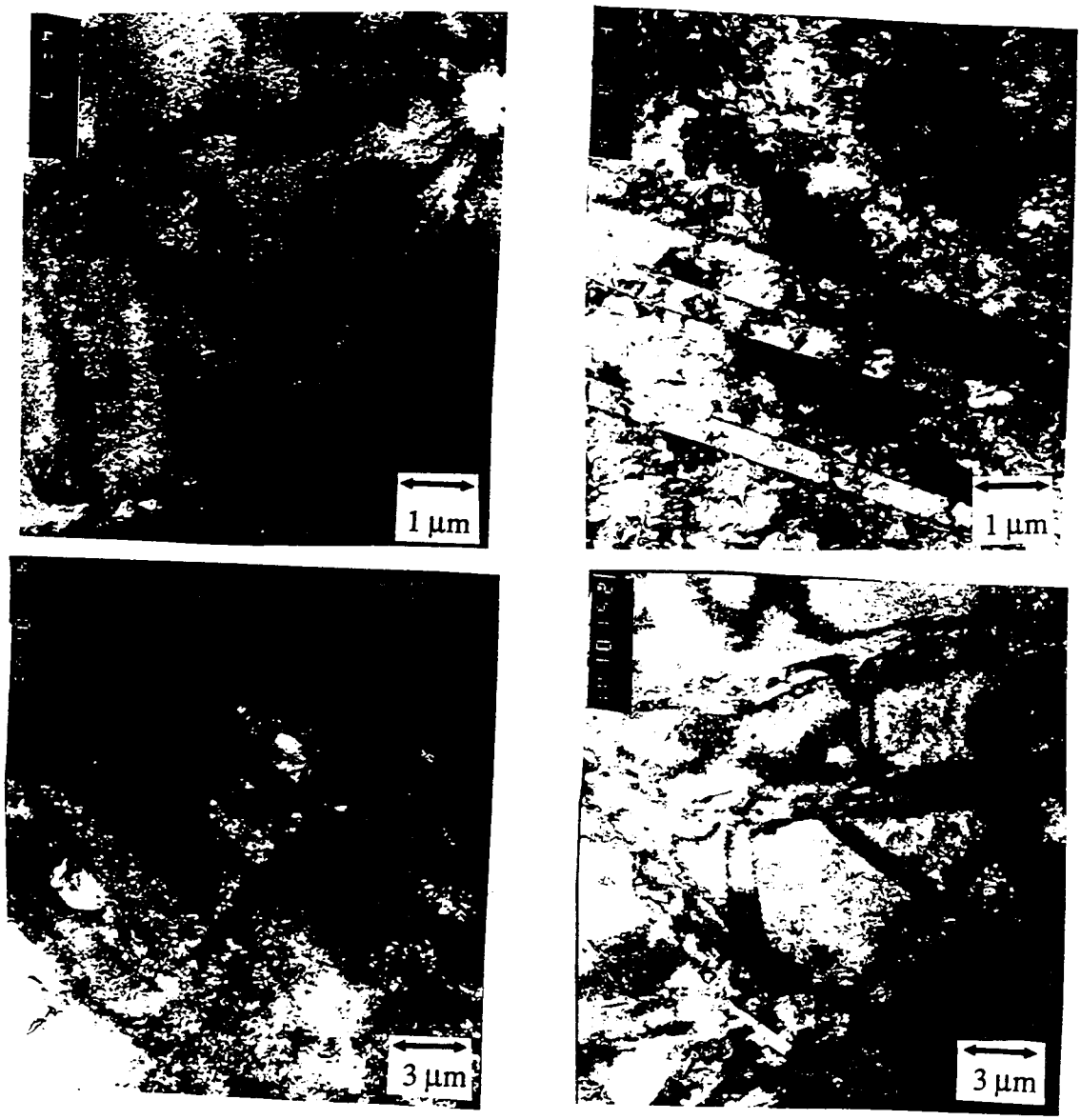

Figure 23 TEM micrographs of the initial shot peened condition at 62 µm below the shot peened surface

Figure 24 TEM micrographs after 0.5 hrs at 300°C at 70 µm below the shot peened surface

Optical Metallography

No changes in grain structure or grain nucleation were observed after elevated temperature exposures using optical metallography under polarized light. This indicates that the changes that occur were indeed a result of classic recovery and not recrystallization. Figure 25, below, illustrates this with some micrographs of the shot peened surface region using polarized light from the initial (pre-annealed) condition to 2790 hours at 300°C.

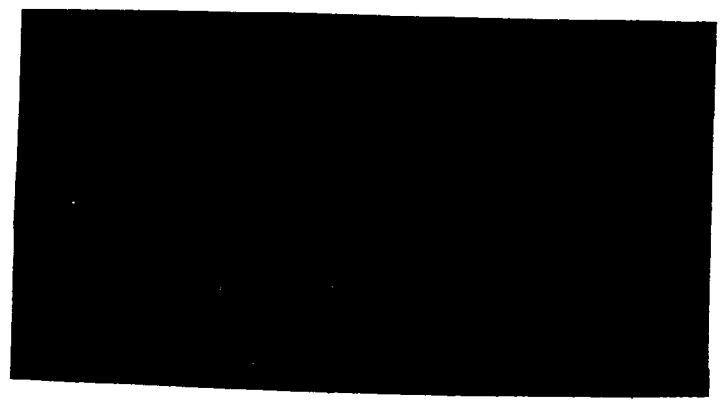

(a)

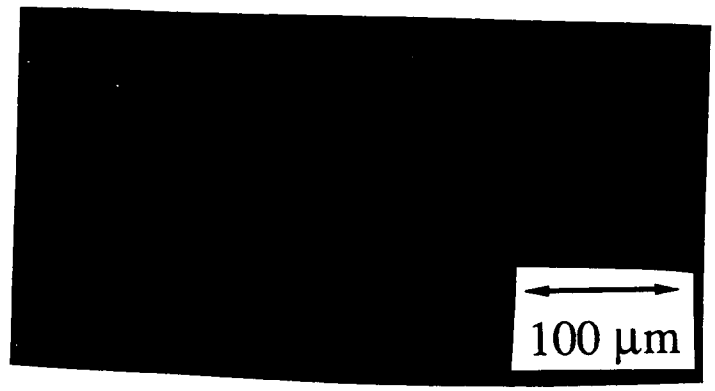

(b)

Figure 25 Micrographs of shot peened surface region in the initial condition (a) and after 2790 hours at 300°C (b)

Discussion of Results

Thermal Stability Study

During cold work, a large amount of elastic strain energy is imparted into the metal as a result of dislocation multiplication. The free energy of a cold worked metal is, of course, higher than that of a fully annealed metal due to the elastic strain fields of the dislocations. This increase in free energy can cause spontaneous reactions to occur to decrease this free energy, even at relatively low temperatures. This is the driving force for recovery, or recrystallization. Here recovery is considered to be the annihilation and/or realignment of dislocations to form low misorientation sub-grain boundaries, decreasing the total strain energy. Recrystallization is the nucleation and growth of new, low dislocation density grains.

The results observed in this study are consistent with the static restoration processes in zirconium observed in other studies. McGeary et al. [2], found that highly cold worked zirconium (97%) can experience 3/4 of the total softening as a consequence of recovery before any grain re-orientation (recrystallization) is observed. Recovery may consist of several mechanisms. First, the highly dense dislocations can change their configuration from an extremely disordered and tangled state to a more ordered state, decreasing the strain energy present in the lattice. Second, some dislocation annihilation of dislocations of opposite sign may occur, decreasing the total dislocation density. The reconfiguration process is known as polygonization. During polygonization, the dislocations re-orient themselves from a random state to form subgrain boundaries [5]. A more complete discussion of polygonization that occurs during recovery has been reviewed by Cahn [39] and by Hibbard and Dunn [40]. The process of polygonization in deformed single crystal zirconium has been observed by Dedo et al. [3] at temperatures as low as 300°C. The

polygonization process of recovery is illustrated in Figure 26 below by Askeland [41]. Third, there may be some recovery of point defects.

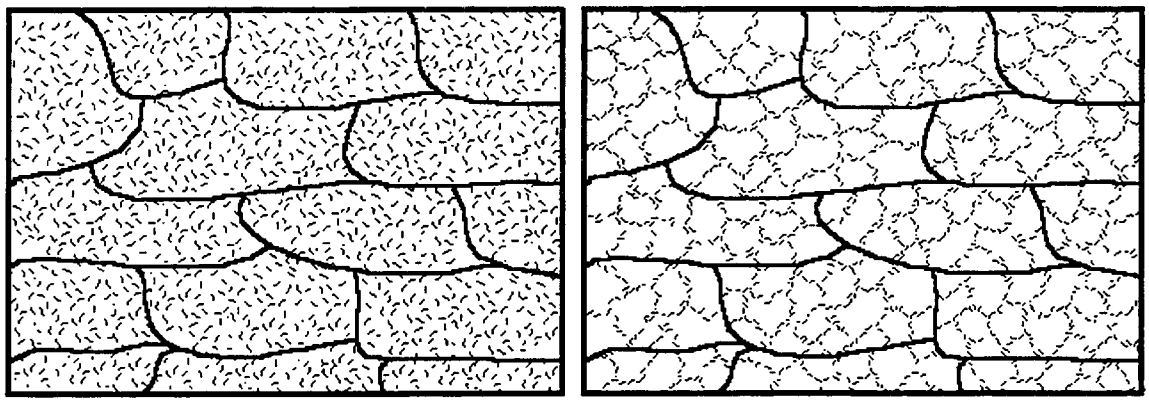

(a) (b)

Figure 26 (a) initial microstructure (dislocation configuration) of cold worked zirconium and (b) the microstructure after recovery

Recovery may be associated with decreased hardness. Of course, recovery occurs at 300°C more readily than at 200°C, because more thermal energy is available to mobilize point and line defects.

Our observation that softening or recovery occurred about 2 orders of magnitude more quickly at 300°C than at 200°C is consistent with the results of McGeary and Lustman [2] (see Figure 21). In the McGeary et al. study, the same reduction in hardness that occurred after 8 minutes at 295°C as experienced after about 4500 minutes at 198°C (2.5 orders of magnitude).

The recovery process can be described by Arrhenius-type behavior, or,

$$\frac{1}{t} = M e^{-\frac{Q}{RT}} \qquad (16)$$

where **t** is the time required to recover a given fraction of the hardness, **M** is a constant, **Q** is the activation energy for recovery in zirconium, **R** is the ideal gas constant and **T** is the absolute temperature. For two different temperatures that experience the same amount of recovery (same reduction in hardness),

$$t_1 M e^{-\frac{Q}{RT_1}} = t_2 M e^{-\frac{Q}{RT_2}} \qquad \textbf{(17)}$$

M is associated with a fixed amount of softening and, therefore,

$$\frac{t_1}{t_2} = \frac{e^{-\frac{Q}{RT_2}}}{e^{-\frac{Q}{RT_1}}} = e^{-\frac{Q}{R}\left(\frac{1}{T_2} - \frac{1}{T_1}\right)} \qquad \textbf{(18)}$$

An activation energy determination maybe helpful to determine the atomic process(es) associated with the softening observed in this study,. Solving for the activation energy from equation 18,

$$Q = -\frac{R \, Ln\left(\frac{t_1}{t_2}\right)}{\left(\frac{1}{T_2} - \frac{1}{T_1}\right)} \qquad \textbf{(19)}$$

Substituting the times $\mathbf{t}_1$ = 557 hrs at 200°C, $\mathbf{t}_2$ = 5.5 hrs at 300°C yields an activation energy of 24,834 cal/mol (104.1 KJ/mol). The activation energies for lattice self diffusion in zirconium have been reported between 22,000 and 75,000 cal/mol [42-47] for temperatures ranging from 506°C to 860°C (no self diffusion data reported below 506°C). Although the reason for such scatter is not clear, it has been suggested that the lower values (e.g. 22,000 and 27,000 cal/mol) may

actually reflect short circuit diffusion along dislocation lines, even in annealed zirconium [48-51]. We expect that the activation energy for self diffusion in our shot peened zirconium at 200°C to 300°C to be that of short circuit diffusion. The activation energy of 24,834 cal/mol calculated in this study is in good agreement with the lower activation energies of 22,000 cal/mol [42, 43] and 27,000 cal/mol [44] reported for self diffusion. If one assumes that these values are low due to short circuit diffusion along dislocations, then the activation energy calculated in the current study suggests that a diffusion controlled process such as dislocation climb (necessary for recovery processes such as edge dislocation annihilation and polygonization) may be associated with the observed softening or recovery. This argument is somewhat complicated by the fact that the activation energy appears to be a function of temperature (Horvath et al. [51] reported increases with decreasing temperature from an apparent maximum of about 84,000 cal/mol using the two data nearest the transition temperature to about 27,000 cal/mol using the two lowest temperature data near 500°C) for unexplained reasons [51] for a given mechanism (i.e. bulk or short circuit diffusion). The activation energy in the present study may also be decreased by the very fine grain size (about 30 μm) and an increase or supersaturation of vacancies (above the equilibrium concentration) with the heavy cold work associated with shot peening.

Hardness/ Cold Work Study

When comparing the hardness versus cold work curves for the cold rolling study (see Figure 19), one notes that the longitudinal and transverse curves have a fairly consistent shape and experience the most rapid change in hardness over the early rolling reductions. This is consistent with the zirconium 702 stress versus strain behavior, illustrated in Figure 22. As was stated

previously, the difference between the two behaviors (from longitudinal and transverse orientations) may be due to a texture in the zirconium.

Although the hardness of the cold rolled samples when extrapolated to near 100% cold work (~230 VHN) and the hardness extrapolated to the surface of the shot peened specimens (~230 VHN) appeared to be fairly coincident, the deformation mechanisms involved in the cold rolling were not identical to that of shot peening. The surface layer of the shot peened zirconium exhibited substantial twinning as illustrated in Figure 27a. The grains throughout the cold rolled zirconium exhibited little twinning as illustrated in Figure 27b. There were changes in the grain morphology as well; greater elongation in rolling than shot peening. With rolling, deformation is generally "unidirectional" whereas some of the hardening associated with shot peening may involve reversals of the direction of plasticity. The grains of the zirconium plate have a strong preferred orientation after rolling. Slip can only occur along the prism planes in zirconium [52]. If the grains are oriented for twinning ({1 0 $\bar{1}$ 2} [52]) rather than for slip under a particular deformation, twinning is, initially, the primary deformation mode (upon twinning, regions inside the twins become favorably oriented for prism slip). It is possible, therefore, that deformation by shot peening occurred in an orientation that favored twinning whereas slip was favored during the rolling deformation. Orientation measurements were not made to confirm this possibility. Twinning is also strain rate dependent. Twinning is, initially, the primary deformation mechanism for favorably oriented crystals even at low strain rates (3×10^{-4} at ambient temperature [52]). For grains not perfectly oriented for slip or for twinning, a twinning mechanism may be activated at high strain rates where more twinning modes become strongly active [52], while a slip mechanism may predominate at lower strain rates. It is possible then, that the relatively high deformation rates associated with shot peening (~10^4 s^{-1}) activated a twinning mechanism, while the more modest deformation rate experienced in rolling (~10^1 s^{-1}) did not. Changes in deformation mode may affect the hardness/ cold work relationship. However, in order to compare the results from this study to those

from previous studies, the hardness profile resulting from shot peening must be converted to percentages of cold work. The outlined procedure appeared to be the most practical method.

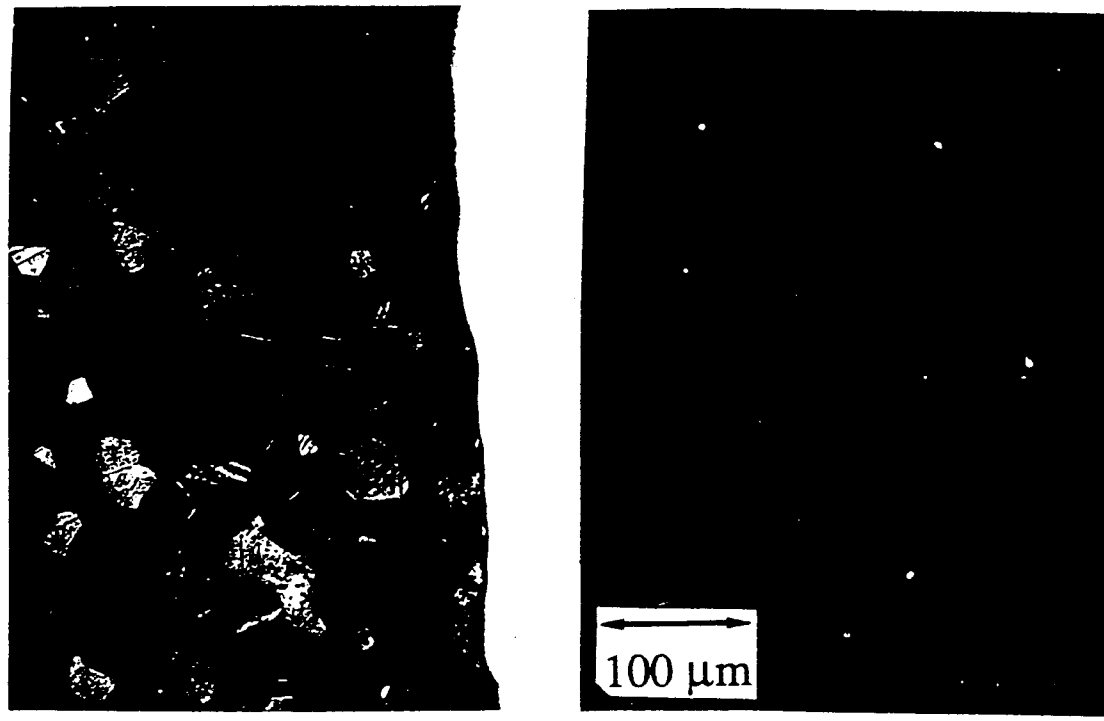

(a) (b)

Figure 27 Comparison of (a) shot peened grains to that of (b) cold rolled grains

Conclusions

1.) Significant softening of the surface of the shot peened zirconium was observed after annealing at both 200°C and 300°C. The mechanism of this softening is not presently known.

2.) The softening appears to be due to static recovery, consistent with some earlier studies of cold rolled zirconium.

3.) The apparent activation energy for the softening was consistent with the activation energy that would be expected for a short circuit diffusion recovery process.

4.) Initial transmission electron microscopy has not shown any conclusive evidence as to the softening mechanism.

Bibliography

1. Society of Automotive Engineers, "Procedures for Using Standard Shot Peening Test Strip," SAE J443, JAN84.

2. R.K. McGeary, and B. Lustman, "Kinetics of Thermal Reorientations in Cold Rolled Zirconium," *Transactions of the American Institute of Mining and Metallurgical Engineers*, 197 (1953) pp. 284-291.

3. A. Dedo, D. Mills, and G.B. Craig, "The Formation of Polygonized Substructure in Deformed Single Crystals of α-Zirconium," *Journal of Nuclear Materials*, 24 (1967) pp. 237-239.

4. A. Desalvo, and F. Zignani, "Electrical Resistivity Study of Recovery Phenomena in Cold-Worked Zirconium," *Journal of Nuclear Materials*, 20 (1966)pp. 108-118.

5. D.L. Gray, "Recovery and Recrystallization of Zirconium and its Alloys: Part 2 - Annealing of Cold-Worked Zirconium," Hanford Laboratories Report HW-69679, 1961.

6. P.M. Kelley and P.D. Smith, "Strain-Ageing in Zirconium-Oxygen Alloys," *Journal of Nuclear Materials*, 46 (1973) pp23-34.

7. M.L. Swanson, A.F. Quenneville, and H. Schultz, "Stage I Recovery of Deformed Zirconium," *Applied Physics Letters*, 6 (1965) pp. 49-51.

8. P. Merle, C. Vauglin, G. Fantozzi, J. L. Derep, and D. Charquet, "Study by Thermoelectric Power Measurements of Recovery and Recrystallization of Cold-Rolled Zircaloy-4 Sheets," Zirconium in the Nuclear Industry: Seventh International Symposium, ASTM STP 939, R.B. Adamson and L.F.P. Van Swam, Eds., American Society of Testing and Materials, Philadelphia, 1987, pp. 555-576.

9. W.A. Bostrom and S.A. Kulin, "Recovery of Cold-Worked Zirconium," Zirconium and Zirconium Alloys, American Society for Metals, Cleveland, 1953, p 186.

10. O.M. Katz, "Recovery and Recrystallization Kinetics of Cold-Worked Zircaloy-4 Plate and Tubing," Technical Report WAPD-TM-590, Bettis Atomic Power Laboratory, Pittsburgh, 1968.

11. R.M. Treco, "Recrystallization and Grain Growth in Iodide Zirconium," *Journal of Metals, Transactions AIME* (1956) pp. 1304-1311.

12. D. Amick, Teledyne Wah Chang, Albany, Oregon, private communication, May 1994.

13. Unpublished Data, Analytical Request Sheet, Teledyne Wah Chang, Albany Oregon, 1992.

14. R. Vogel, and W. Tonn, "A Transition Point for Zirconium," *Zeitschrift für anorganische und allgemeine Chemie*, 202 (1931) p. 292.

15. Leco Corporation, Metallography Principals and Procedures, 1989.

16. Military Specification, "Shot Peening of Metal Parts," MIL-S-13165C, June 7, 1989.

17. American Society of Mechanical Engineers, "Surface Texture Surface Roughness, Waviness and Lay", ANSI B46.1 - 1978, 1978 pp. 30-32.

18. Society of Automotive Engineers, "Test Strip, Holder and Gage for Shot Peening", SAE J442 AUG79.

19. Steel Founders Society of America, "Standard Specification for Cast Steel Abrasives," SFSA 20-66, 1980.

20. P. Danielson, "Zirconium and Hafnium and Their Alloys," Metals Handbook, Metallography and Microstructures, American Society for Metals (ASM), Vol. 9, 1985, pp. 497-499.

21. J.E. Bailey, "Electron Microscope Studies of Dislocations in Deformed Zirconium," *Journal of Nuclear Materials*, 7, No. 3 (1962) pp. 300-310.

22. C.E.L. Hunt, and E.M. Schulson, "Recrystallization of Zircaloy-4 During Transient Heating," *Journal of Nuclear Materials*, 92 (1980) pp. 184-190.

23. W. Chubb, G.T. Muehlenkamp, F.R. Shober, and A.D. Schwope, "Mechanical Properties of Zirconium and Its Alloys," in The Metallurgy of Zirconium, (Lustman, B., Kerze, F.), McGraw-Hill Book Company, 1955, pp. 490-552.

24. M.E. Sauby and D. Lee, "Recovery Behavior of Cold-Worked and Quenched Zircaloy with Varying Oxygen Content," *Journal of Nuclear Materials*, 50 (1974) pp. 175-182.

25. C.O. De Gonzalez, and E.A. Garcia, "Determination of the Diffusion Coefficients of Oxygen in Zirconium by Means of XPS," *Applied Surface Science*, 44 (1990) pp. 211-219.

26. T. Tanabe, and M. Tomita, "Surface Oxidation of Zirconium Above Room Temperature," *Surface Science*, 222 (1989) pp. 84-94.

27. M. Tomita, T. Tanabe, and S. Imoto, "An AES Study of Surface Oxidation of Zirconium," *Surface Science*, 209 (1989) pp. 173-182.

28. R. Charles, S. Barnartt, and E. Gulbransen, "Prolonged Oxidation of Zirconium at 350° and 450°C," *Transactions of the American Institute of Mineral (Metallurgical) Engineers*, 212 (1958) p101.

29. H. Porte, J. Schizlein, R. Vogel, and D. Fischer, "Oxidation of Zirconium and Zirconium Alloys," *Journal of the Electrochemical Society*, 107 (1960) pp. 506-515.

30. K. Sense, "On the Oxidation of Zirconium," *Journal of the Electrochemical Society*, 109 (1962), pp. 377-382.

31. I. Korobkov, D. Ignatov, A. Yevstyukhin, and V. Yemel'yanov, *Metallurgiya i Metallovedniye Chistykh Metallov*, 1 (1959) p 144.

32. D. Douglass, and J. Van Landuyt, "The Oxidation of Zirconium: an Electron Microscopy Study of Zirconia Formed in the Thin-Film Region," *Acta Metallurgica*, 13 (1965) pp. 1069-1079.

33. J. Wanklyn, C. Britton, R. Silvester, and N. Wilkens, "Influence of Environment on the Corrosion of Zirconium and Its Alloys in High-Temperature Steam," *Journal of the Electrochemical Society*, 110 (1963) pp. 856-866.

34. P. Shewmon, Diffusion in Solids, McGraw-Hill, 1983.

35. Unpublished data, Spectrographic Analysis, Teledyne Wah Chang, Albany Oregon.

36. Teledyne Wah Chang, "ME-271 Flat Tensile Specimen," (Drawing T-B57), 1973.

37. J.C. Haygarth, and L.J. Fenwick, "Improved Wear Resistance of Zirconium by Enhanced Oxide Films," *Thin Solid Films*, 118 (1984) pp. 351-362.

38. R.M. Treco, "Technical Progress Report for July Through September 1953, "Report MIT-1114, Nov. 24, 1953 & "Technical Progress Report for October Through December 1949," Report MIT-1040, Feb. 8, 1950 in The Metallurgy of Zirconium (B. Lustman, and F. Kerze), McGraw-Hill Book Company, 1955, p 387.

39. R.W. Cahn, ed., Physical Metallurgy, North-Holland Publishing Company - American Elsevier Publishing Company Inc., New York, 1970.

40. W.A. Hibbard Jr., and C.G. Dunn, Creep and Recovery, ASM, Cleveland, 1957, pp. 52-78.

41. D.R. Askeland, The Science and Engineering of Materials, Brooks/Cole Engineering Division (Wadsworth Inc.), Belmont California, 1984, pp. 220-221.

42. P.L. Gruzin, V.S. Yemel'yanov, G.C. Ryabova, and G.B. Federov, "Study of the diffusion and distribution of the elements in Zirconium and Titanium base alloys by the radioactive isotope method," 2nd International Conference on Peaceful Uses of Atomic Energy, *Geneva*, 19 (1958), p. 187.

43. G.B. Federov, and F.I. Zhomov, "Diffusion of Zirconium and Tin in Tin Alloys of Alpha-Zirconium," *Metallurgiya i Metallovedenie chistykh Metallov*, 1 (1959), p. 162.

44. F. Dyment, and C.M. Libanati, "Self-Diffusion of Ti, Zr, and Hf in their HCP Phases, and Diffusion of Nb95 in HCP Zr," *Journal of Materials Science*, 3 (1968) pp. 349-359.

45. P. Flubacher, "Selbst-Diffusionsversuche in α-Zirkon," EIR-Bericht Nr. 49 (1963).

46. V.S. Lyashenko, V.N. Bykov, and L.V. Pavlinov, "A Study of Self-Diffusion in Zirconium and Its Alloys With Tin," *Physics of Metals and Metallography*, 8 No. 3 (1960) pp. 40-46.

47. G.M. Hood, "Diffusion and Vacancy Properties of α-Zr," *Journal of Nuclear Materials*, 139 (1986) pp. 179-184.

48. M.C. Naik, and R.P. Agarwala, "Self and Impurity Diffusion in Alpha-Zirconium," *Acta Metallugica*, 15 (1967) pp. 1521-1525.

49. N.L. Peterson, "Diffusion in the Anomalous," *Comments on Solid State Physics*, 8 (1978) pp. 93-106.

50. G.M. Hood, and R.J. Schultz, "Tracer Diffusion in α-Zr," *Acta Metallurgica*, 22 (1974) pp. 459-464.

51. J. Horvath, F. Dyment, and H. Mehrer, "Anomalous Self-Diffusion in a Single Crystal of α-Zirconium," *Journal of Nuclear Materials*, 126 (1984) pp. 206-214.

52. R.E. Reed-Hill, "The Role of Deformation Twinning in the Plastic Deformation of Zirconium," Proc. USAEC Symposium on Zirconium Alloy Development, GEAP-4089 II 12-0 (1962).

Appendices

Appendix A Heat Treatments

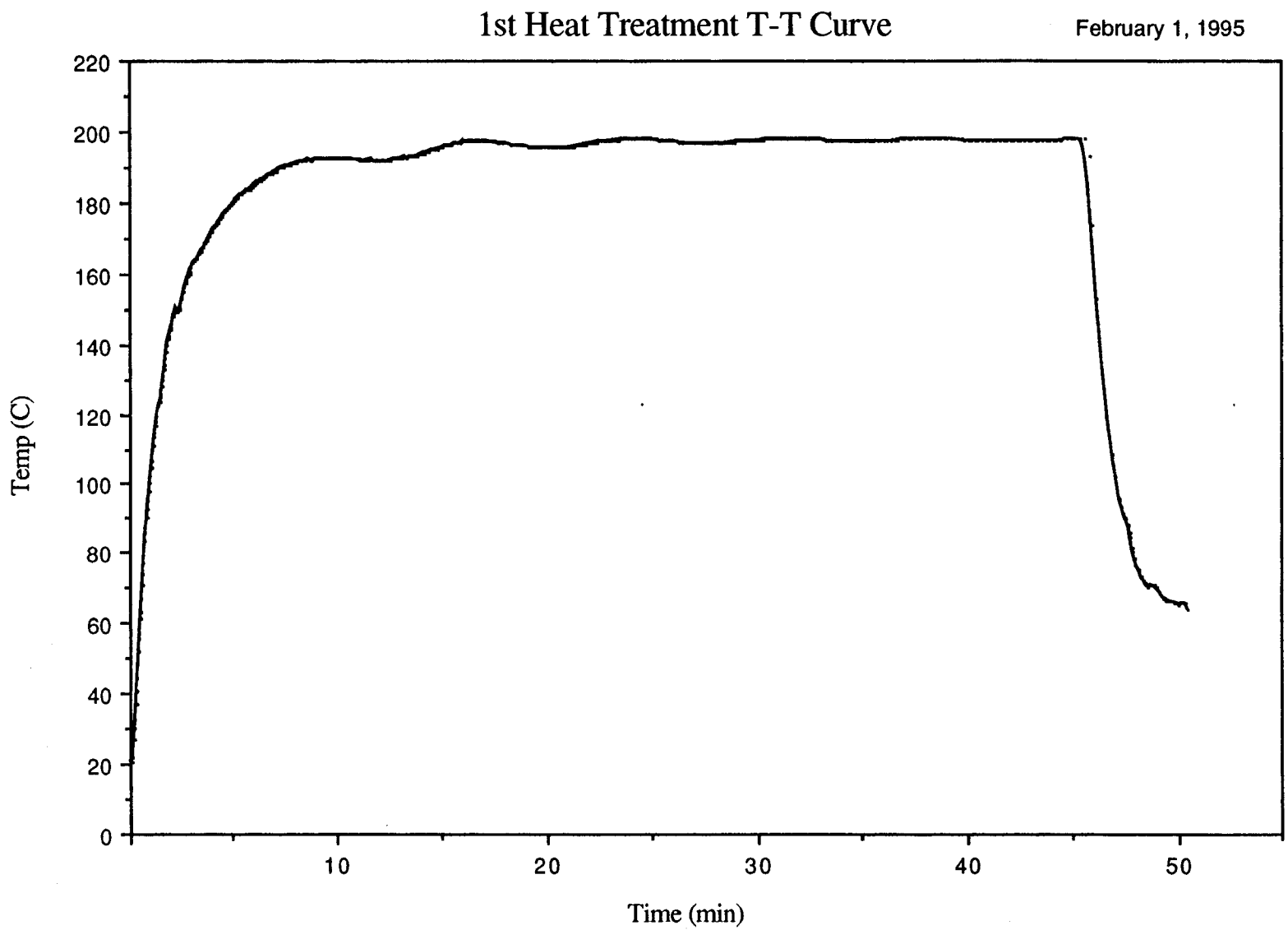

Figure A1 Time - Temperature plot for 0.5 hrs at 200°C

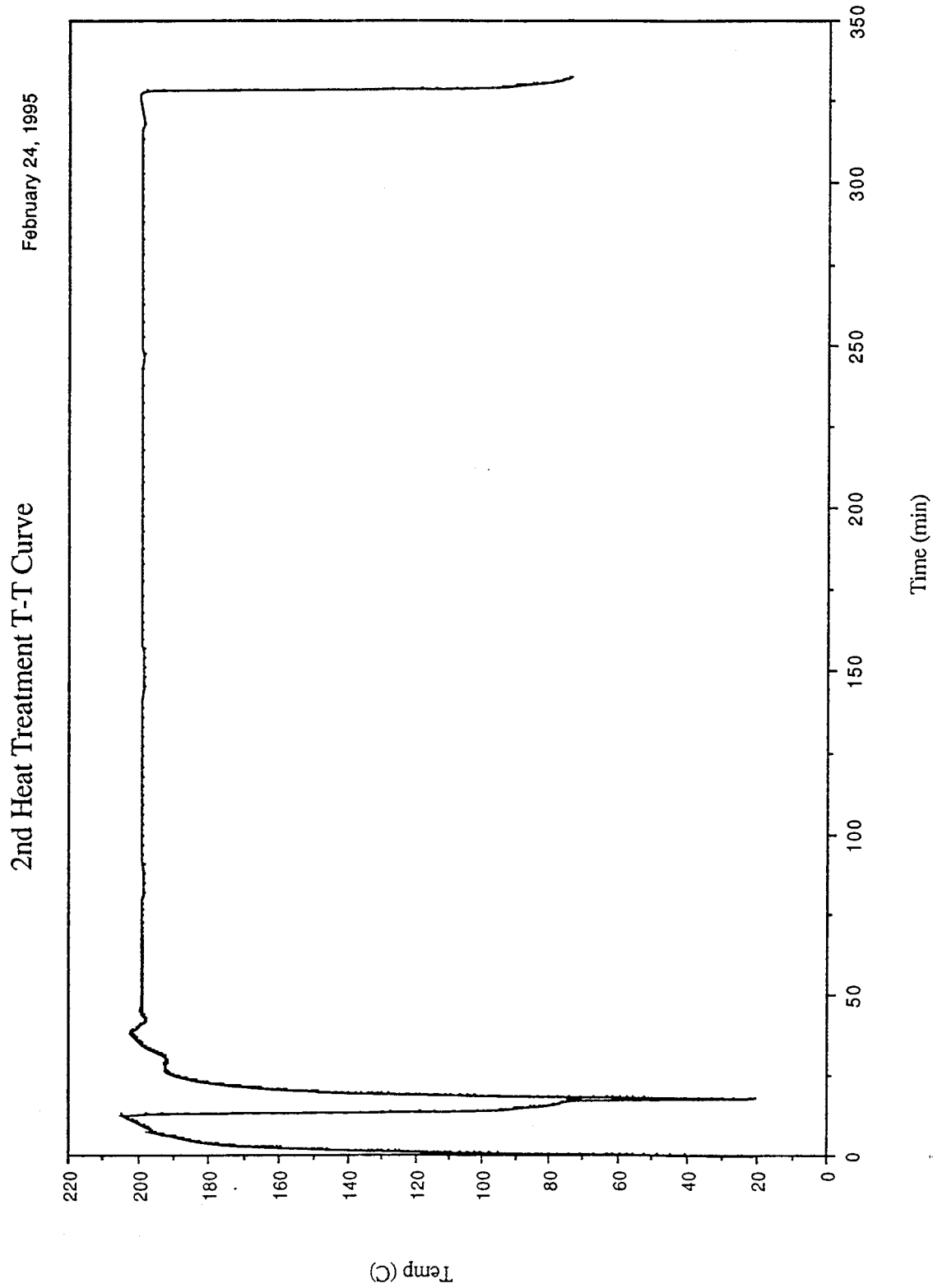

Figure A2 Time - Temperature plot for 5 hrs at 200°C

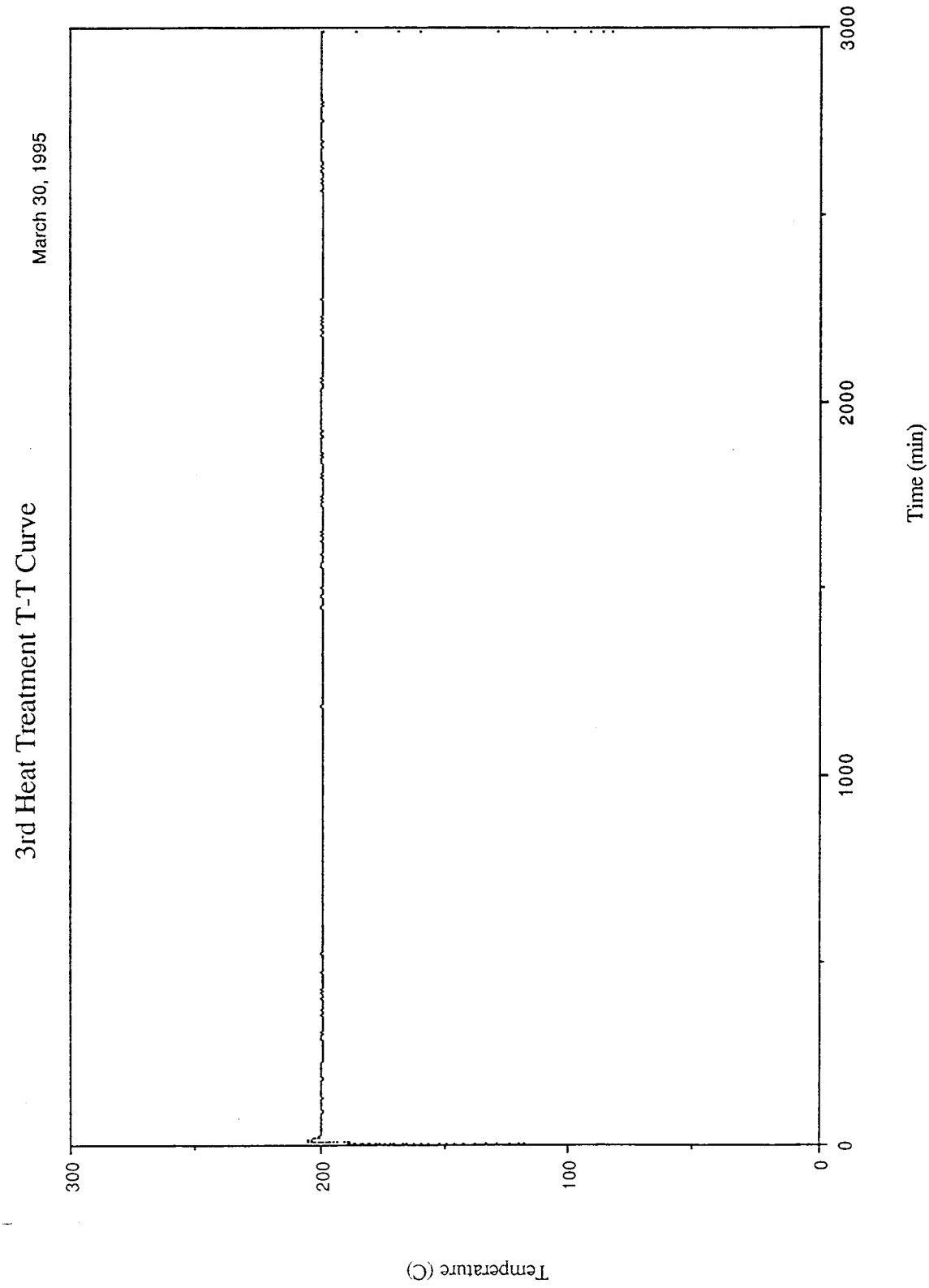

Figure A3 Time - Temperature plot for 50 hrs at 200°C

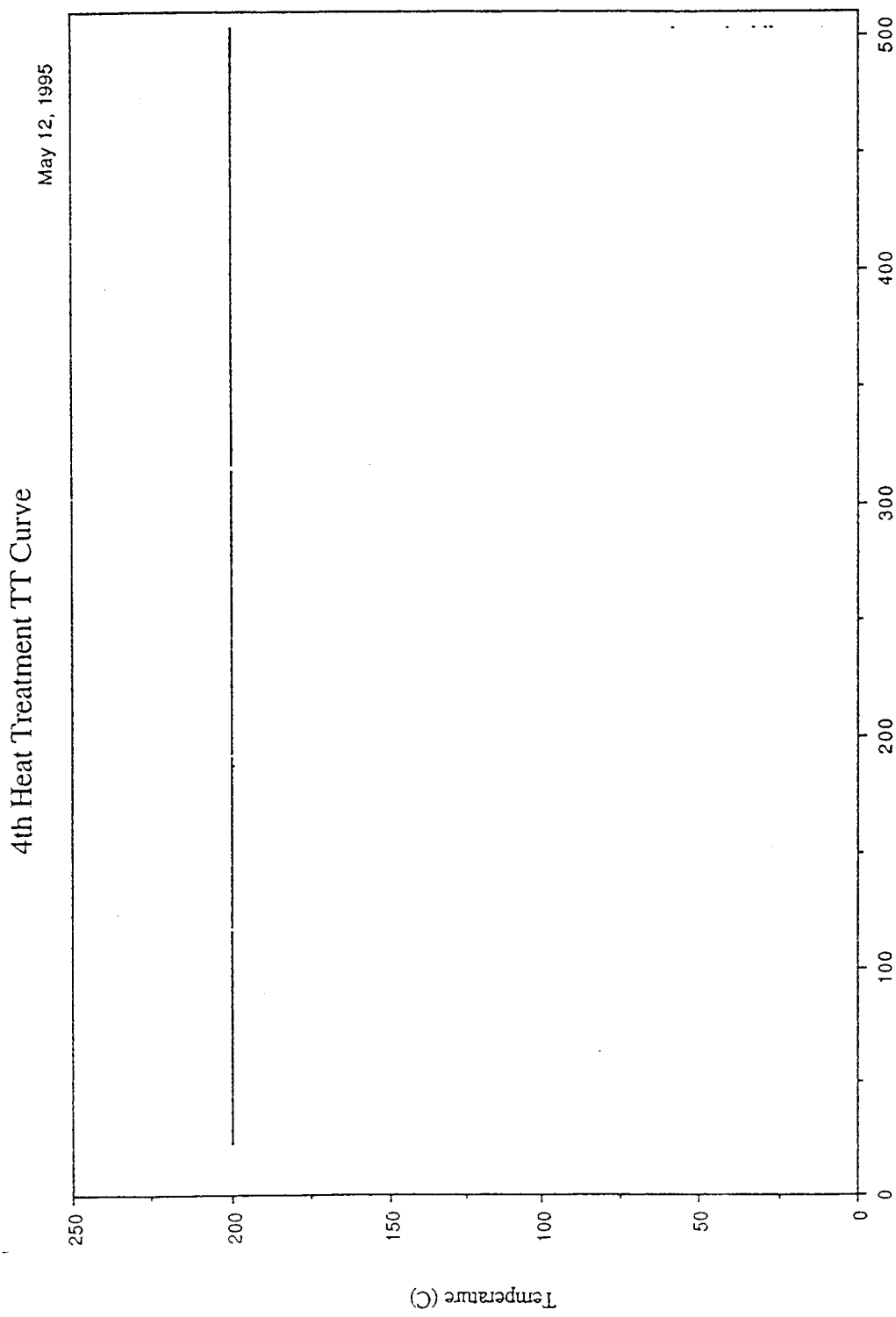

** The 4th heat treatment (500 hrs @ 200C) was performed after moving the oven away from the window. In the previous tests, the sample experienced about one degree C of variation throughout the day and night (199C to 200C).

Figure A4 Time - Temperature plot for 500 hrs at 200°C

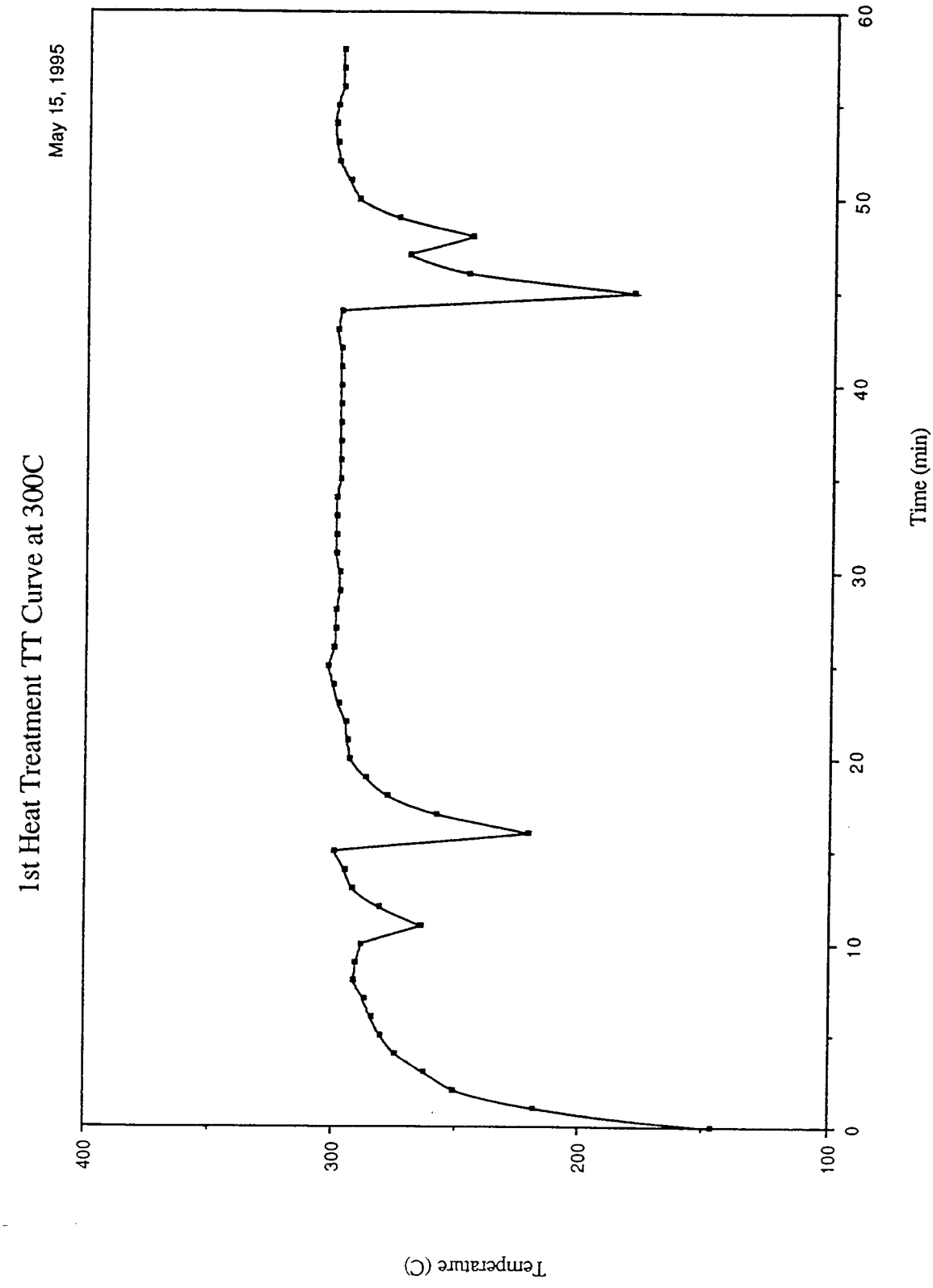

Figure A5 Time - Temperature plot for 0.5 hrs at 300°C

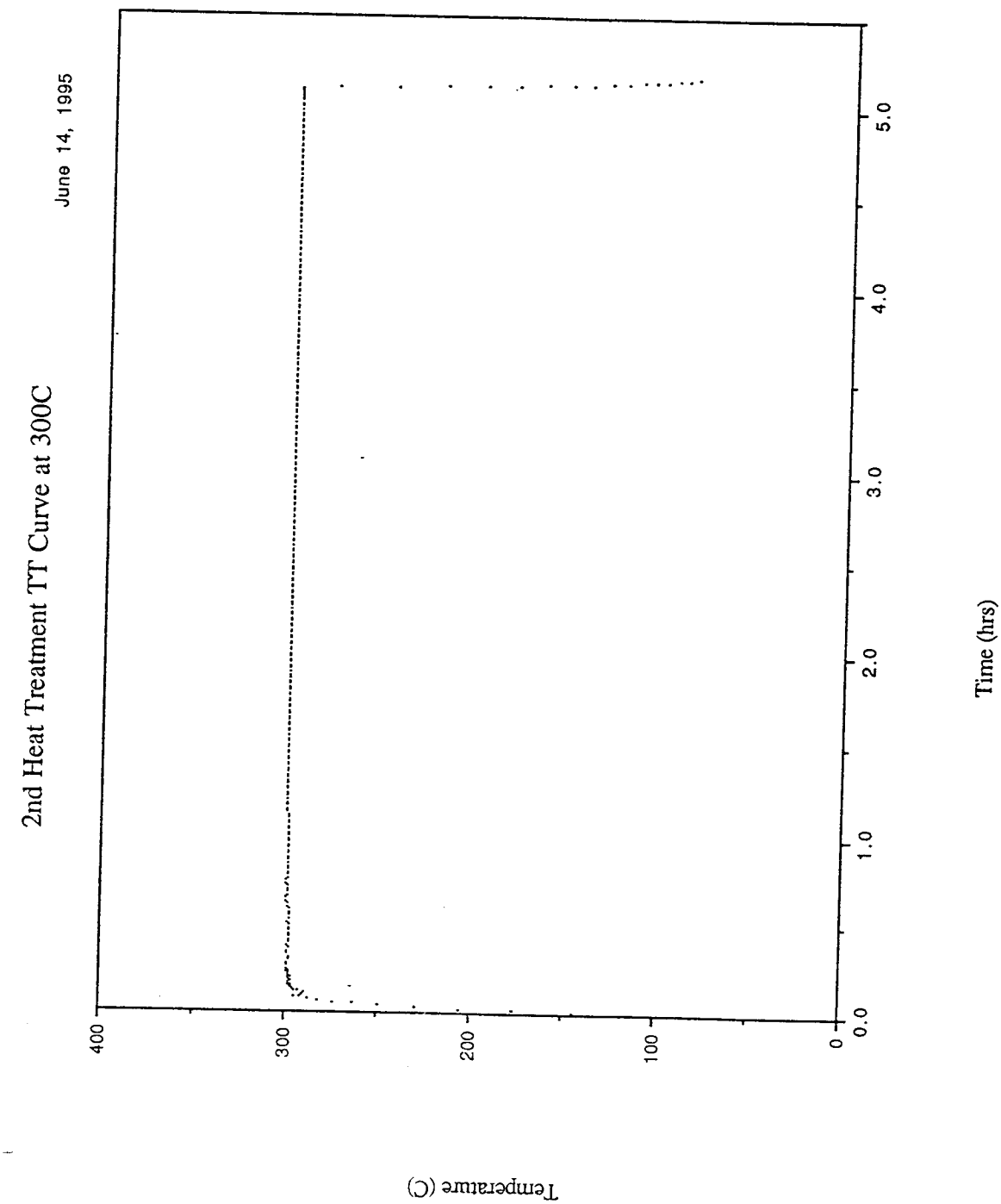

Figure A6 Time - Temperature plot for 5 hrs at 300°C

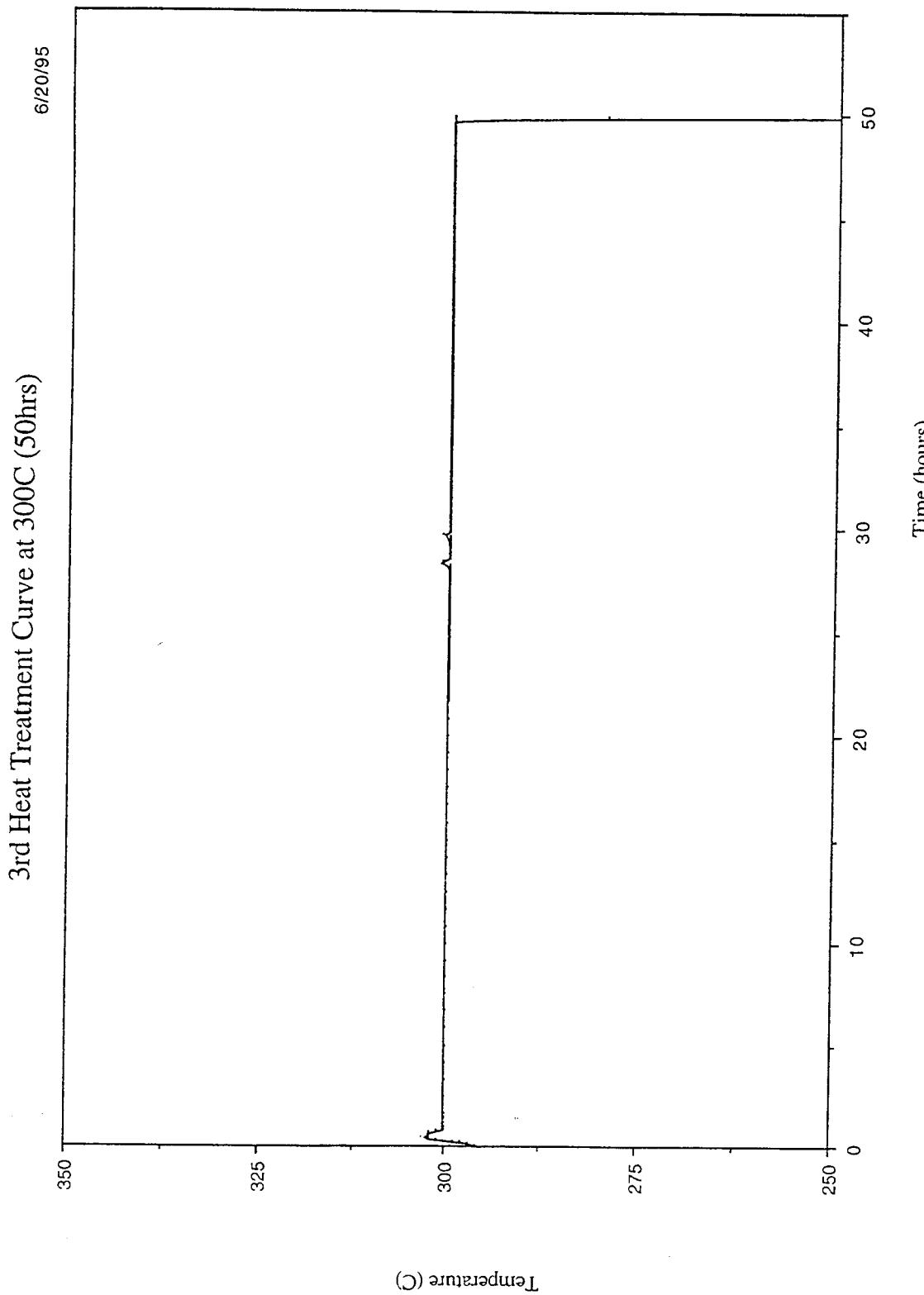

Figure A7 Time - Temperature plot for 50 hrs at 300°C

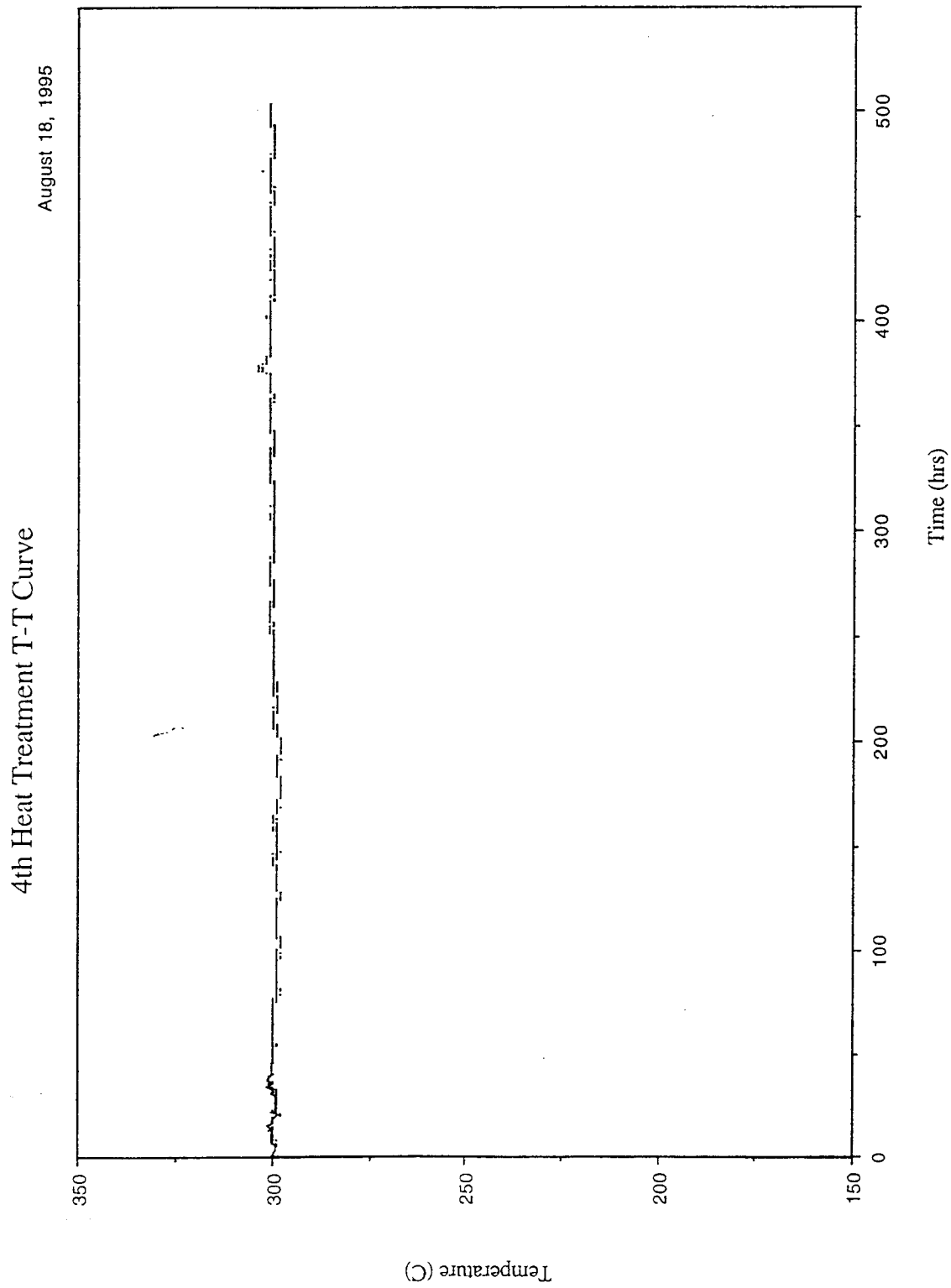

Figure A8 Time - Temperature plot for 500 hrs at 300°C

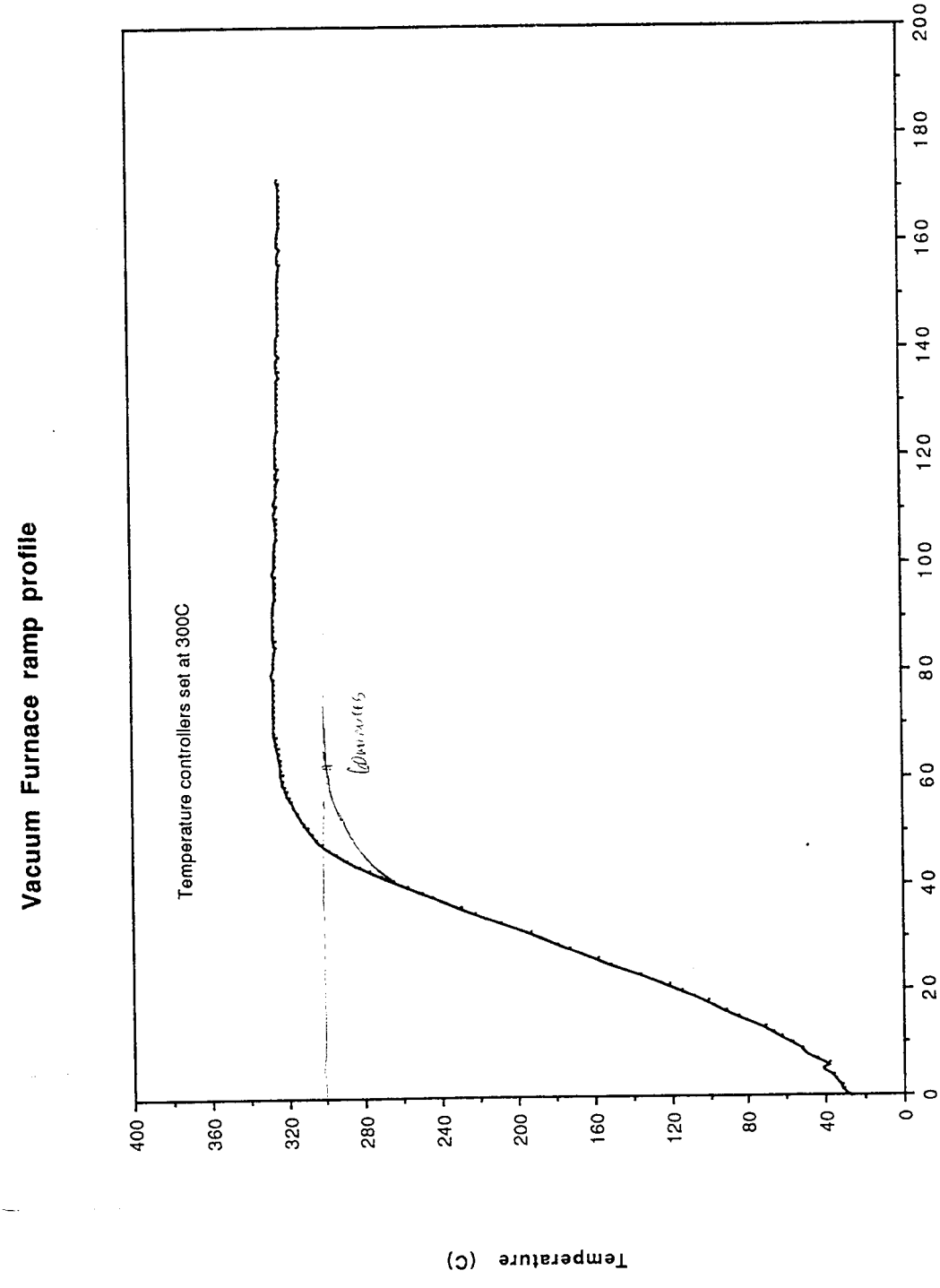

Figure A9 Vacuum furnace temperature ramp up profile

Appendix B Hardness Profiles

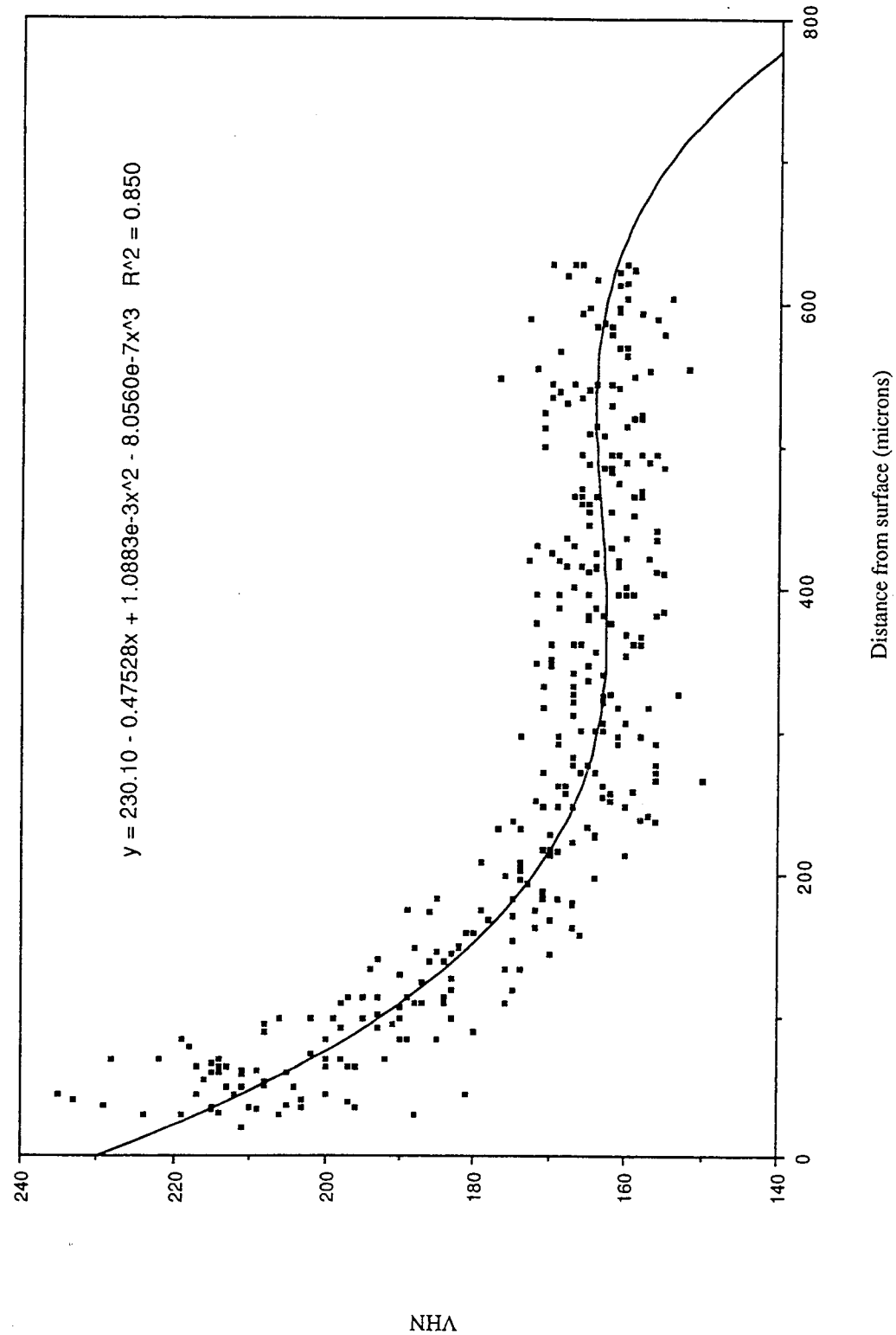

Figure B1 Hardness profile for the initial condition for samples AA1, BB1, and CC1 (for 200°C annealing)

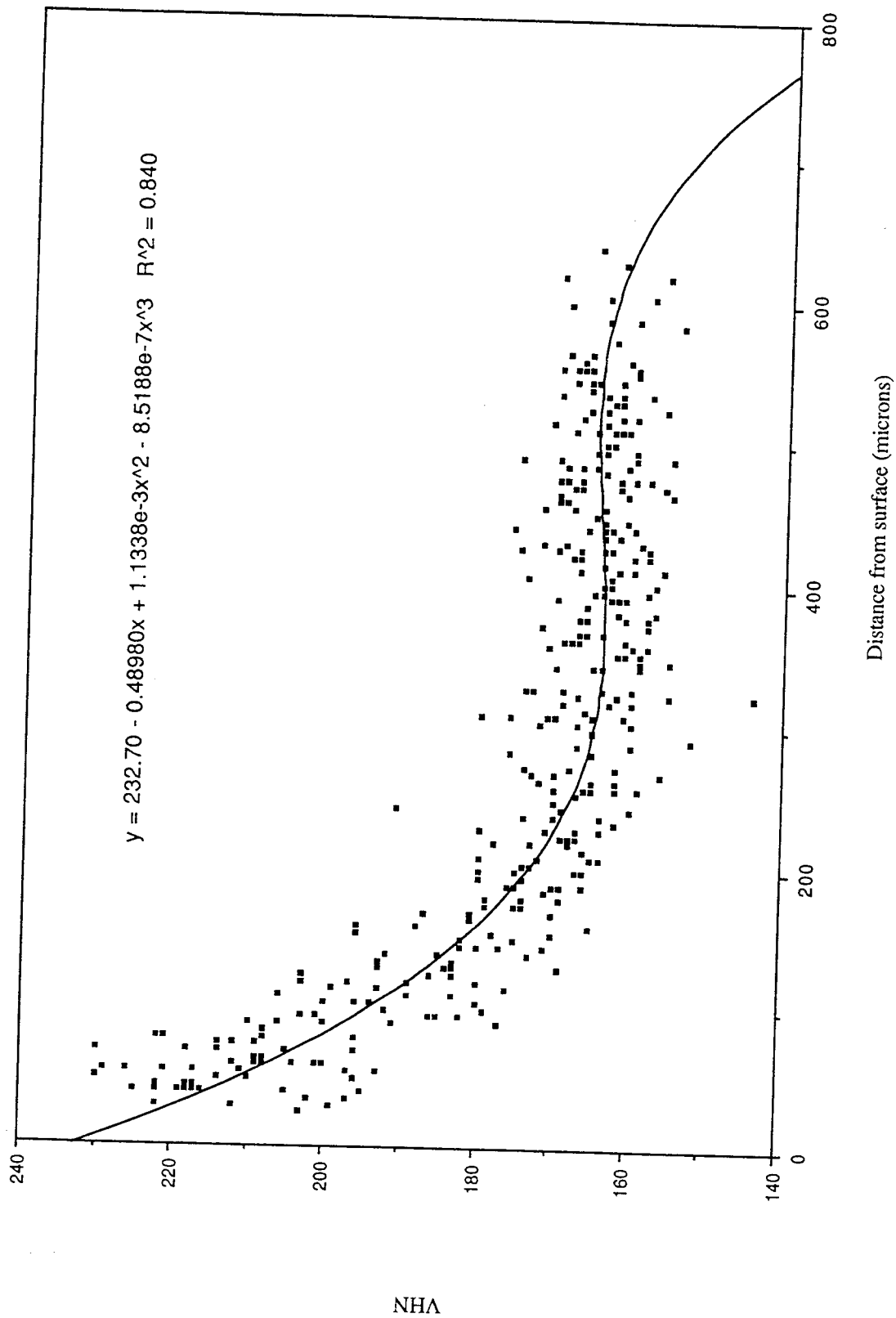

Figure B2 Hardness profile after 0.5 hours at 200°C

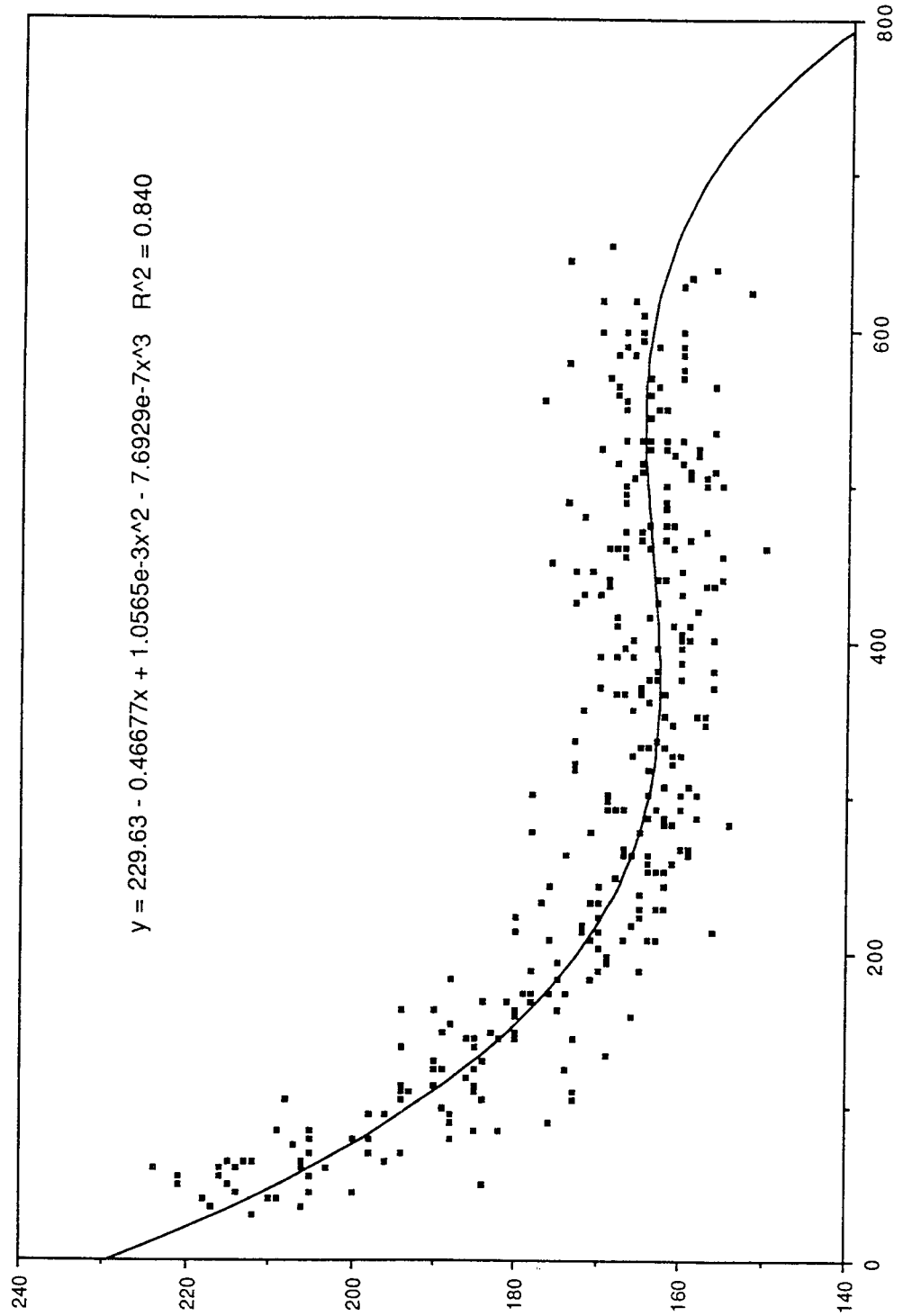

Figure B3 Hardness profile after 5.5 hours at 200°C

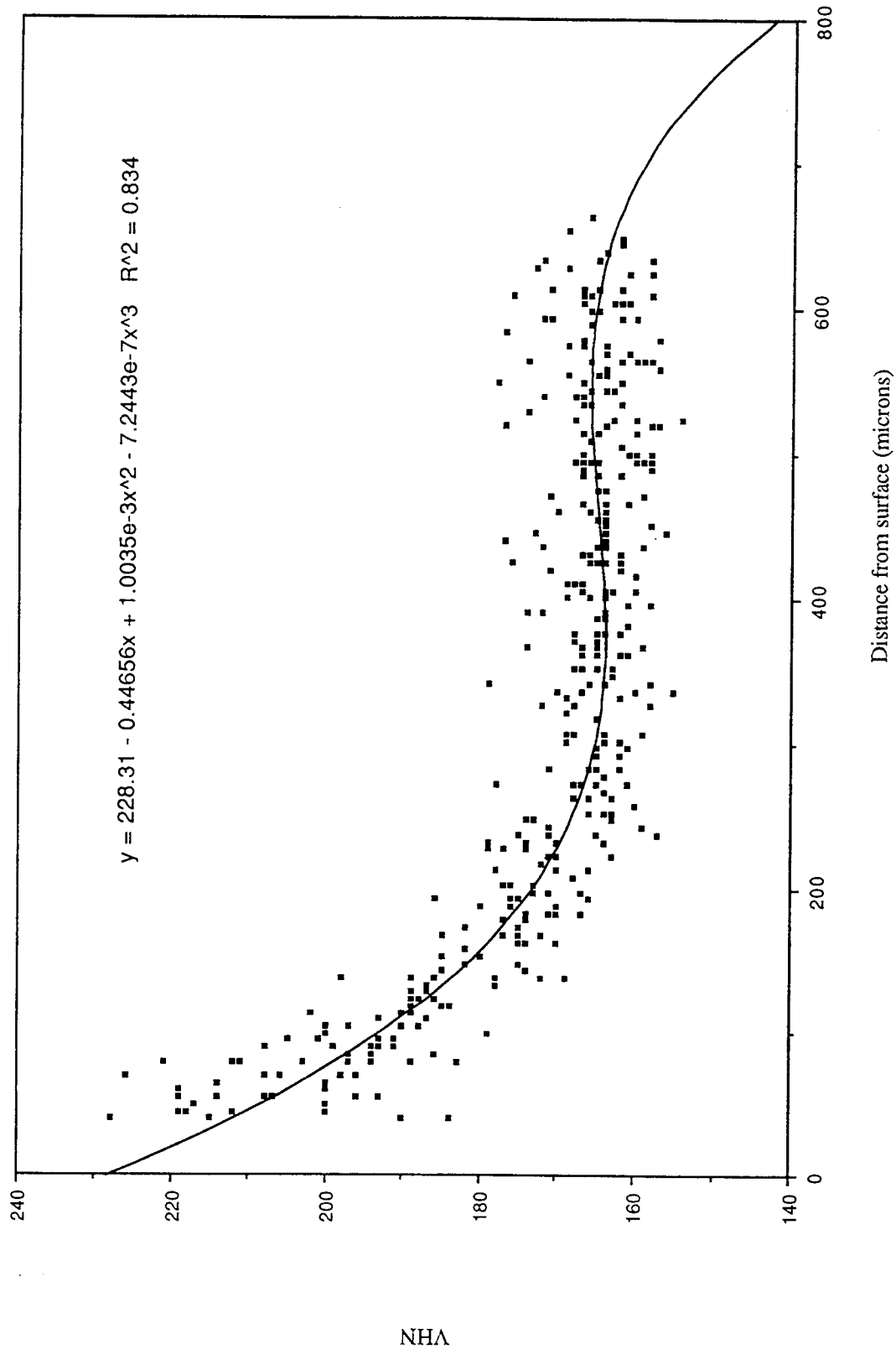

Figure B4 Hardness profile after 55.5 hours at 200°C

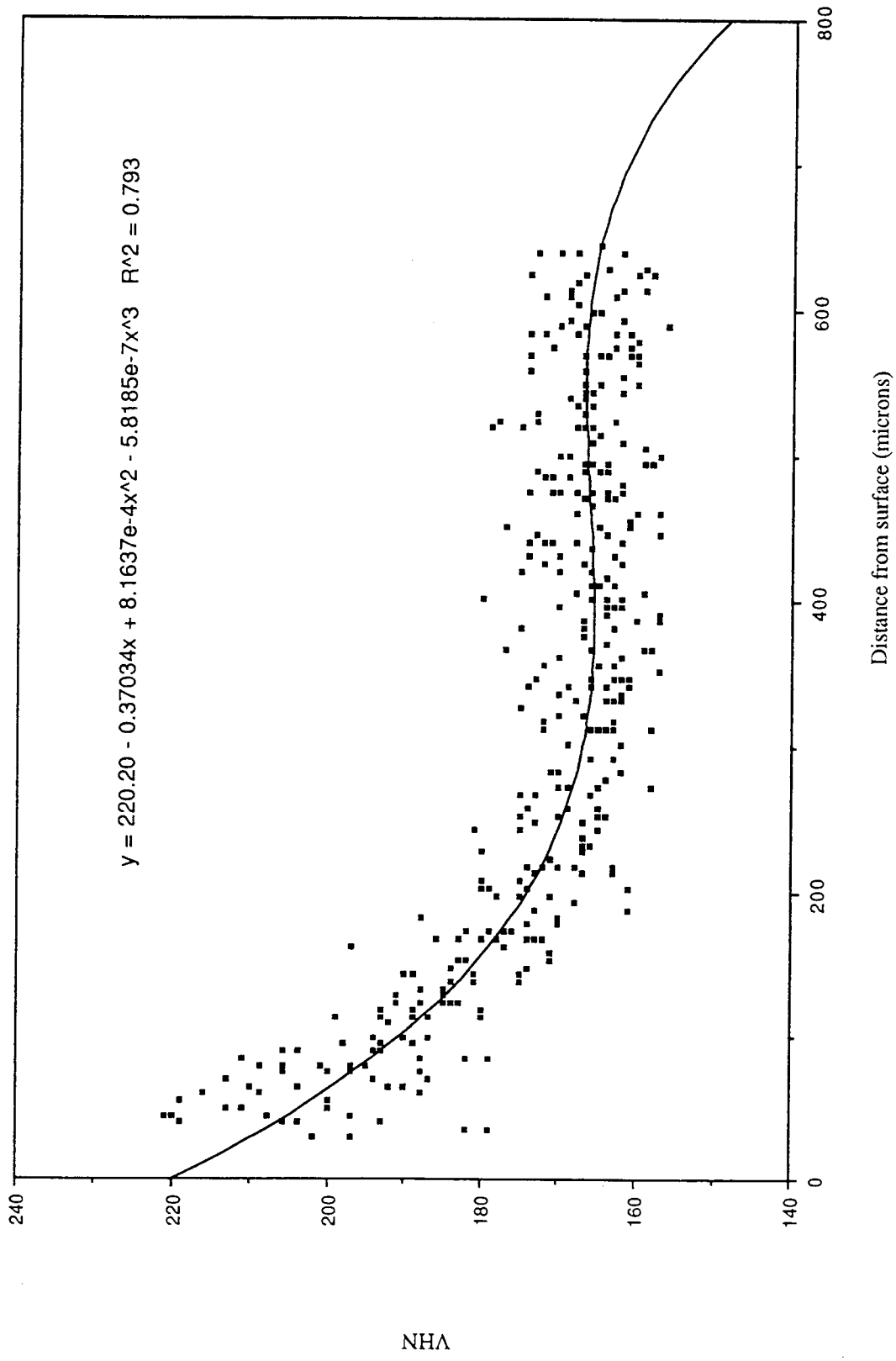

Figure B5 Hardness profile after 560 hours at 200°C

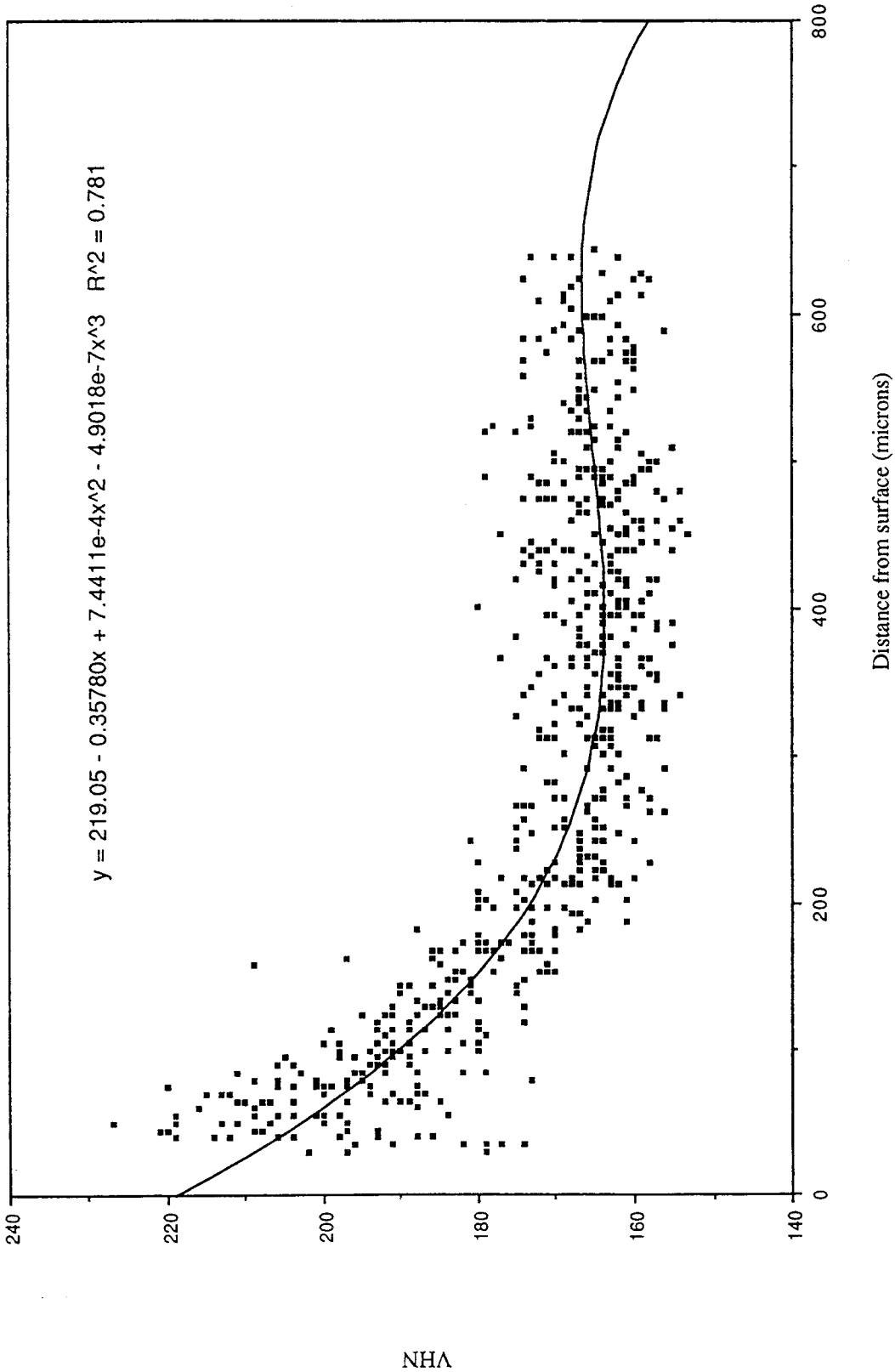

Figure B6 Hardness profile/ and reprofile after 560 hours at 200°C

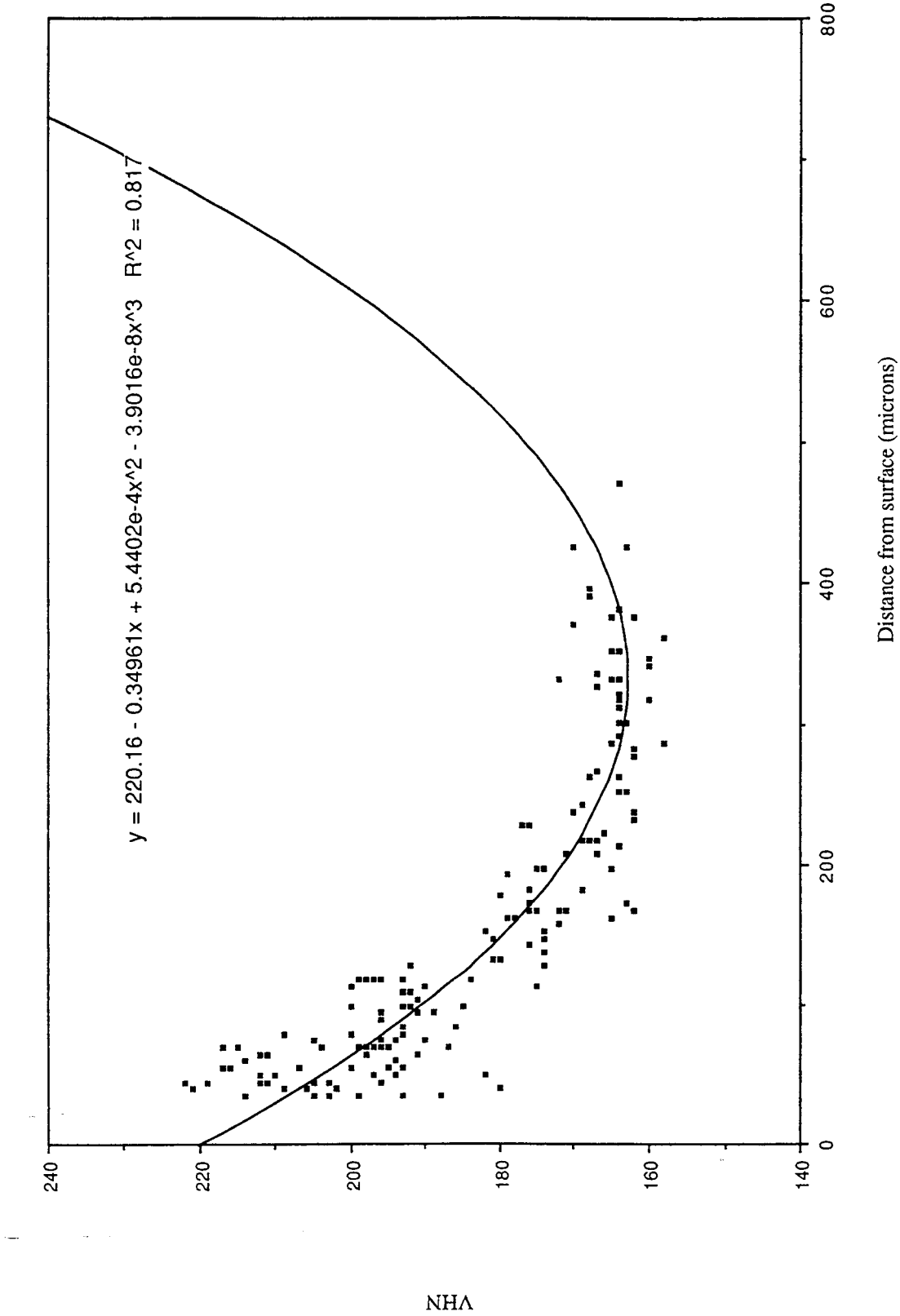

Figure B7 Hardness profile after 2244 hours at 200°C

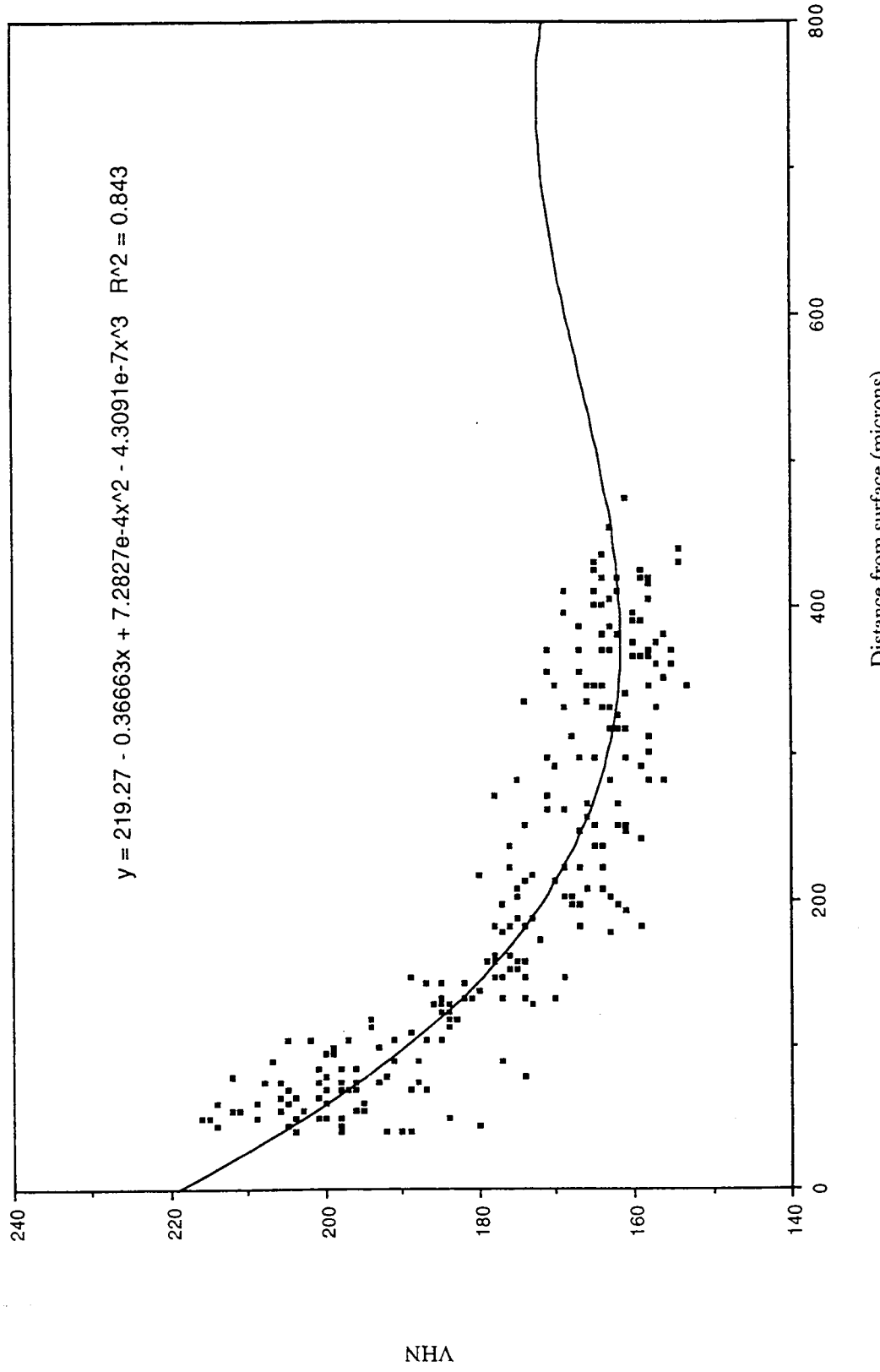

Figure B8 Hardness profile after 4458 hours at 200°C

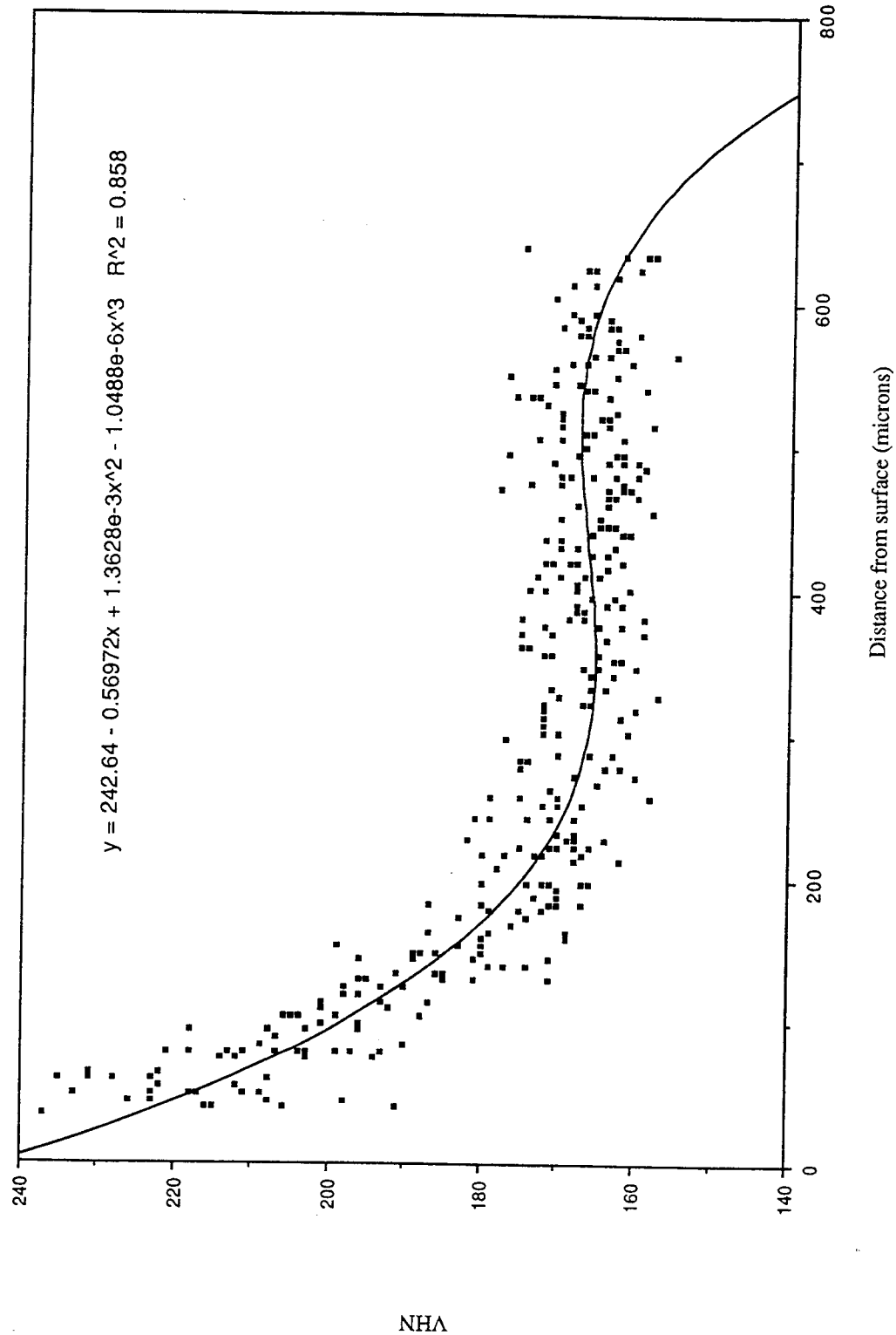

Figure B9 Hardness profile for the initial condition for samples AA2, BB2, and CC2 (for 300°C annealing)

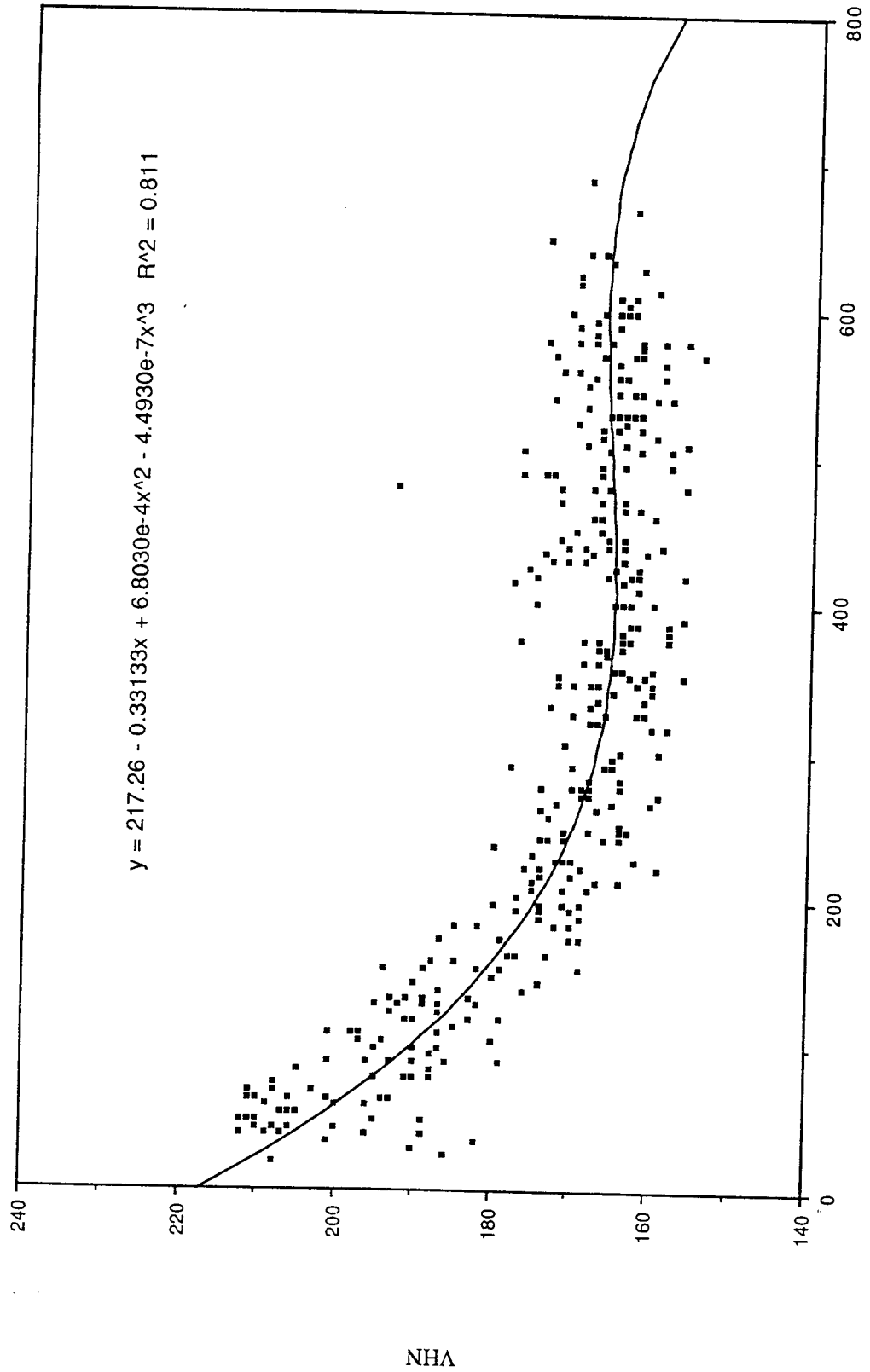

Figure B10 Hardness profile after 0.5 hours at 300°C

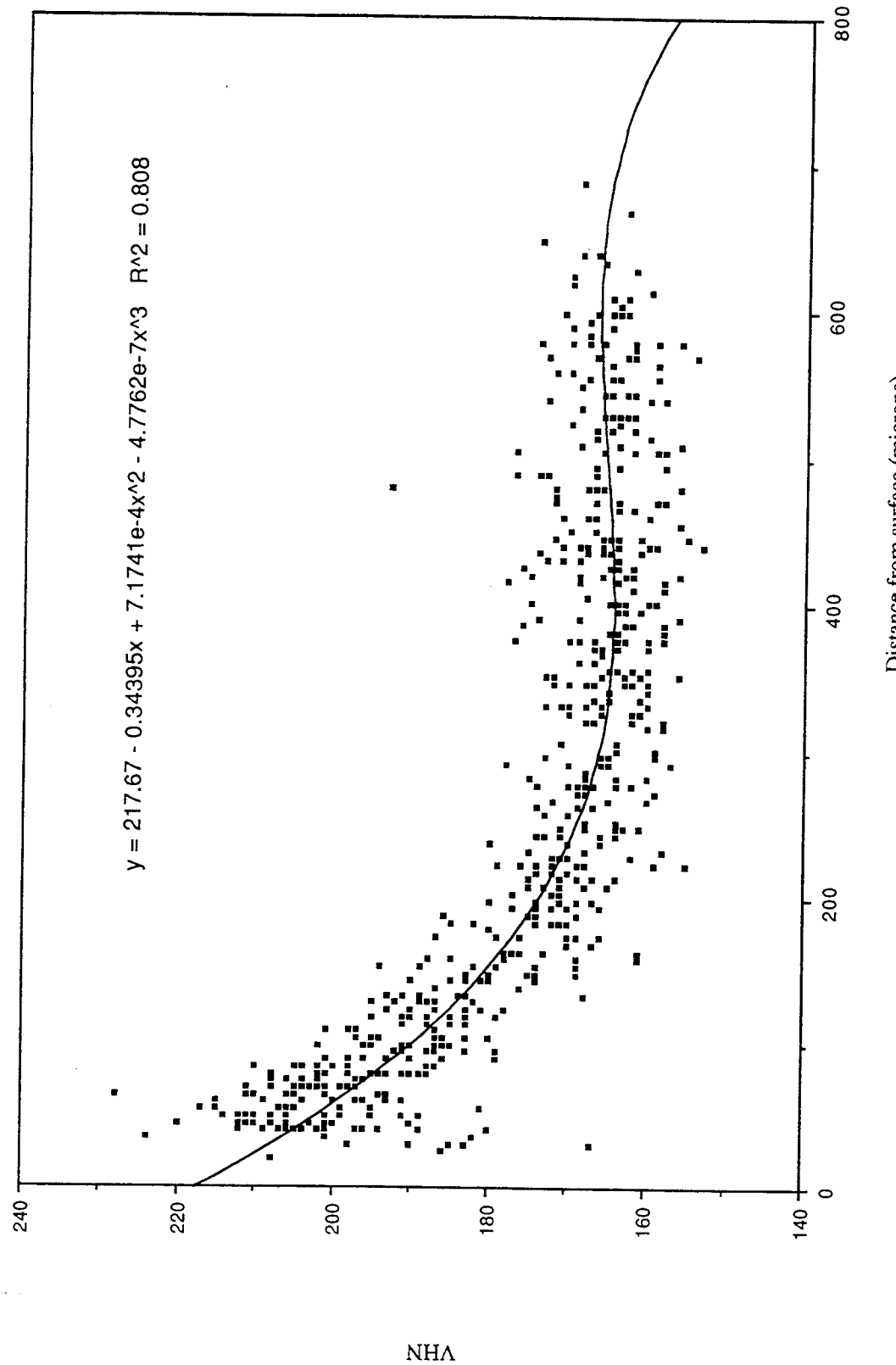

Figure B11 Hardness profile/ reprofile after 0.5 hours at 300°C

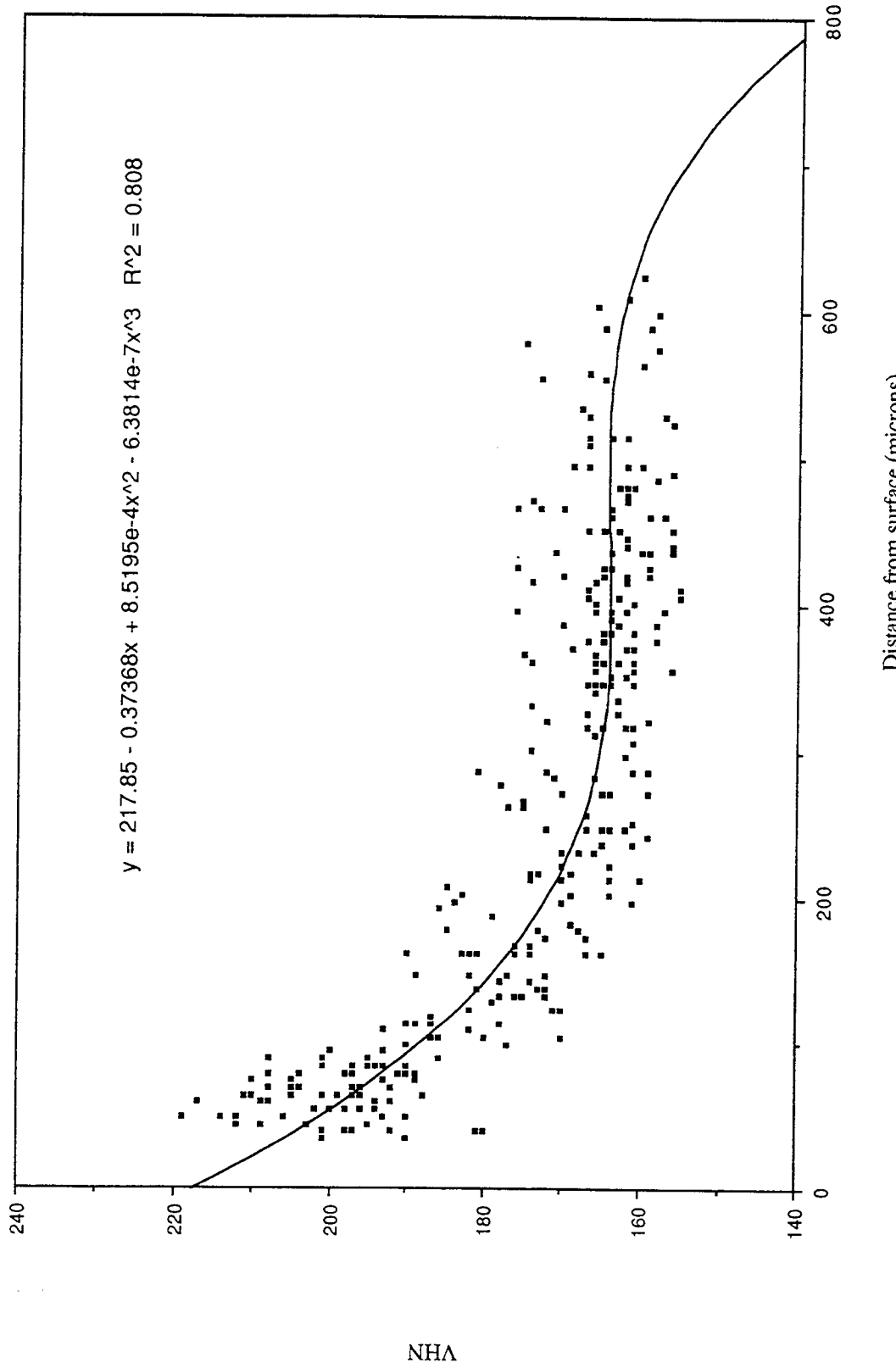

Figure B12 Hardness profile after 5.5 hours at 300°C

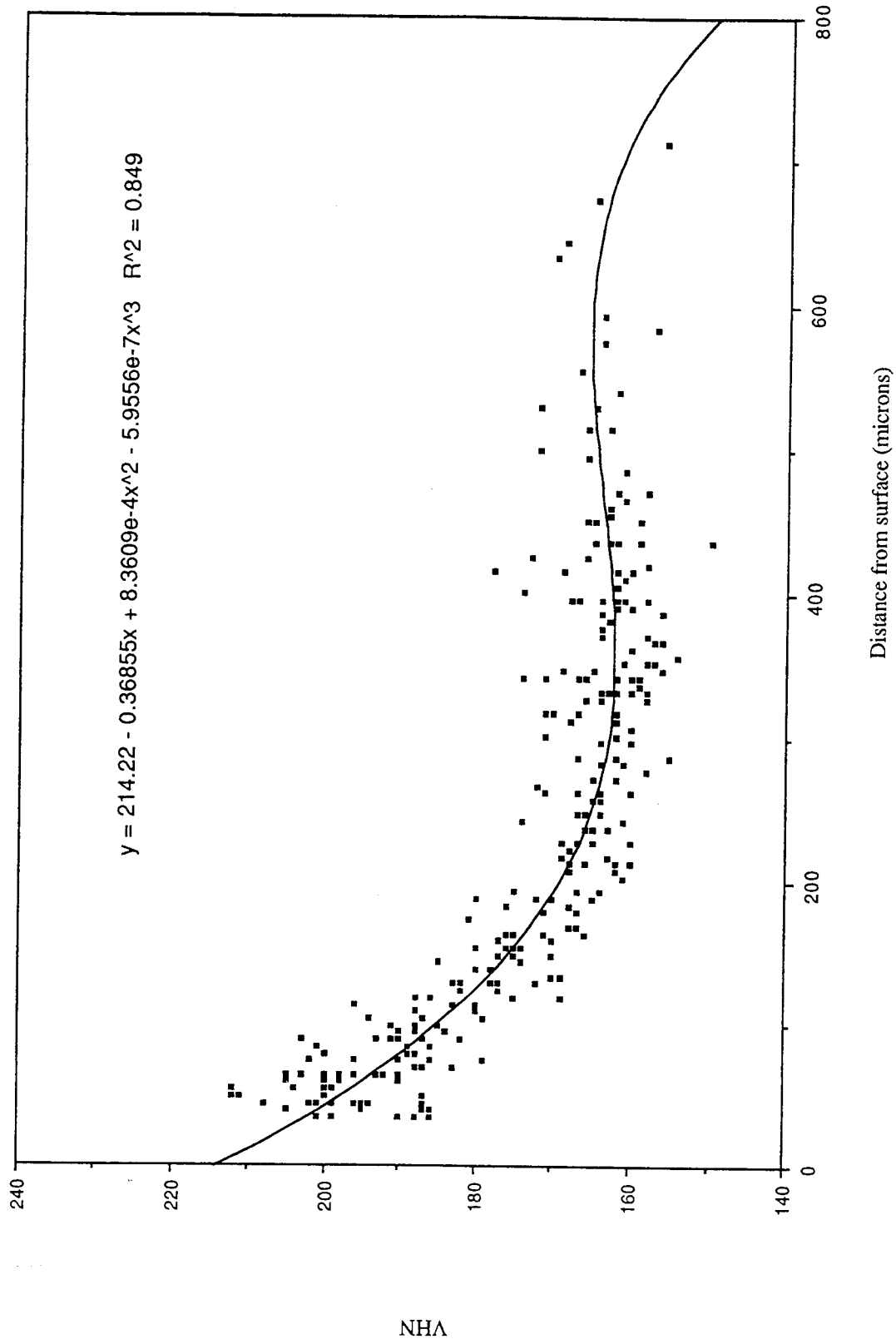

Figure B13 Hardness profile after 55.5 hours at 300°C

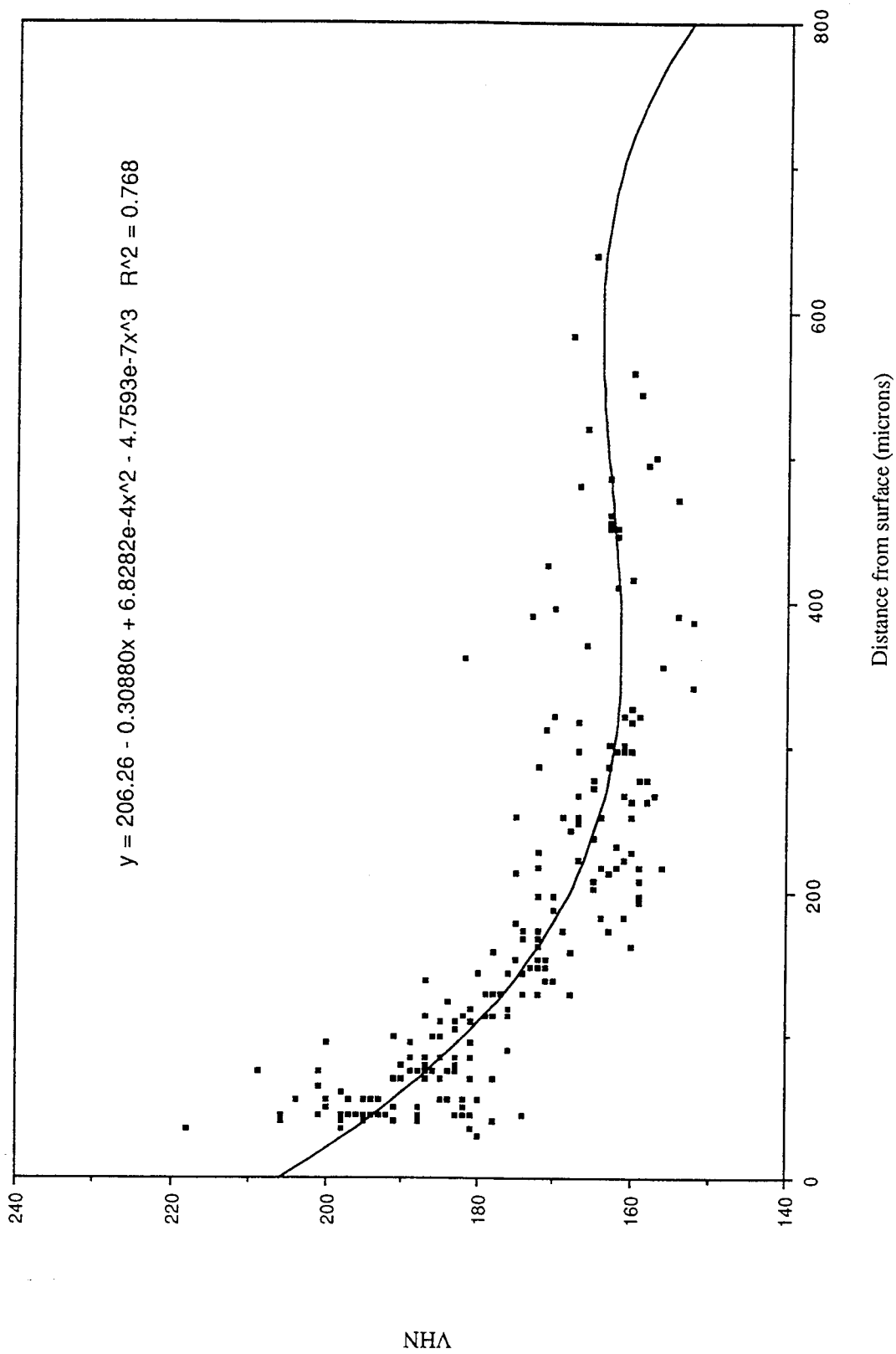

Figure B14 Hardness profile after 557 hours at 300°C

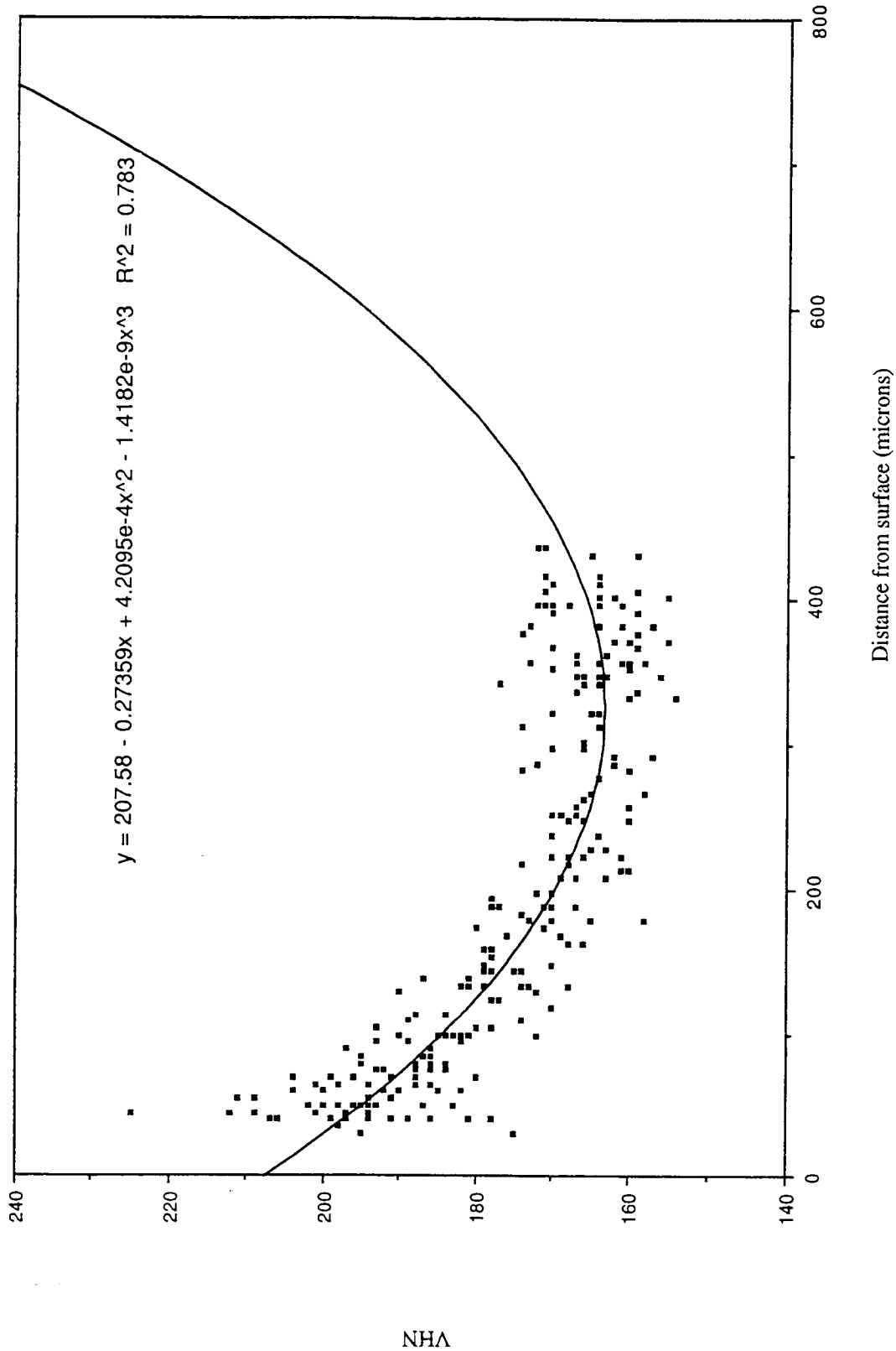

Figure B15 Hardness profile after 2790 hours at 300°C

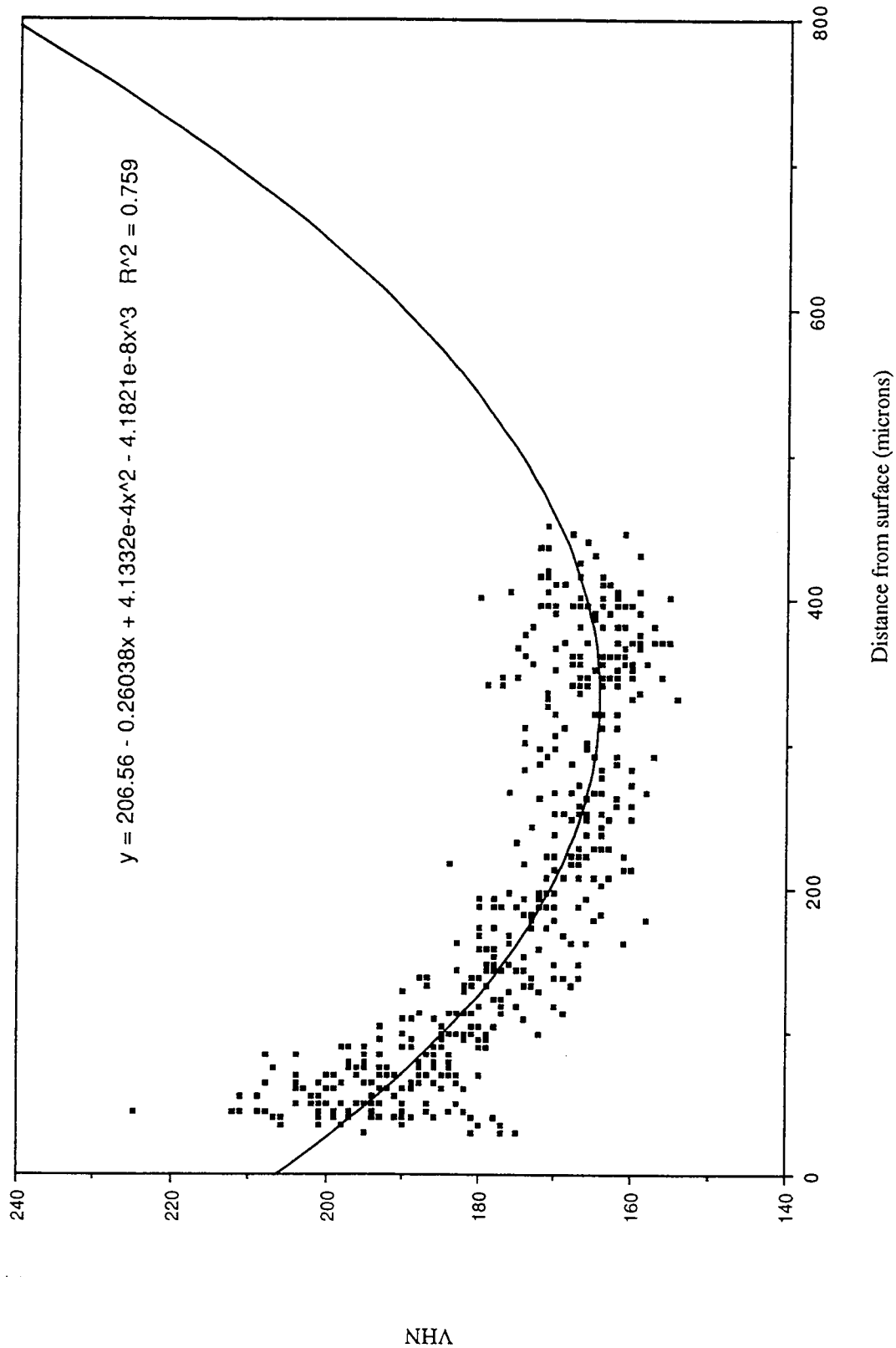

Figure B16 Hardness profile/ reprofile after 2790 hours at 300°C

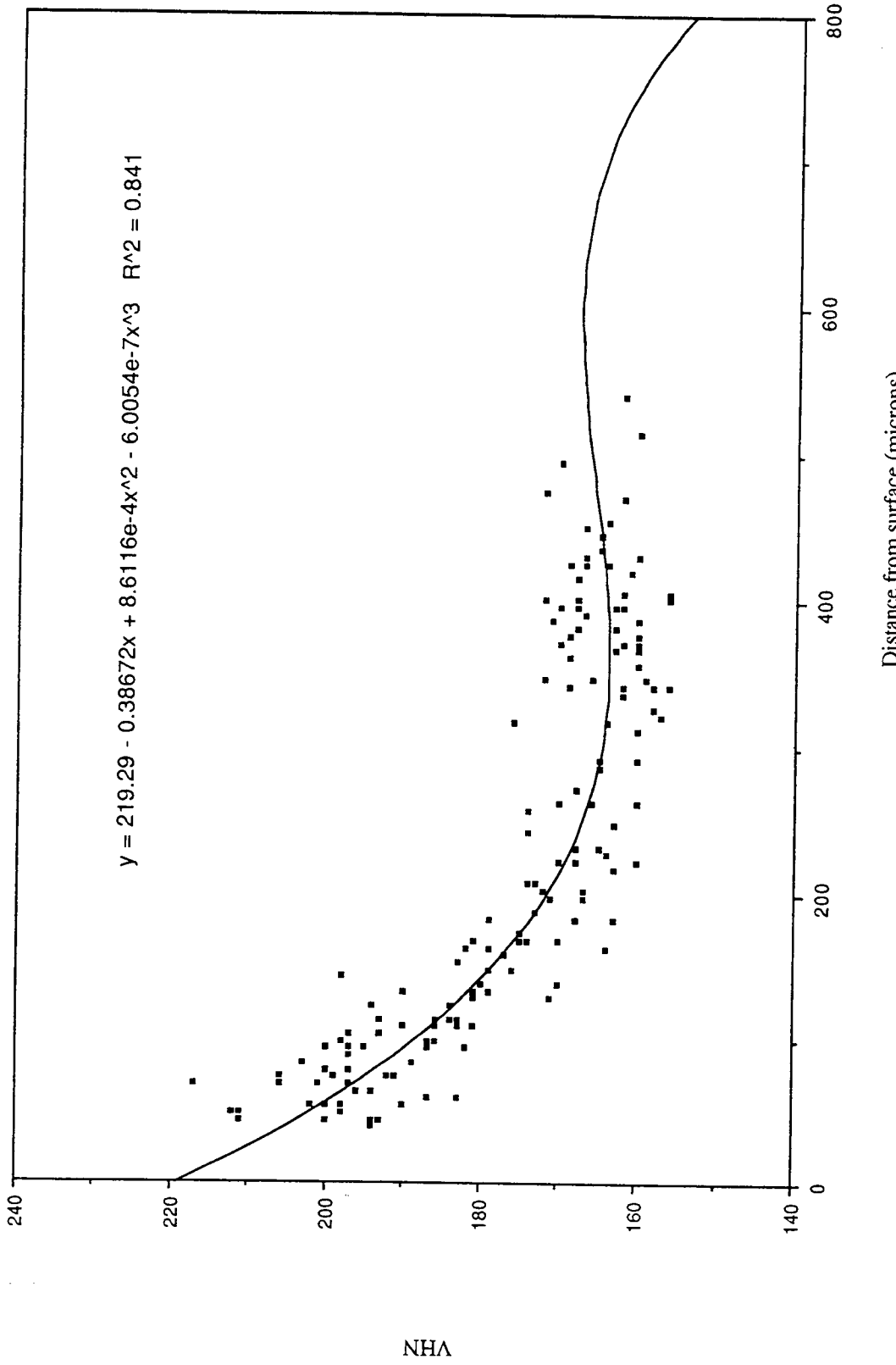

Figure B17 Hardness profile after 1.5 hours at 300°C under vacuum

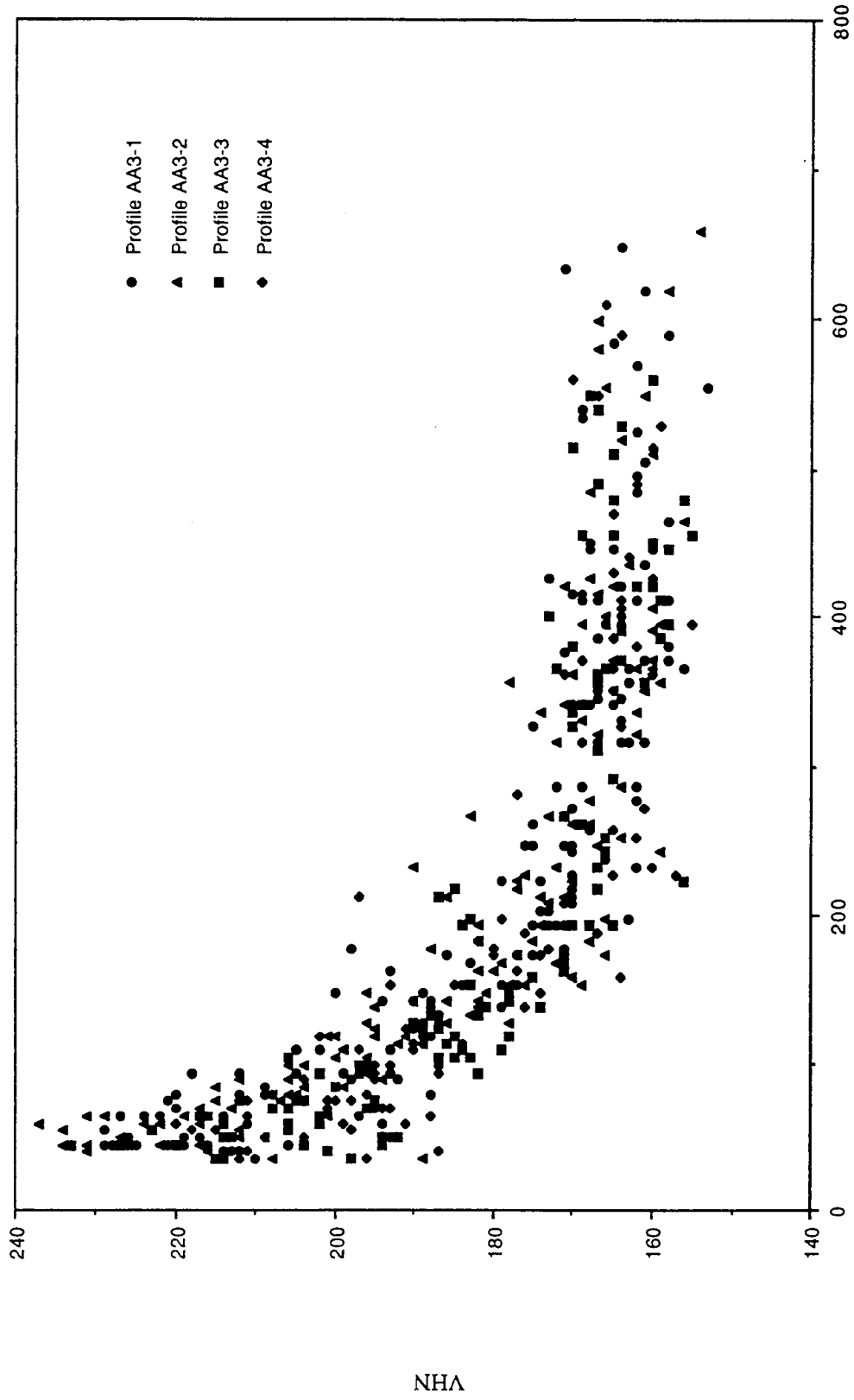

Figure B18 All AA3 (control) hardness data

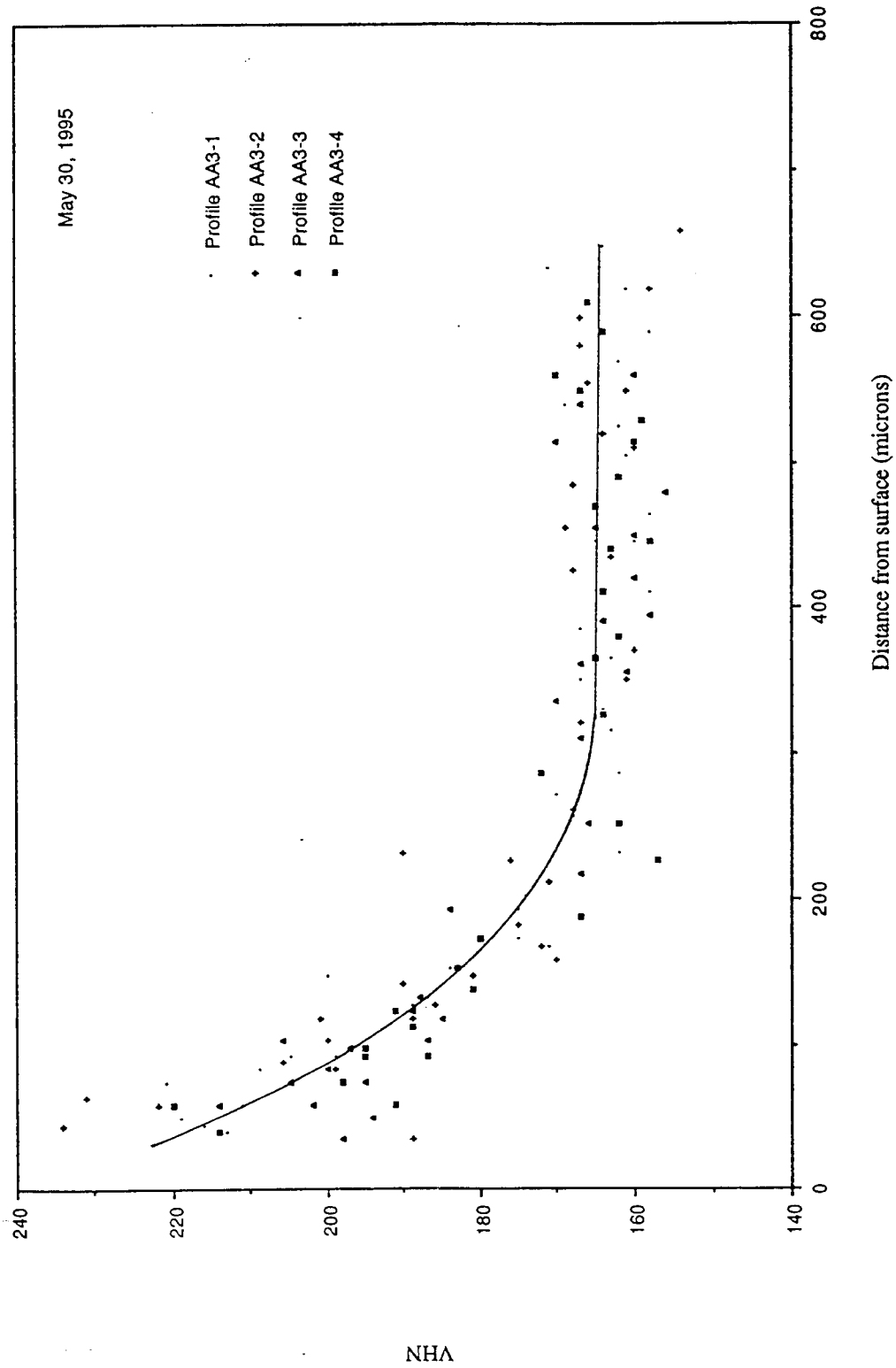

Figure B19 Control (AA3) hardness profile after 560 hours at 200°C and 0.5 hours at 300°C

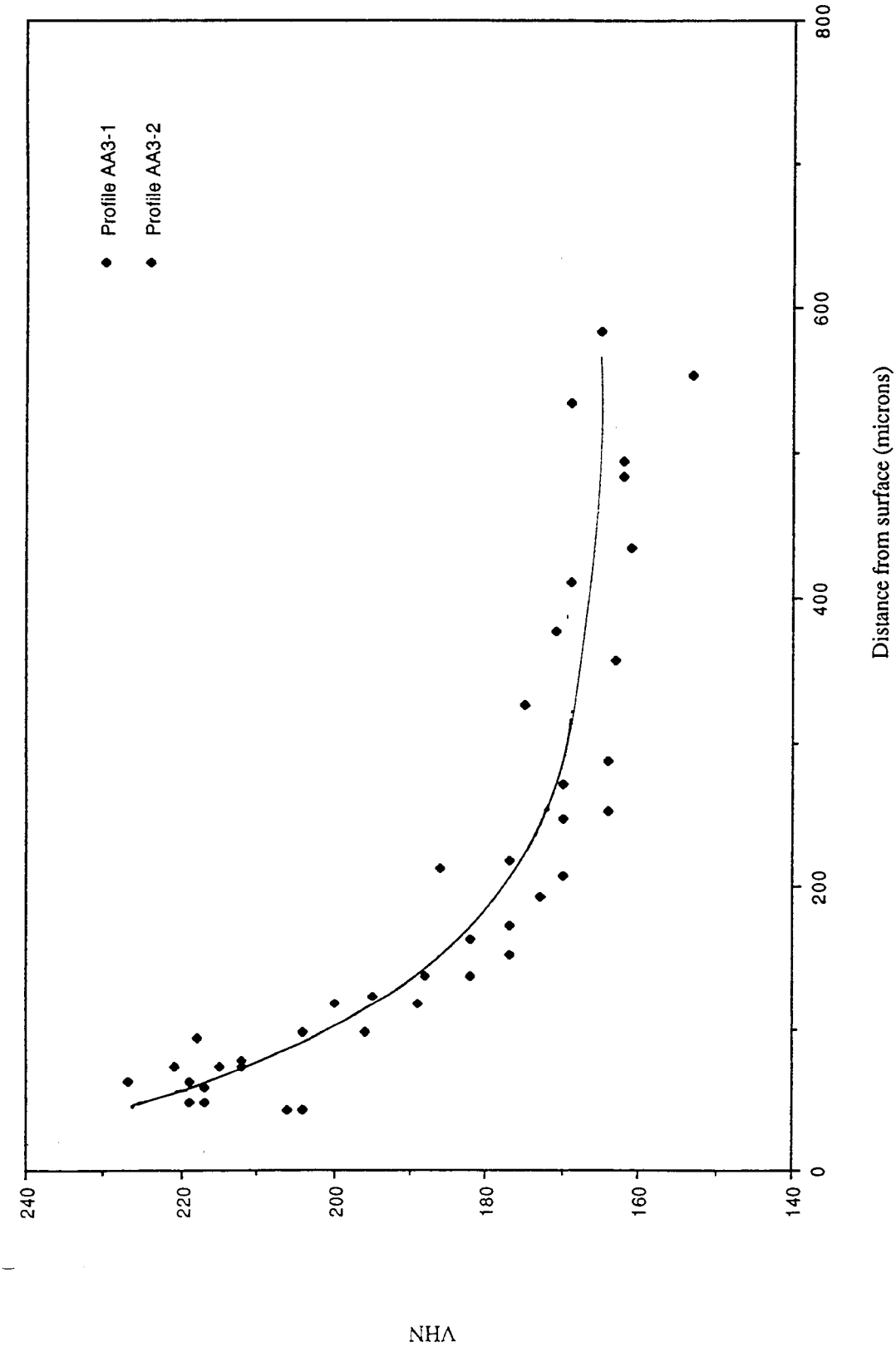

Figure B20 Control (AA3) hardness profile after 5.5 hours at 300°C

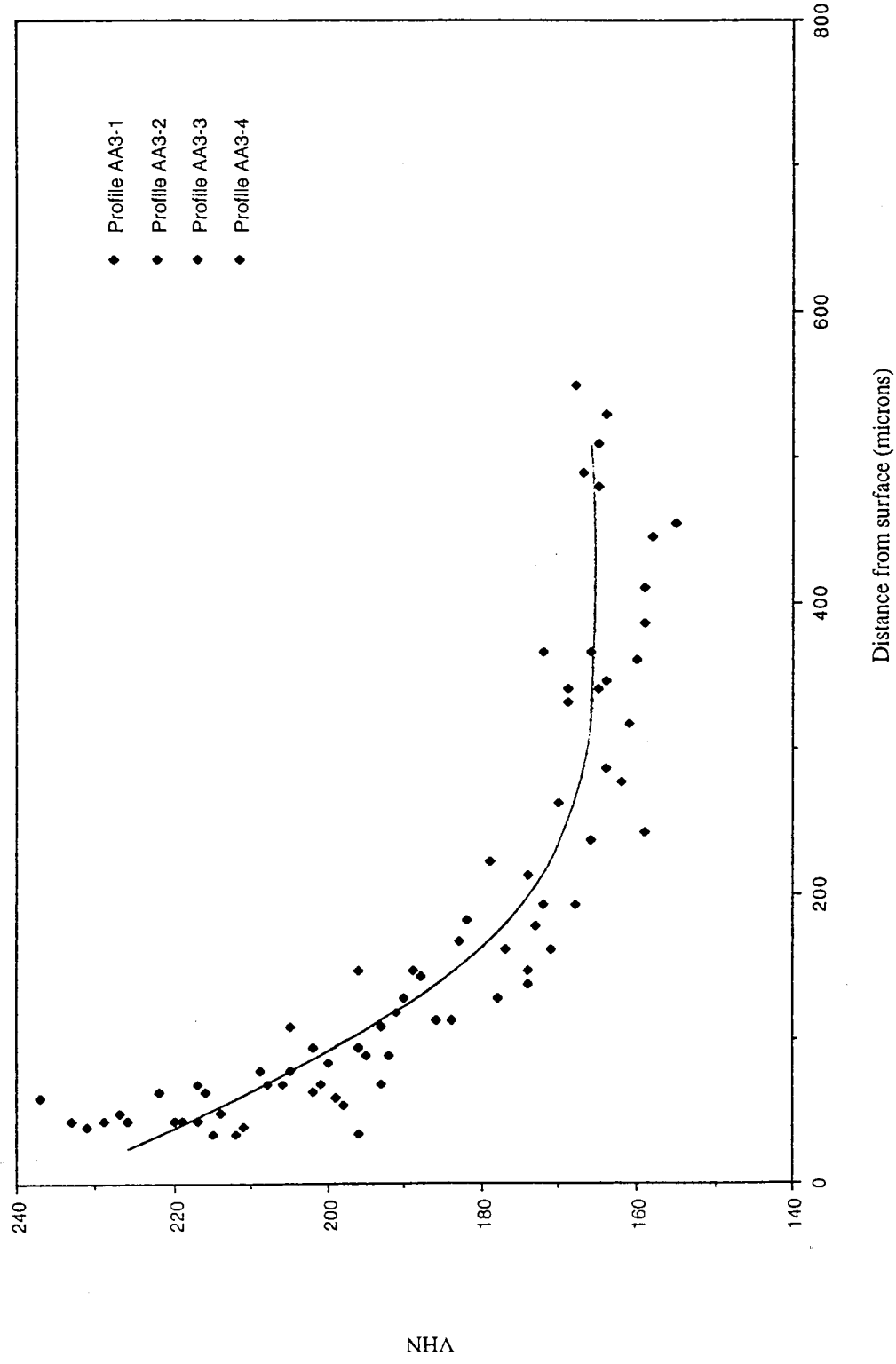

Figure B21 Control (AA3) hardness profile after 55.5 hours at 300°C

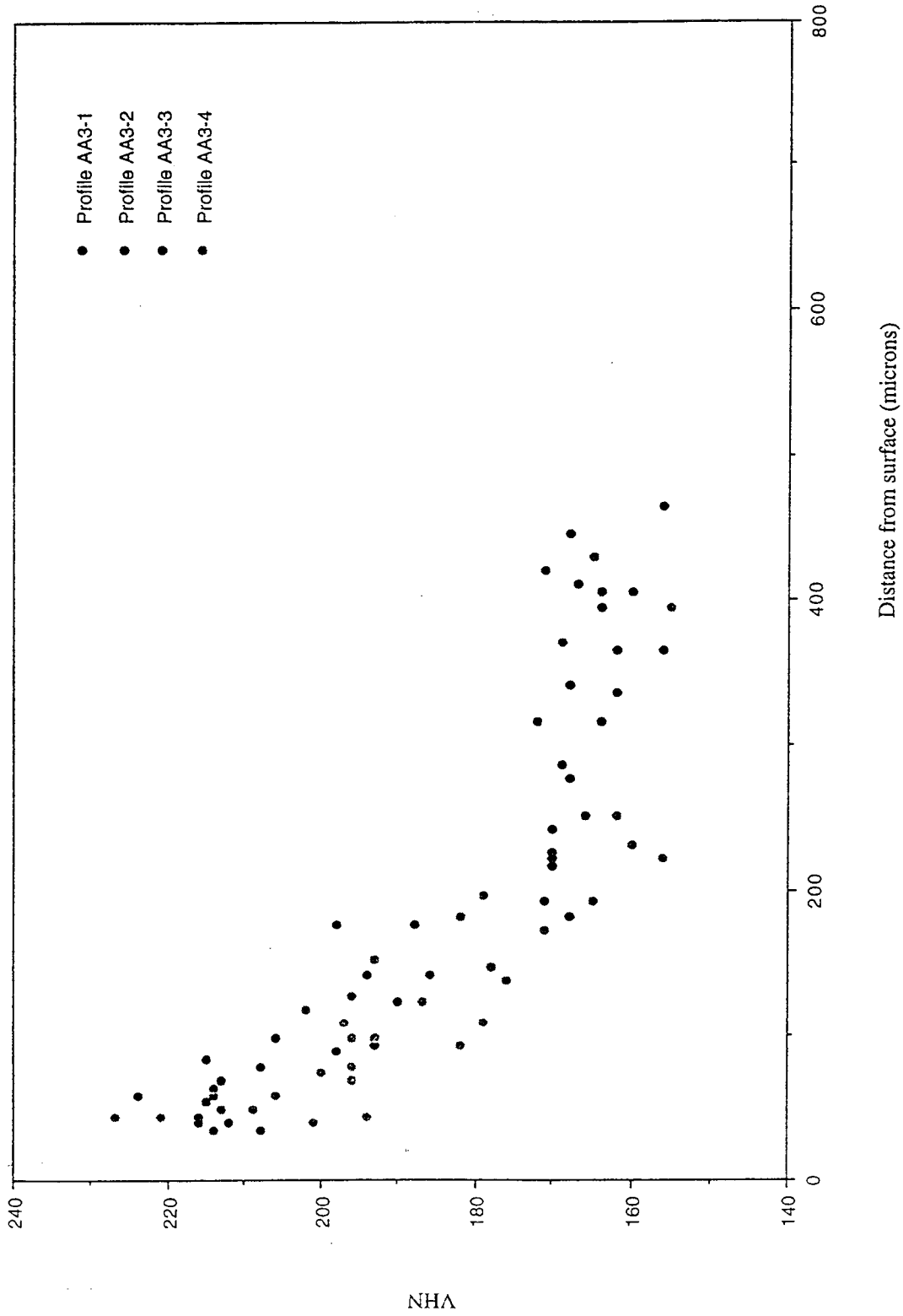

Figure B22 Control (AA3) hardness profile after 2244 hours at 200°C and 557 hours at 300°C

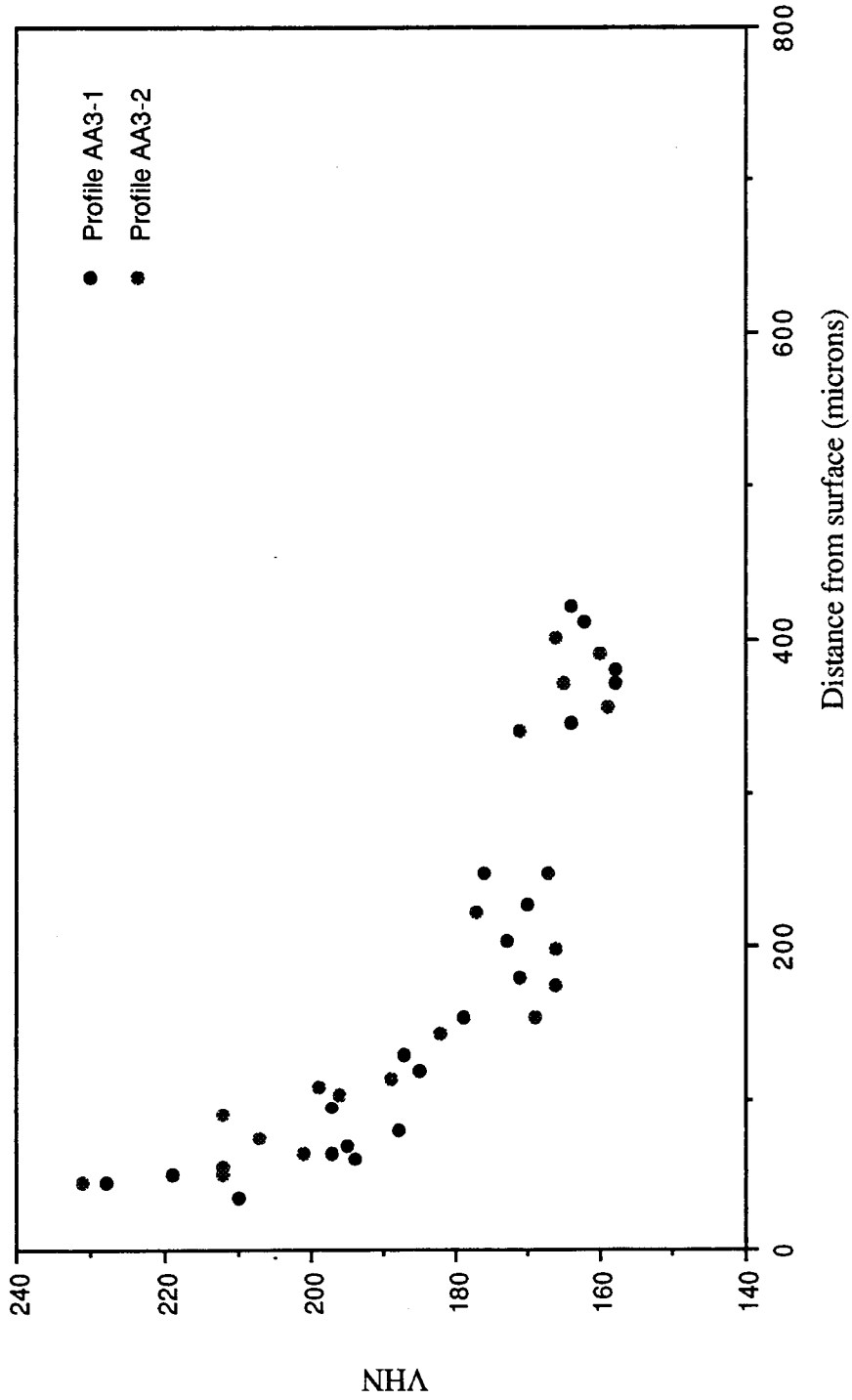

Figure B23 Control (AA3) hardness profile after 4458 hours at 200°C and 2790 hours at 300°C

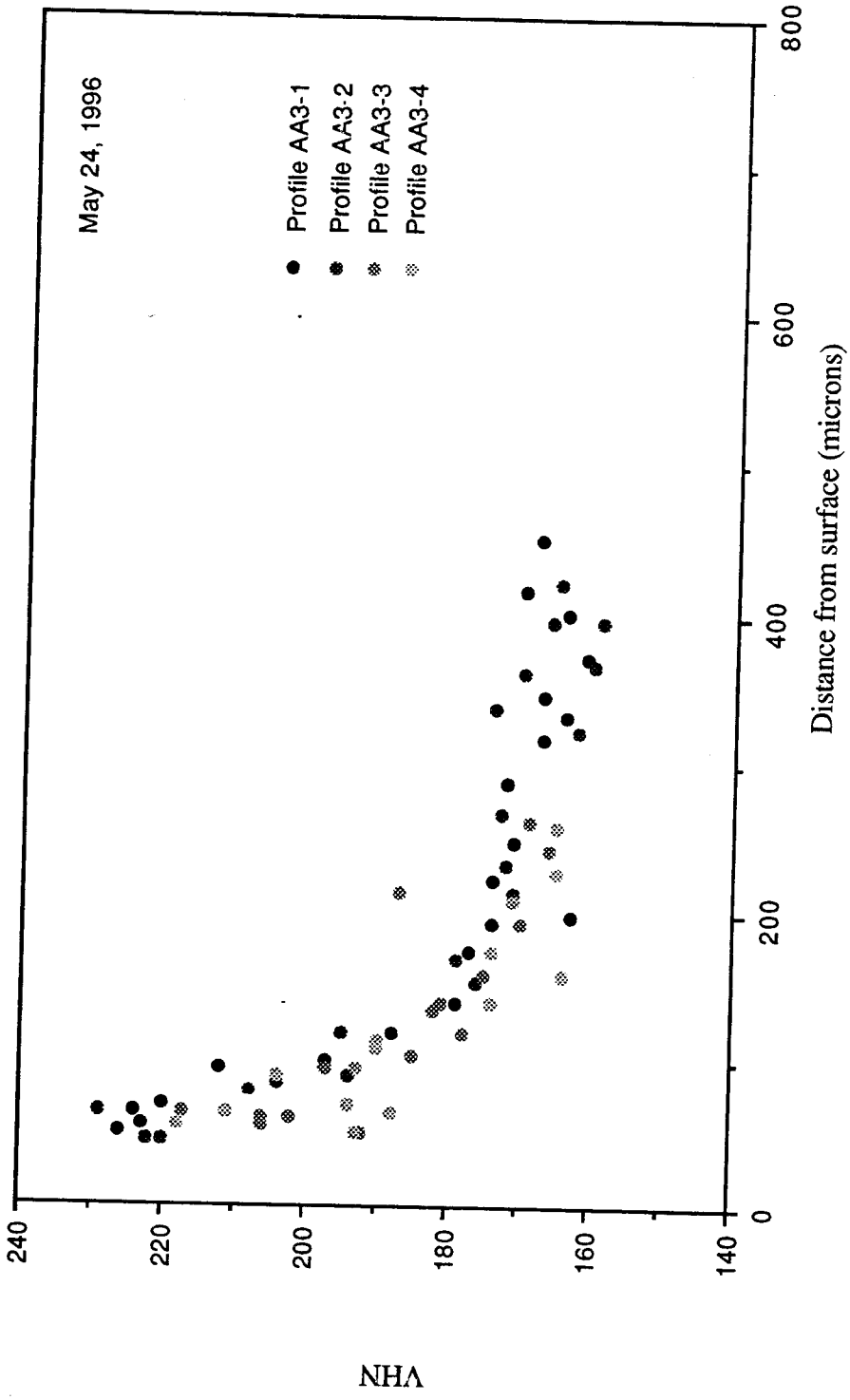

Figure B24 Control (AA3) hardness profile after 1.5 hours at 300°C under vacuum

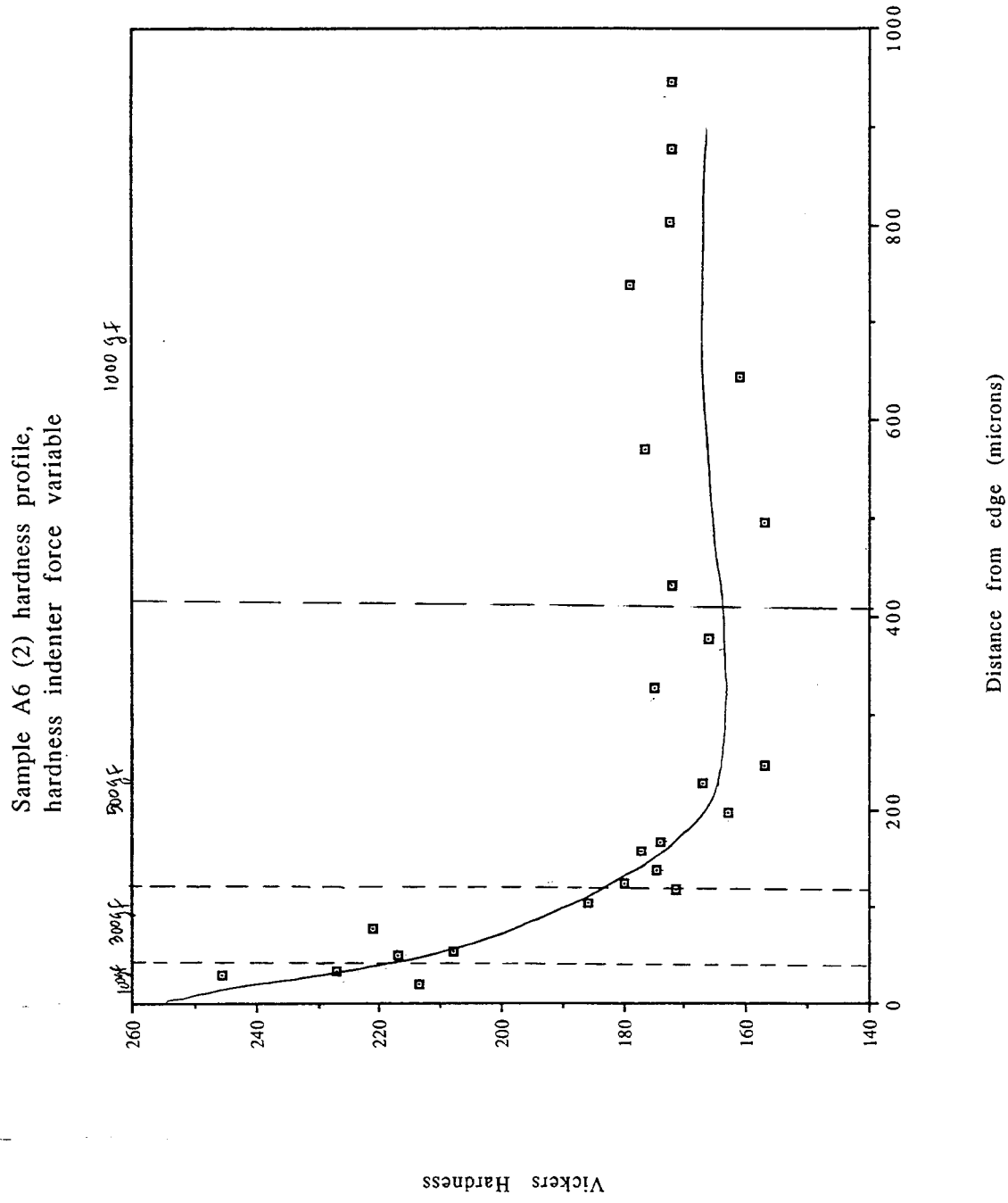

Figure B25 Hardness profile using variable indenter force

Figure B26 Hardness profile using 100 gf indenter

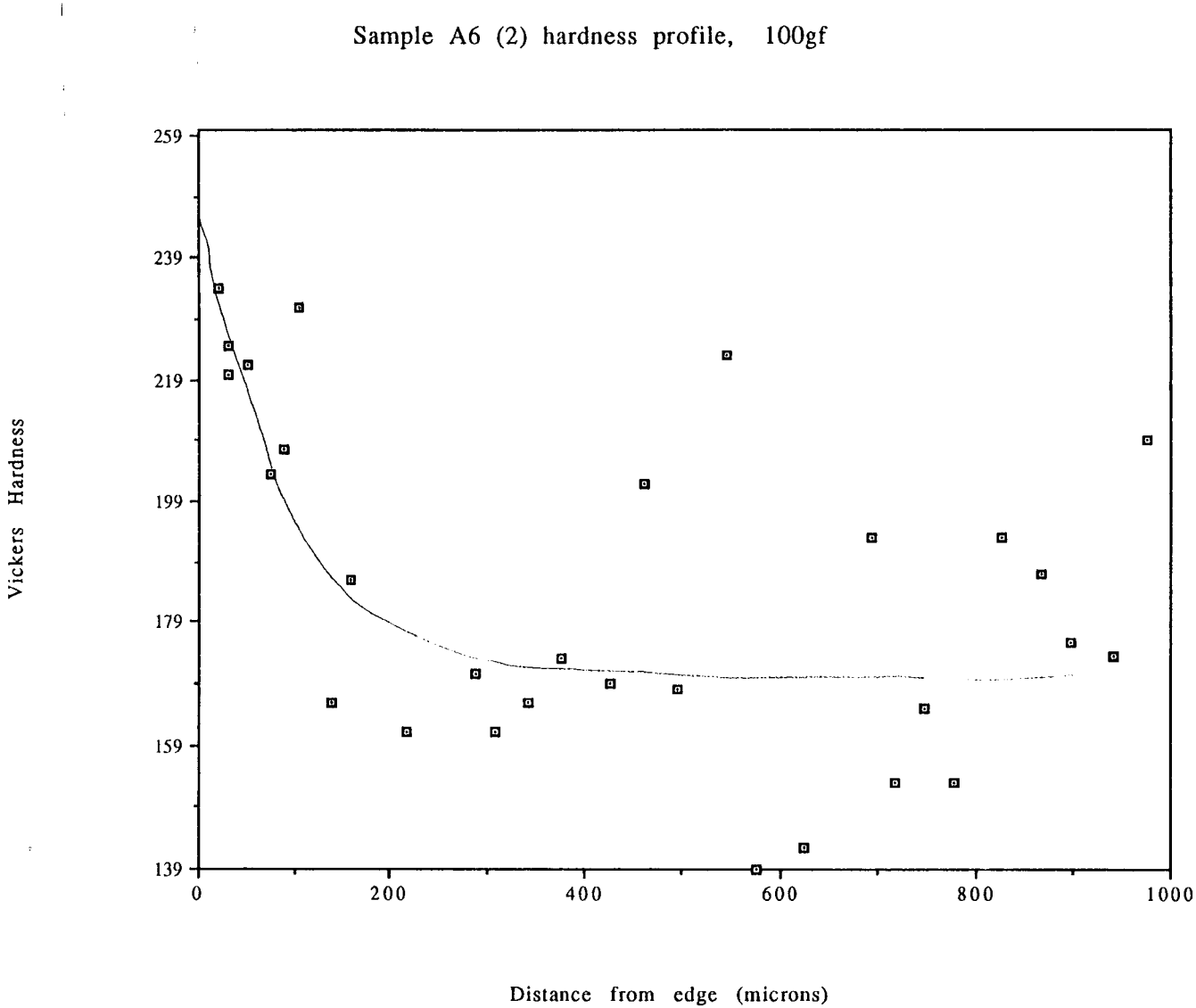

Figure B27 Hardness profile using 300 gf indenter

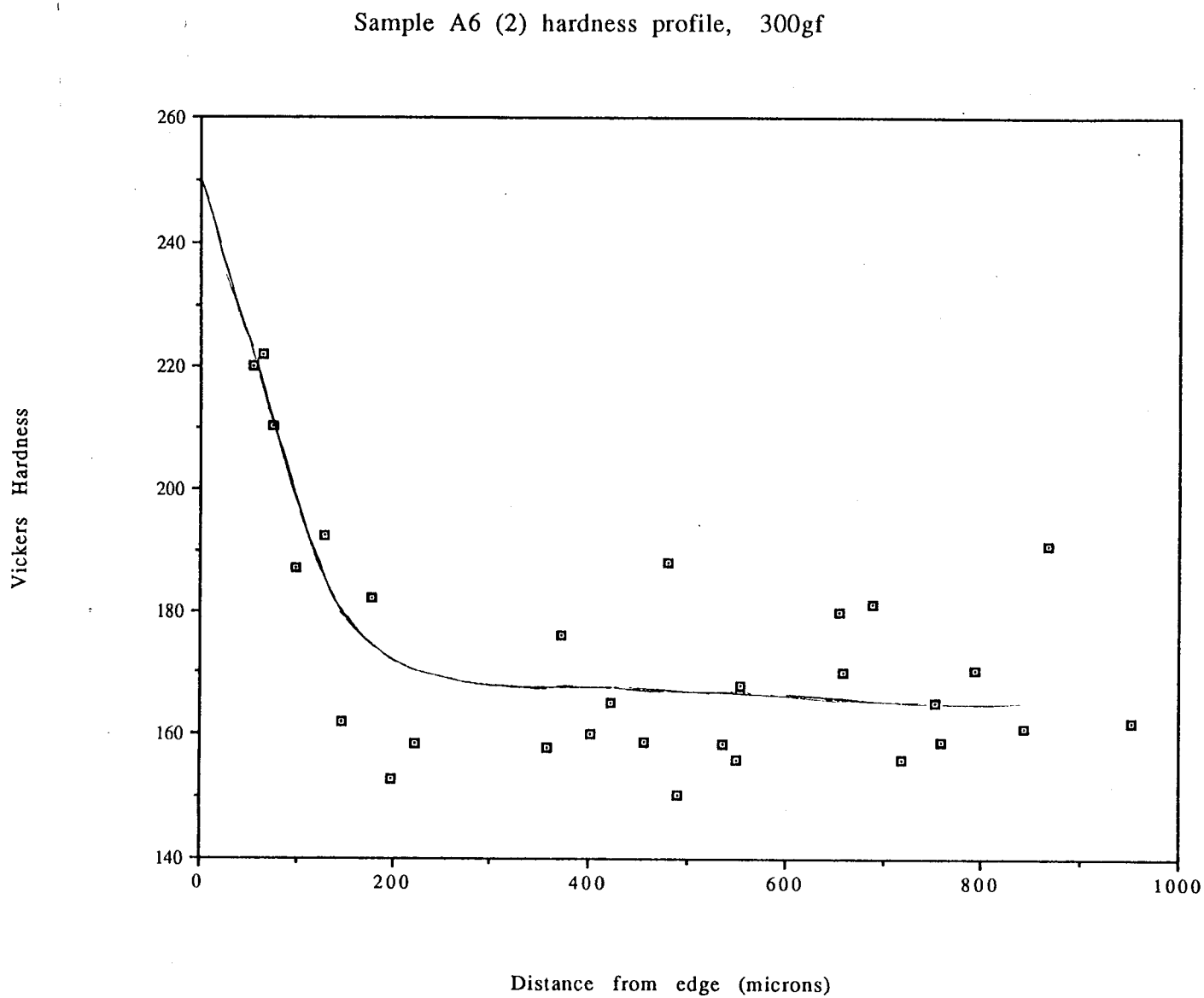

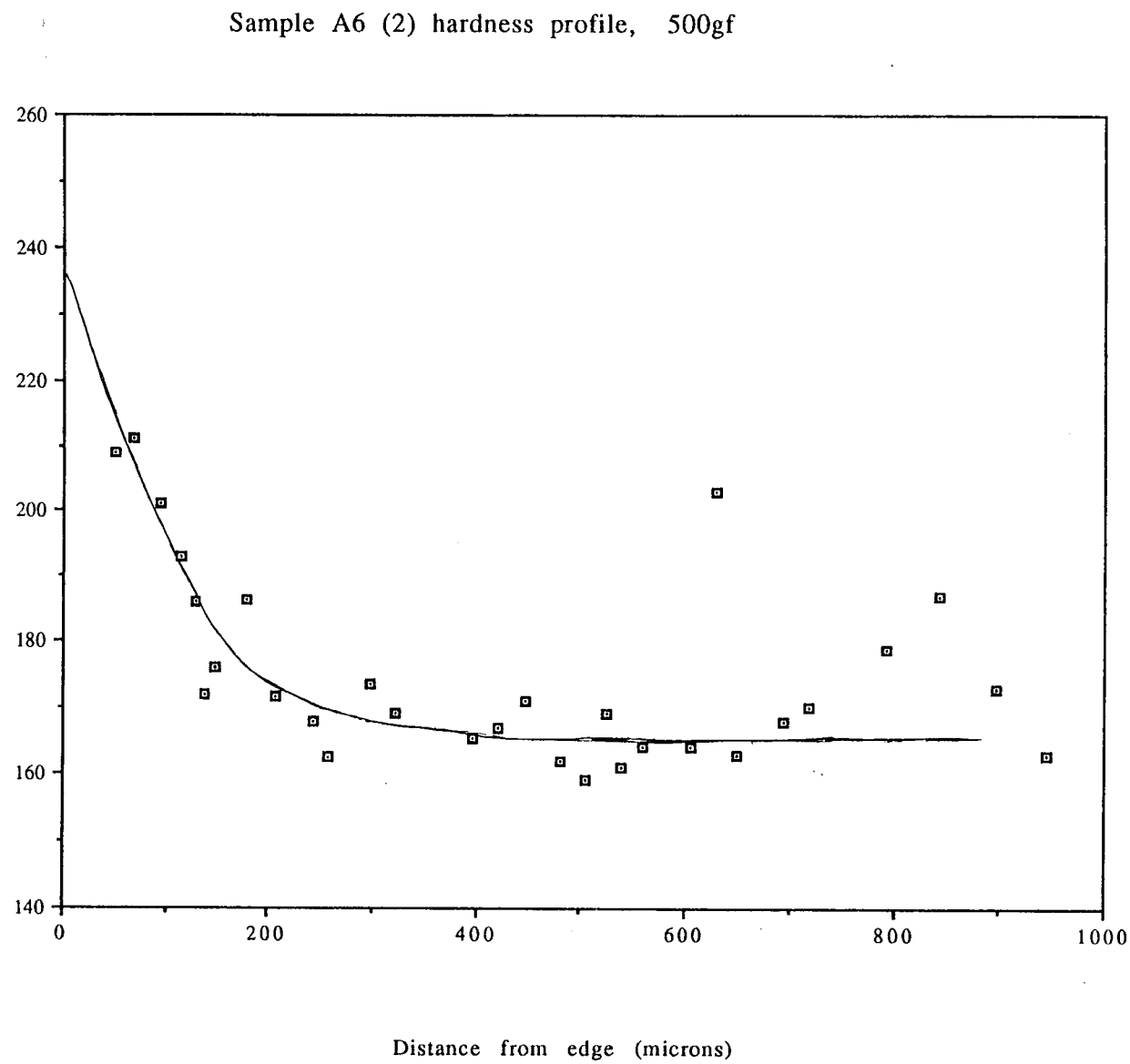

Figure B28 Hardness profile using 500 gf indenter

Appendix C Tensile Testing

Date: Tensile Test of Troy Zr

Specimen No. 1 L

			ave	Time
~~Diameter:~~ width	0.2485	0.248	0.249 .2485	σ_b= 58004.3
~~Length:~~ thickness	0.1885	0.1875	0.1865 0.1875	σ_{uts}= 70944.206
			Area: 0.0466	$\sigma_{0.2}$=
Energy:				ε_1=
				ε_2=
Peak Load:				RA= 39.1%
			ω_f .191	
Elongation:			t_{hf} .149	A_f = 0.0284

Specimen No. 2 L

			ave	Time
~~Diameter:~~ width	0.2485	0.248	0.249 .249	σ_b= 58326.2
~~Length:~~ thickness	0.1885	0.187	0.186 0.1878	σ_{uts}= 71223.18
			Area: 0.0466	$\sigma_{0.2}$=
Energy:				ε_1=
				ε_2=
Peak Load:			ω_f = 0.189	RA= 40.3%
			t_{hf} = .147	
Elongation:			A_f = 0.0278	

Specimen No. 3 L

			ave	Time
~~Diameter:~~ width	0.249	0.250	0.249 0.249	σ_b= 58763.3
~~Length:~~ thickness	0.1885	0.1885	0.188 0.1883	σ_{uts}= 71130.064
			Area: 0.0469	$\sigma_{0.2}$=
Energy:				ε_1=
				ε_2=
Peak Load:			ω_f = .188	RA= 42.7%
			t_{hf} = .143	
Elongation:			A_f = 0.0269	

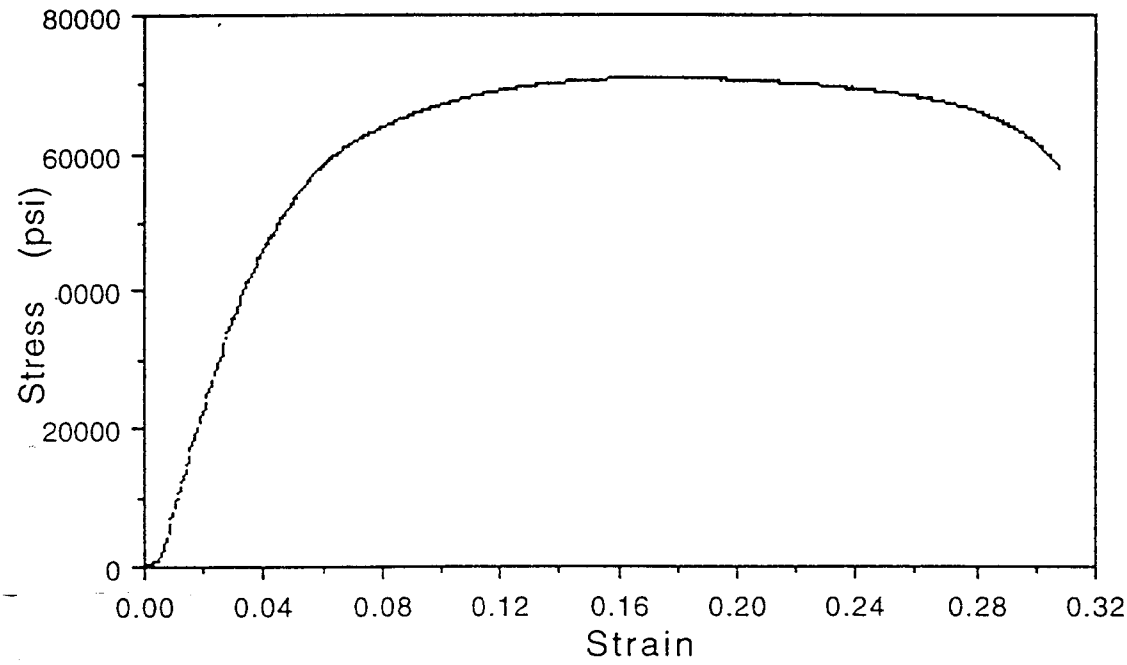

Figure C1 Sample 1L longitudinal engineering stress-strain curve

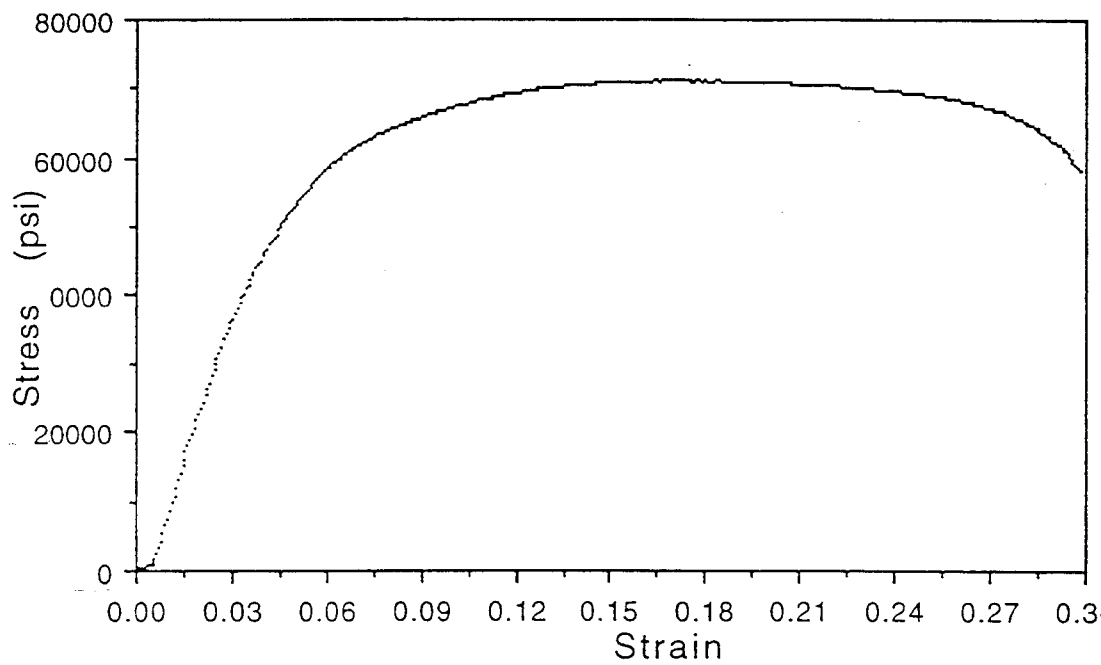

Figure C2 Sample 2L longitudinal engineering stress-strain curve

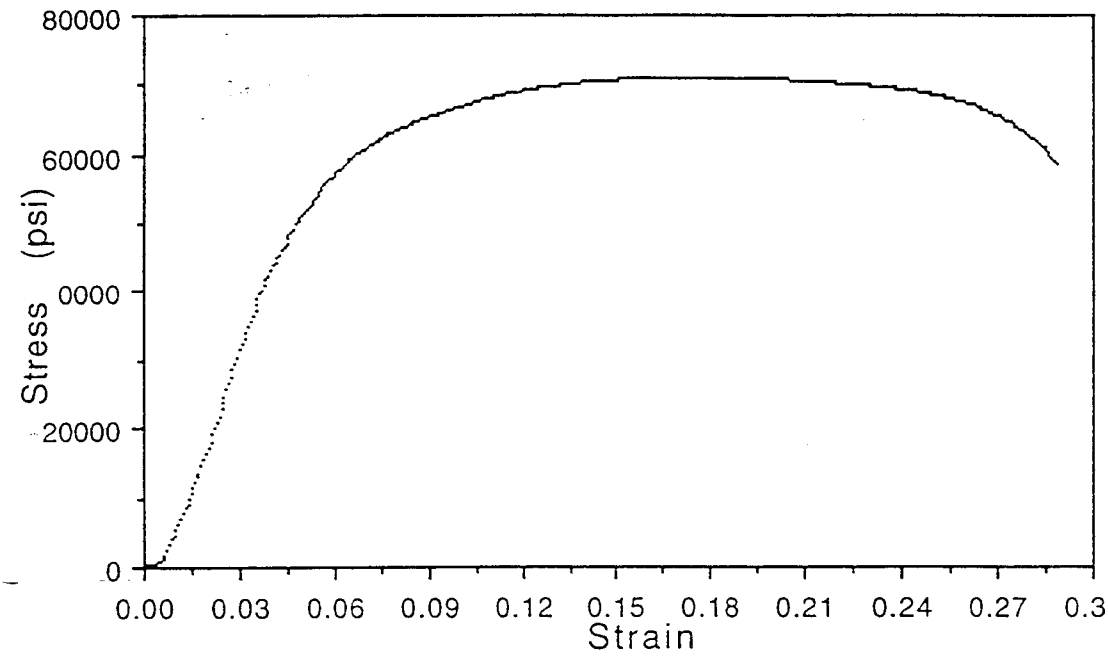

Figure C3 Sample 3L longitudinal engineering stress-strain curve

Troy's Zr

Date: Tensile Test of

Specimen No. 1 ω

				avg	Time
width ~~Diameter:~~	0.248	0.248	0.249	0.2483	σ_b= 51901.7
thickness ~~Length:~~	0.189	0.188	0.188	0.1883	σ_{uts}= 71047.009
				A_0 = 0.0468	$\sigma_{0.2}$=
Energy:					ε_1=
					ε_2=
Peak Load:			ω_f = 0.159	A_f = 0.0250	RA= 46.6%
			th_f = 0.157		
Elongation:					

Specimen No. 2ω

				avg	Time
width ~~Diameter:~~	0.250	0.255	0.250	0.252	σ_b= 50847.4
thickness ~~Length~~:	0.1875	0.1870	0.1870	0.1872	σ_{uts}= 68008.474
				A_0 = 0.0472	$\sigma_{0.2}$=
Energy:					ε_1=
					ε_2=
Peak Load:			ω_f = 0.157		RA= 46.8%
			th_f = 0.160	A_f = 0.0251	
Elongation:					

Specimen No. 3ω

				avg	Time
width ~~Diameter~~:	0.249	0.295	0.2485	0.264	σ_b= 49736.3
thickness ~~Length~~:	0.187	0.1865	0.1870	0.1868	σ_{uts}= 65476.673
				A_0 = 0.0493	$\sigma_{0.2}$=
Energy:					ε_1=
					ε_2=
Peak Load:			ω_f = 0.161	A_f = 0.0254	RA= 48.4%
			th_f = 0.158		
Elongation:					

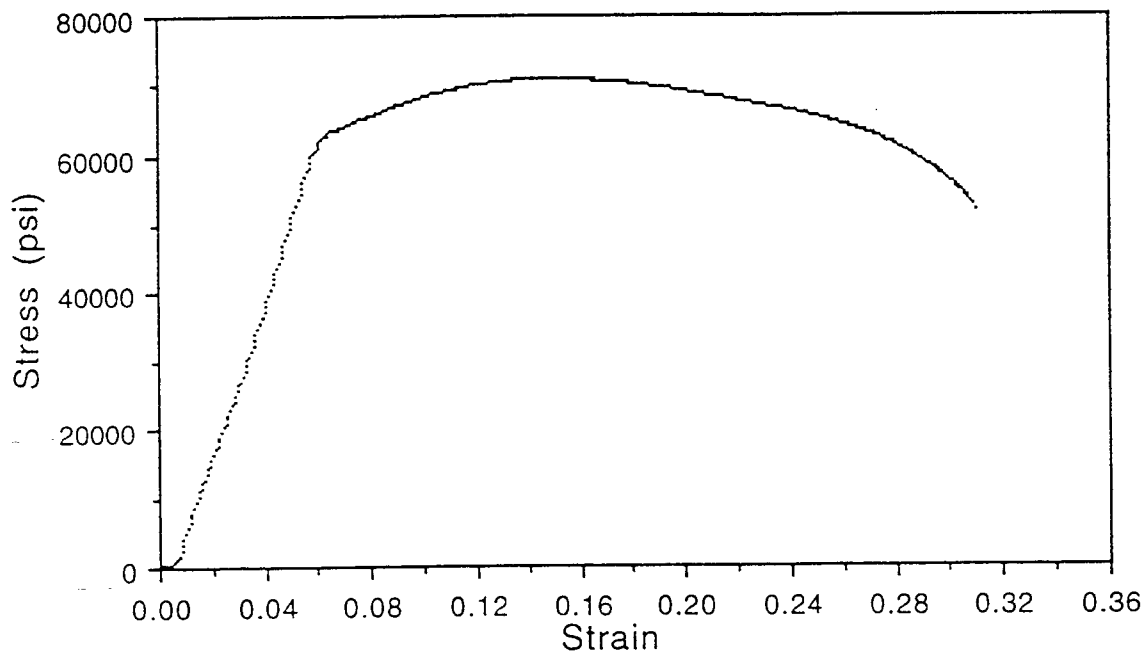

Figure C4 Sample 1W transverse engineering stress-strain curve

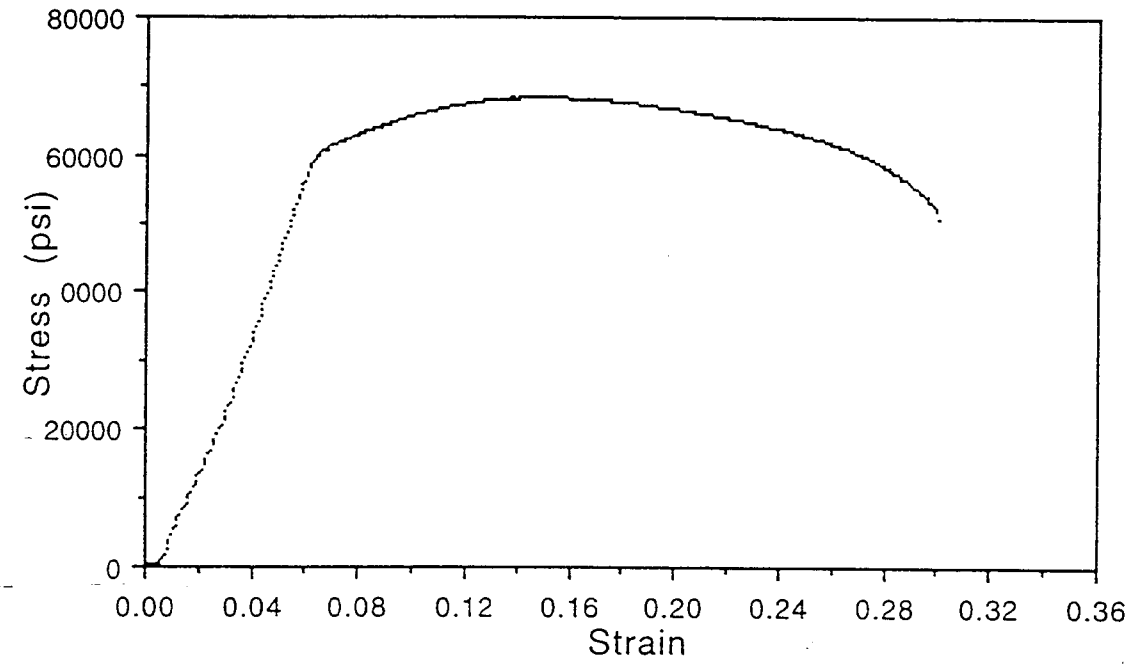

Figure C5 Sample 2W transverse engineering stress-strain curve

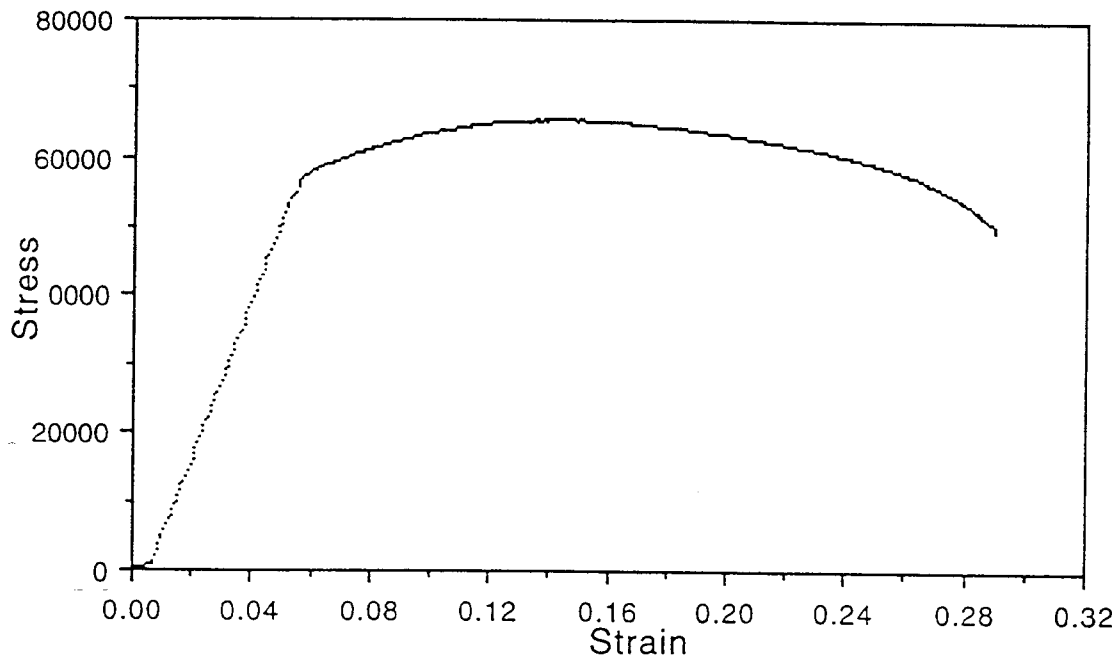

Figure C6 Sample 3W transverse engineering stress-strain curve

Appendix D Shot Peening Fabrication Stress Calculation

The bending stress resulting from the shot peening of the shot peened test plate was estimated because each side of the test plate was shot peened independently. Shot peening the sides independently caused some bowing of the plate until the reverse side was peened. The bowing was quantified by measuring the maximum height (arc height) that the test plate experienced after one side of the plate was shot peened. An arc height of 0.457 mm was measured to the center of the 15.0 cm by 21.6 cm by 0.65 cm thick test plate.

Two methods were used in order to estimate the bending stress in the plate after one side of the plate was shot peened. The first method modeled the shot peened surface as a uniformly distributed load where the load was determined by the center deflection. The stress was determined using the radius of curvature of the plate with the second method. These methods are described in more detail below.

Method 1 Uniformly Distributed Load

Assuming the plate acts as a simply supported beam under a uniformly distributed load, the center deflection is given as

$$\delta = \frac{5\,q\,L^4}{384\,E\,I}$$

where δ is the center deflection, q is the load per unit length, L is the length, E is Young's modulus and I is the bending moment of inertia around the bending axis. Solving for the distributed load,

$$q = \frac{384\,E\,I\,\delta}{5\,L^4}$$

Because the plate is approximated as a beam in this analysis, the bending

moment is given by

$$I = \frac{b\,h^3}{12}$$

where b is the beam (plate) width and h is the plate thickness. The above measured arc height would most closely correspond to a beam the length of the diagonal of the plate (since the maximum height is at the middle of the plate, not at an edge), however, this would make the determination of the moment of inertia difficult. Instead, the long axis of the plate was used as the beam length. This will yield a conservative estimate. The moment of inertia can then be calculated using the plate width of 150 mm and the plate thickness of 6.5 mm:

$$I = \frac{(150\text{mm})(6.5\text{mm})^3}{12} = 3433\ \text{mm}^4$$

Using the above values and 99.4 x 109 N/m^2 for Young's modulus, the equivalent distributed load to cause the 0.457 mm deflection is:

$$q = \frac{384\ (99.4 \times 10^9\ \frac{\text{N}}{\text{m}^2})(\frac{1\text{m}^2}{1000000\text{mm}^2}(3433\text{mm}^4)\ 0.457\text{mm}}{5\ (216\text{mm})^4} = 5.5\frac{\text{N}}{\text{mm}}$$

The stress can then be solved for using the relation

$$\sigma_{max} = \frac{M\,y_{max}}{I}$$

where M is the maximum internal bending moment (at the center of the beam) and y_{max} is the maximum distance from the neutral axis (half the thickness). The maximum stress is then:

$$\sigma_{max} = \frac{(32076\ \text{N mm})(3.25\ \text{mm})}{3433\ \text{mm}^4} = 30.4\ \text{MPa}$$

Method 2 Curvature Method

The second method uses the relationship:

$$\frac{1}{\rho} = -\frac{M}{E\,I}$$

where ρ is the radius of curvature of the plate, M is the internal bending moment in the plate, E is Young's modulus and I is the moment of inertia. The radius of curvature can be calculated using the relationship:

$$\rho = \frac{c^2}{8m} + \frac{m}{2}$$

where the variables are defined in the following illustration.

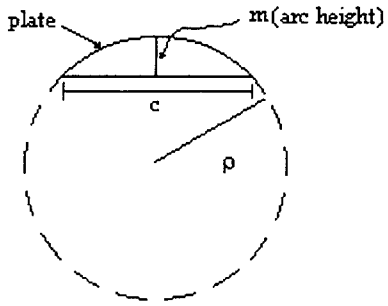

Again, for simplicity, the long dimension (216 mm)has been chosen as the chord length. The height m is the arc height (0.457 mm). The radius of curvature was then calculated to be 12800 mm. Solving for M, using the same moment of inertia and Young's modulus used in method 1, yields a value of 26.7 KN mm. The maximum stress at the plate surface is 25 MPa.

The maximum stress calculated by either method (30.4 MPa) is much smaller than the measured yield strength of zirconium of 186 MPa. This suggests that the bending due to shot peening was completely elastic and did not result in any plastic deformation.